AN INVESTIGATION INTO THE VENTILATION CHARACTERISTICS OF A LONGWALL DISTRICT IN A COAL MINE

FINAL REPORT

Submitted to the U.S. Department of Energy under
Contract No. DC AC03-768 F00098
A 75 15 20

Malcolm J. McPherson and Daniel J. Brunner

Department of Materials Science and Mineral Engineering
University of California, Berkeley

SEPTEMBER, 1983

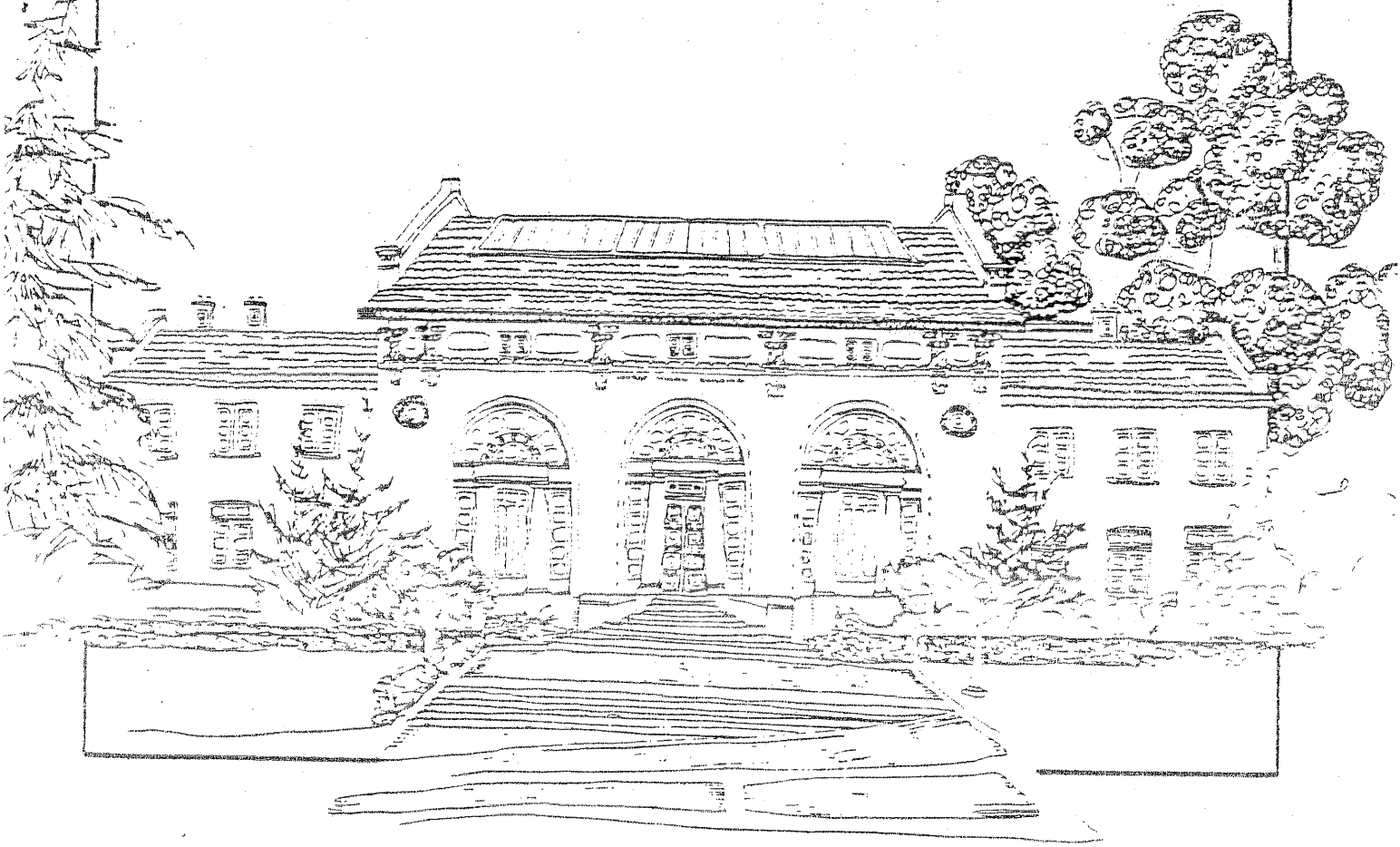

University of California, Berkeley

EXECUTIVE SUMMARY

The project described in this report arose out of the Snowmass Coal Company, Colorado, making available their Thompson Creek No. 1 Mine to the U.S. Department of Energy for research investigations during the summer months of 1982. The opportunity was taken to carry out controlled experiments on the ventilation characteristics of a longwall district employing waste ventilation through bleeder intake and return airways.

Four major tests were conducted, namely: (i) detailed measurements of the variation in airflow along the face front, conveyor track, travelling track and chock track of the longwall; (ii) measurements that led to the establishment of resistance values for the face ends, across the shearer and along the faceline; (iii) an experiment to determine the relationship between frictional pressure drop and air volume flowrate through the face, and (iv) an examination of the leakage characteristics of the caved area.

The major Sections of the report describe the conduct of these tests and the data obtained. The information gained was combined with theoretical analyses to produce improved procedures for the design, planning and control of ventilation in longwall mines. These procedures are illustrated by worked examples.

CONTENTS

LIST OF FIGURES

LIST OF TABLES

1. BACKGROUND

In July, 1982, the U.S. Department of Energy (DOE) agreed to provide funding for a field study and analysis of the ventilation of a longwall district in an underground coal mine. A major problem facing any in-depth study of ventilation on a fully equipped longwall face is the continuous movement of equipment, cramped conditions and strata movement as the face advances and caving occurs in the waste areas. The steady-state conditions, freedom of access, and utilization of sensitive and delicate instruments that are necesary for accurate ventilation measurements are neither available nor welcome in the activity of a working longwall.

During the summer months of 1982 the Thompson No. 1 mine, owned and operated by the Snowmass Coal Company, Carbondale, Colorado, was placed on standby, except for some development and essential maintenance work. This mine included a longwall face, fully equipped with a shearer and powered supports. The Company offered to make the mine available for experimental field studies funded by DOE. This provided a rare opportunity to conduct detailed ventilation measurements on a longwall face.

In mid-August 1982, a team of four spent two weeks at the mine carrying out both survey and experimental data acquisition. The personnel in the team were:

Principal Investigator:	Dr. Malcolm J. McPherson
Graduate students:	Dan Brunner
	Satya Harpalani
	Keith G. Wallace Jr.

This report describes the practical work carried out at the mine, a detailed analysis of data, and develops guidelines for the planning of ventilation in a longwall mine.

2. INTRODUCTION

The two major reasons for the steady increase in the number of longwall faces operated in U.S. coal mines are (a) the greater productivity potential and (b) the limitations on room and pillar workings imposed by depth below surface. There are, however, several factors that inhibit the growth of longwall mining. One of the more important is the difficulty experienced in meeting mandatory environmental standards on longwall faces. Coal is mined at a greater rate from a single production location than in room and pillar workings. This gives rise to increased problems of dust, gas and in some cases, heat and humidity. Furthermore the resistance to airflow offered by the longwall face and its associated airways is significantly higher than the multiple airflow routes of a room and pillar panel. This results in fans of higher pressure being required, and, consequently, greater pressure differentials across leakage paths within the mine ventilation system. In order to ensure that adequate airflows are supplied on longwall faces it is important that design procedures for the planning of ventilation are accurate and reliable.

In 1952, techniques of ventilation planning for underground mines moved from being an essentially empirical art to a quantified procedure through the development of electrical analogs to simulate large scale airflow systems. These, in turn, were superceded early in the 1960s by digital computer programs designed to model mine ventilation networks. Such programs are now used widely in all major mining countries. Five ventilation network programs were compared in a report on mine ventilation planning submitted to the Department of Energy in September 1981.[1]

Much of the recent work in network modelling has been concerned with improving the accuracy of the technique for specific mining layouts. In the case of longwall districts, a number of assumptions and simplifications are made, including the following:

(a) A single value of resistance is taken for the longwall face and this is usually assumed to be a linear function of face length for any given height. Due to shock losses and concentration of equipment at the face end it is most probable that the resistance is non-linear and higher at these locations than the rest of the face.

(b) It is assumed that the relationship between frictional pressure drop, p, and the airflow, Q, follows the normal square law,

$$p = RQ^2$$

where R is the face resistance. Whilst the square law has been verified many times for airways, its accuracy has been questioned when applied to longwall faces. Theory indicates that this law is applicable for airways whose "roughness" is around the periphery of the cross section, i.e. wall type roughness. On a longwall face, however, the majority of supports are sited within the main body of the airstream and offer aerodynamic drag.

(c) For the purposes of ventilation network analysis it is usually assumed that the air flows around a longwall district along discrete and continuous routes. The fact that only a fraction of the air entering a district actually reaches the face indicates that this is not true. Considerable leakage occurs through the caved waste and bleeder airways. This is often ignored, or treated in a cursory manner, in ventilation network planning.

This report describes a series of tests that were carried out on a standing, but fully equipped, longwall face at the Thompson No. 1 mine owned by the Snowmass Coal Company, Carbondale, Colorado. The field work was followed by a period of intensive analysis of the results and the development of design data and procedures that will improve the accuracy of ventilation network planning for longwall mines.

Section 3 outlines the methods of approach employed in the conduct of the tests and ensuing analyses. Section 4 gives a brief description of the mine and Section 5 deals with the calibration of instruments used in the field tests. A pressure-volume survey was carried out along the main intake and return airflow routes of the mine. This is described in Section 6 and provides details of the ventilation infrastructure within which the longwall face was located.

Four major tests were conducted in the longwall district. Section 7 of the report deals with the variation in airflow along the faceline and its distribution across the face track, the conveyor track, the travelling track and between the chock legs. The system of bleeder airways around the caved zone behind the face was found to be working well along the upper (return) half of the face, with air leaking from the face into the gob and, hence, preventing waste area methane from polluting the face airflow. However, a fault located approximately halfway along the face had combined with the effect of the elapsed time since the face had last operated (several weeks) to produce a well consolidated zone of collapsed waste at the back of the shield supports in this area. The test results indicated that this was causing some of the bleeder air to leak from the gob back into the face upstream of the fault.

The test described in Section 8 enabled a detailed evaluation of the resistance of the longwall to be made. The resistances of the face ends, faceline and shearer were measured. Procedures were developed to allow the corresponding resistances to be established for other longwall faces. These procedures were correlated with the field test data and the Section concludes with a worked example.

Section 9 is concerned with an investigation into the background of the Square Law, $p = RQ^2$, and the reasons for suspecting its accuracy when applied to a longwall face. However, a very carefully controlled test at the Snowmass mine gave a very convincing result showing that the square law did, indeed, hold for that face. This test also allowed the resistance of the faceline to be measured independently. The value obtained correlated well with data from the

other tests, indicating that confidence could be placed on the accuracy of the observational data.

The leakage of air through the caved waste is examined in Section 10. Considerable attention is paid to the modelling of leakage airflows through the caved material. Several models were considered. One of these, named the "Simplified Representative Resistance Model" was incorporated into an existing ventilation network analysis program and gave a good correlation with the observed data. This model takes into account the effects of the caved bleeder airways bordering the gob, the variation in consolidation of the caved material and laminar flow in the gob. A design procedure is proposed for modelling a caved waste and including it within the network analysis of a mine ventilation system. This Section concludes with a worked example showing the effect of shearer position on the airflow patterns along the faceline and in the adjoining gob.

Some of the field observations were utilized in more than one of the test analyses. However, an attempt has been made to make the four sections that describe the tests and corresponding analyses as self contained as possible. This should enable the selective reader to turn directly to any of those sections.

3. RESEARCH METHODS

The approach to the project involved an initial planning phase, field experiments, and an extensive and detailed sequence of data analyses. The overall philosophy has been to conduct a rigorous investigation into the ventilation patterns in, and around, a longwall district, based on hard data, and to produce design procedures for those involved in the planning of ventilation for longwall mines.

The project was divided into the following sub-tasks:

3.1 Instrument Calibration

During the week preceding the commencement of the field study, the anemometers and pressure gauges were calibrated against primary instruments at the Mine Ventilation Laboratory of the University of California, Berkeley.

3.2. Pressure-Volume Survey of the Mine

A pressure survey of the major airflow routes in the mine was conducted during the first four days of the field observations. The gauge-and-tube method was employed using calibrated magnehelic diaphragm gauges and a 100m length of pressure tubing. Concurrent airflow measurements were taken by anemometer traverse. The purpose of the pressure-volume survey was to provide the essential network infrastructure within which the longwall face was situated. Although it was not the intention to carry out any ventilation planning exercises for the mine these surveys did, in fact, provide sufficient information to permit network analyses of the system.

3.3. Distribution of Airflow on the Face

The field observations for this phase of the project consisted of taking 14 to 16 air velocity measurements on a grid covering the cross-section at each of six locations along the longwall face. Velocity contours were plotted on scale drawings of each cross-section.

The data analysis consisted of examining the variation in airflow along the faceline and the role of the bleeder airways in producing the pressure differentials that cause such variation. A further analysis was carried out on the distribution of airflow across the face, i.e. (a) close to the coal front, (b) in the conveyor track, (c) in the travelling track and (d) between the chock legs. The results were further examined from the viewpoint of gas and dust control.

3.4. Longwall Face Resistance

Detailed measurements were made of the frictional pressure drops and corresponding airflows across the face ends, shearer and incremental lengths along the mechanized longwall face. The pressure differentials were measured by magnehelic pressure gauges connected by pressure tubing between pitot tubes, and the airflows by spot measurements on a grid of points covering the cross-section of each measuring site. These observations allowed the variation in resistance (per meter length) along the faceline, across the shearer and at the face ends to be established.

An analysis of the data produced a range of friction factors (k values) applicable to longwall faces equipped with powered supports. These were incorporated into nomograms for rapid estimation of faceline resistances. A theoretical examination of shock losses at face ends and at the shearer was combined with measured data to facilitate the estimation of the additional equivalent resistances of those areas. The overall result was the development of an improved procedure to enable mining engineers to assign values of airway resistance to longwall faces during the design of ventilation systems.

3.5. Law of Airflow for a Longwall Face

A pressure tube was laid out along the full length of the face, with a magnehelic gauge connected in line. A fixed point anemometer station was established on the face. The airflow was adjusted in increments between the maximum attainable to the minimum compatible with safety. This variation was achieved by adjustments of doors and regulators, and by the erection of temporary brattice cloths.

The analyses commenced with an examination of the background derivations that lead to the familiar 'square law' of mine ventilation. The reasons for possible deviations from the square law on mechanized longwall faces were investigated. The data obtained from the field test allowed the law of airflow to be tested for the longwall face. Furthermore, it also enabled cross-checks to be carried out to verify the accuracy and reliability of the data used for the determination of face resistance and airflow distribution along the faceline.

3.6. Leakage though the Caved Waste

Deliberate leakage was allowed through the caved waste behind the longwall at the Snowmass Thompson Creek No. 1 mine, in order to prevent accumulations of methane in the caved area. A survey was conducted which traversed all four boundaries of the caved area,

during which airflow measurements were made in all cross-cuts connecting the bleeder airways to the gob.

The results were employed in a detailed investigation to develop a mathematical model of leakage through a longwall waste. A number of such models were examined, and one (the simplified representative resistance model) was selected as giving satisfactory results and was capable of incorporation into any existing ventilation network simulation program that could handle a mixture of laminar and turbulent flow paths.

The data obtained from the mine was tested against the simulation model, allowance being made for the time-dependent consolidation that had taken place in the gob of the standing face, and for the effect of a small fault that crossed the faceline.

A practical procedure was developed for the simulation of leakage flows though a longwall gob and this was inserted into a ventilation network analysis program. The application of the technique was demonstrated by a worked example.

4. DESCRIPTION OF THE MINE

Thompson Creek No. 1 Mine is owned and operated by the Snowmass Coal Company and is situated in Pitkin County, Co. near the town of Carbondale. All current workings are in the 'A' seam, the layout being shown in Figure 4.1. The seam is some 7ft in thickness and dips to the west at an angle of 30°.

One longwall panel is in operation retreating to the north between two sets of boundary airways. The face is on full dip with the airways maintained along strike lines. The line is equipped with:

(i) 350 ton Hemscheidt Troika shield supports
(ii) an Anderson-Boyes 500 hp radio-controlled chainless shearer
(iii) a Dowty-Meco 150 hp twin outboard armored flexible chain conveyor and
(iv) a Dowty-Meco 150hp stage loader

When operating at full capacity, the face production is rated at 2100 rom tons/day.

The depth of cover is variable due to the dip of the seam and the mountainous nature of the surface terrain. At the time of the field observations, the face was some 1250ft. below surface. The main access points are at the northern outcrops where the surface plant is also concentrated. Coal transport is by belt conveyor along the innermost of the two lower airways serving the longwall and up an inclined ramp to surface. At the time of the field study, development was well advanced for opening up a second panel which would run parallel to the present No. 1 panel. However, it is not intended that more than one longwall will be in operation at any one time.

Ventilation is promoted by two exhaust fans. Fan No. 1 is a 100 hp 6ft diameter Westinghouse axial fan operating at a nominal 60,400 cfm and 1.9 inches w.g.s.p. and is situated at one of the northern portals. Fan No. 2 is sited at an eastern outcrop portal. This is a 200 hp 6 ft diameter Joy axial fan with a nominal duty of 124,200 cfm at 3.1 in. w.g.s.p.

Airflow is ascentional on the face. The lower airways provide the intake air to the face. The haulage way on the upper level is also an intake. However, this air never reaches the longwall face but merely mixes with the return air fom the face before being drawn towards fan No. 2.

The conveyor road is well regulated and MSHA permission had been obtained for the conveyor airflow to continue on to the face. As the face retreats, the inner two airways are allowed to cave whilst the outer airways are maintained open as bleeder passages. Strategic erection and dismantling of stoppings within openings connected to the caved region, and regulators in the bleeder airways, help to dilute methane emissions from the waste area. The mine has no history of spontaneous combustion. All of the face return air is drawn towards fan No. 2 at the eastern outcrop. Fan No. 1, on the other hand, handles most of the air that has ventilated the developments.

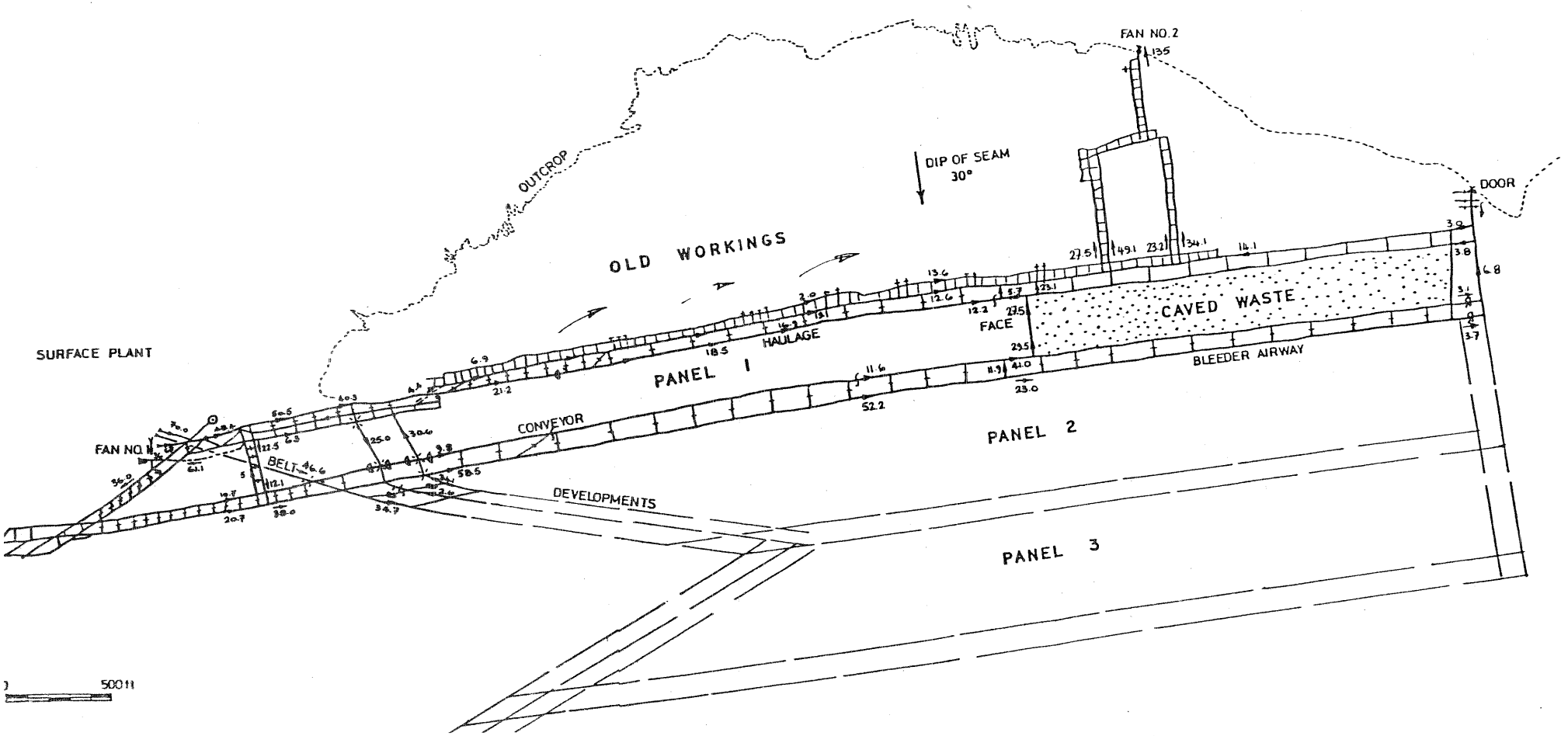

Figure 4.1 Thompson Creek No.1 mine ventilation schematic.

5. INSTRUMENT CALIBRATION

Three Davis Biram anemometers were used during the surveys. These were calibrated in a low turbulence wind tunnel at the Mine Ventilation Laboratory of the University of California, Berkeley.[1] Each anemometer was calibrated against a pitot-static tube over the range of velocities expected in the mine. The positions of the instruments in the wind tunnel are shown in Figure 5.1.

The velocity of the air, u, is related to the velocity head, h_v, registered by the pitot-static tube:-

$$u = 140.07\sqrt{h_v/\rho_a} \quad m/s$$

where h_v = m of water, and
ρa = air density, kg/m^3

or

$$u = 1097.9\sqrt{h_v/\rho_a} \quad ft/min$$

where h_v = inches of water and
ρ_a = air density, lb/ft^3

Air densities were determined from barometric and hygrometric observations throughout the calibration procedure. The anemometer readings were observed by timing an integral number of dial revolutions over a period of not less than 60 seconds.

The pressure gauges employed during the surveys were Dwyer magnehelic instruments. These devices react to differential pressures across a sensitive diaphragm. The slight flexing of the diaphragm is transmitted to an indicator needle via a magnetic linkage with no mechanical contact. Frictional resistance is therefore reduced to a minimum. The gauges employed for this test had ranges varying from 0 - 0.25 through 0 - 4.0 inches w.g., since it had been ascertained that the main fans at Thompson Creek did not exceed a pressure of 4.0 inches water gauge.

Magnehelic gauges were preferred to liquid in glass inclined manometers because of their portability and dependability under mining conditions. It is, however, important that they are calibrated prior to use.

The gauges were attached to a pressure manifold into which was also connected a direct lift manometer. This is a primary laboratory manometer reading directly to 1/1000 inch w.g. and allowing estimates to 1/10,000 inch w.g. Air pressure within the manifold was applied through a damping valve by a simple rubber bulb pump, each magnehelic gauge being removed as its range limit was reached.

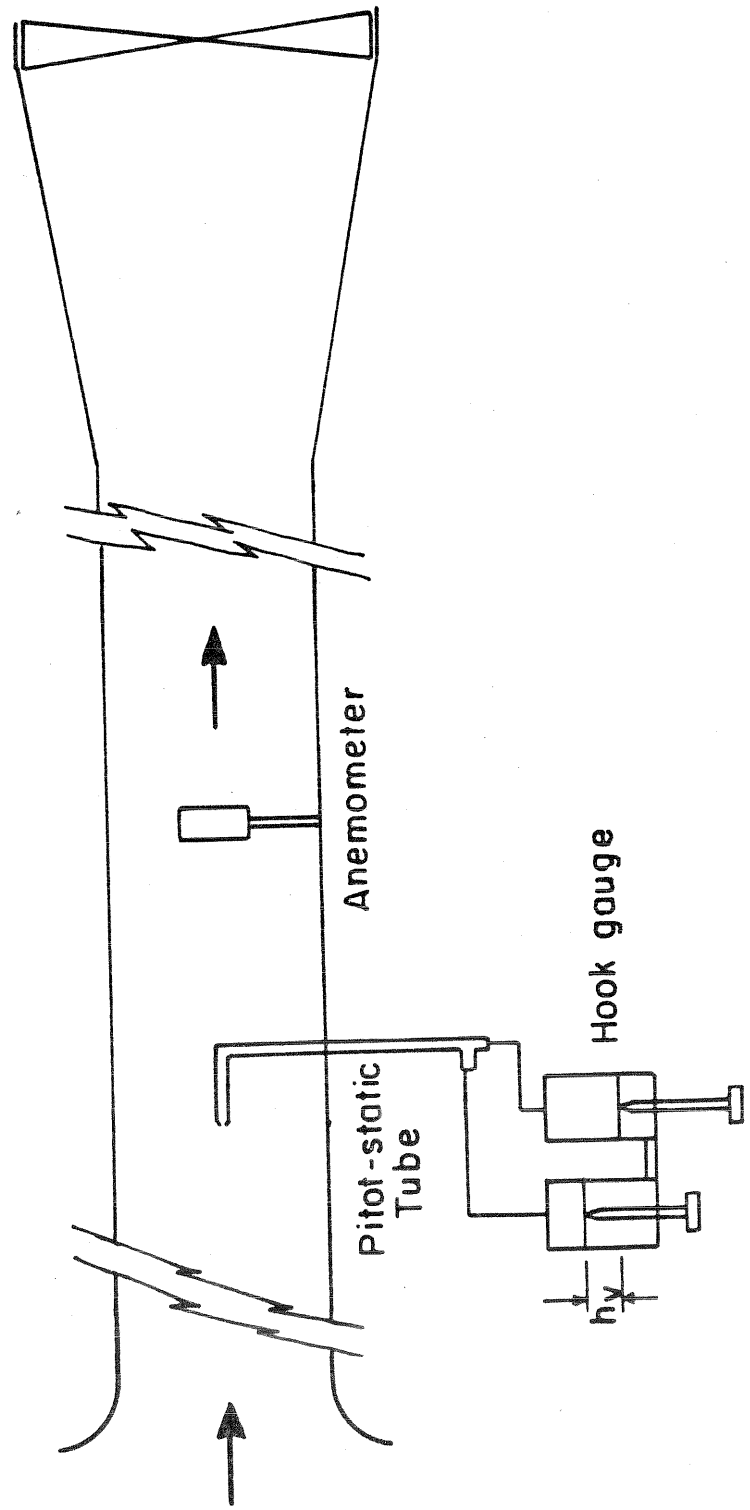

Figure 5.1 Calibration of instruments in wind tunnel.

6. VENTILATION SURVEY OF PRIMARY CIRCUITS

6.1. Survey Procedure and Outline of Results

The four personnel worked as two teams, one responsible for the measurement of frictional pressure drops and the other for airflow determinations. It was important that the pressure drop measurement for each airway was made at a known rate of airflow. Hence, the two teams worked in conjunction with each other.

The first day in the mine was spent on reconnaisance. All of the main ventilation routes were travelled and determinations were made on control points and traverse paths for the ensuing surveys.

On each of the following three days, complete traverses were made, precautions being taken to close each route back to its starting point.

The frictional pressure drops along each airway were determined in 100 m lengths by the gauge and tube method. A 100 m length of pressure tubing (1/8 inch i.d.) was laid out in the airway with a 4 ft pitot tube held facing into the airflow at either end. A 0.25 inch w.g. magnehelic gauge connected into the line allowed a direct reading of the frictional pressure drop. Sufficient time was allowed for transmission of the pressure wave along the tubing. This could be tracked as creep of the gauge needle and in some cases took several minutes. The delay time could have been reduced by employing larger diameter tubing but this would have caused tube handling to be more difficult. Check readings of pressure differentials were taken across all doors, regulators and, where practicable, through stoppings. Such check readings were invaluable in maintaining accuracy of the survey. Independent pressure-volume measurements were also taken at the main fans.

The natural ventilating pressure (NVP) was negative (the air in the mine was cooler than the daytime surface atmosphere) but small in magnitude. Ignoring NVP, the algebraic sum of all frictional pressure drops and fan pressures around any closed traverse should be zero (Kirchhoff's 2nd law). Each evening, the field book data was transcribed on to mine plans and the closing consistency of the pressure-drop traverse checked.

Airflow measurements were made by anemometer traverses and taping in the main airways. The roof of the airways retained the 30° slope of the seam. The floors, on the other hand, had been levelled. The shape of most of the airways was therefore a distorted trapezium - not at all suitable for precise airflow measurements. Airflow stations were chosen at sites where the airway areas could most conveniently be measured by taping and, as far as was possible, well away from junctions or sudden changes in cross section. Three or more traverses were taken at each station using a Davis anemometer and extension rod until repeatability within 5 per cent was achieved. Corrections from the anemometer calibration and the calculations of airflow were made on the spot.

$$Q = u \times A$$

where
Q = airflow ft^3/min (m^3/s)
u = mean velocity ft/min (m/s)
A = cross-sectional area (ft^2) (m^2)

Again, all airflow measurements were transcribed on to a mine plan each evening and checked for consistency.

During the conduct of the survey, a stopping in one of the cross-cuts connecting the lower bleeder airway to the waste area was found to have collapsed allowing large scale leakage. This was sealed with brattice cloth by mine personnel. A regulator in the lower haulage road was also under construction during the time of the survey. These changes caused considerable difficulty in correlating some of the airflows in succeeding days. However, measuring each airway pressure drop, p, and airflow, Q, at the same time ensured that a reliable value of airway resistance, R, was obtained for each individual branch.

$$R = p/Q^2$$

The larger pressure drops are shown on Figure 6.1.

The purpose of the pressure-volume survey was to determine the network structure containing the longwall face. Hence, the survey was intentionally not as complete as would be the case for ventilation planning purposes. In particular, the areas that were not surveyed were:

(i) the legs leading to fan No. 2
(ii) the upper airway bounding on the old workings (much of this was untravellable)
(iii) the return route from the developments into the drift leading to fan No. 1.

However, much of this data could be calculated by difference from the measurements actually made.

6.2. Network Correlation and Observations on Current System

As a preliminary investigation, the entire ventilation system of the mine was simulated using the network analysis program VNET. A simplified network schematic was designed and values of resistance, as determined from the survey, were assigned to the branches. Since the survey was incomplete, the resistances of several branches, such as the caved airways surrounding the gob, were calculated using assumed cross-sectional areas. The caved gob region was represented by branches leading to a single sink located in the center of the gob.

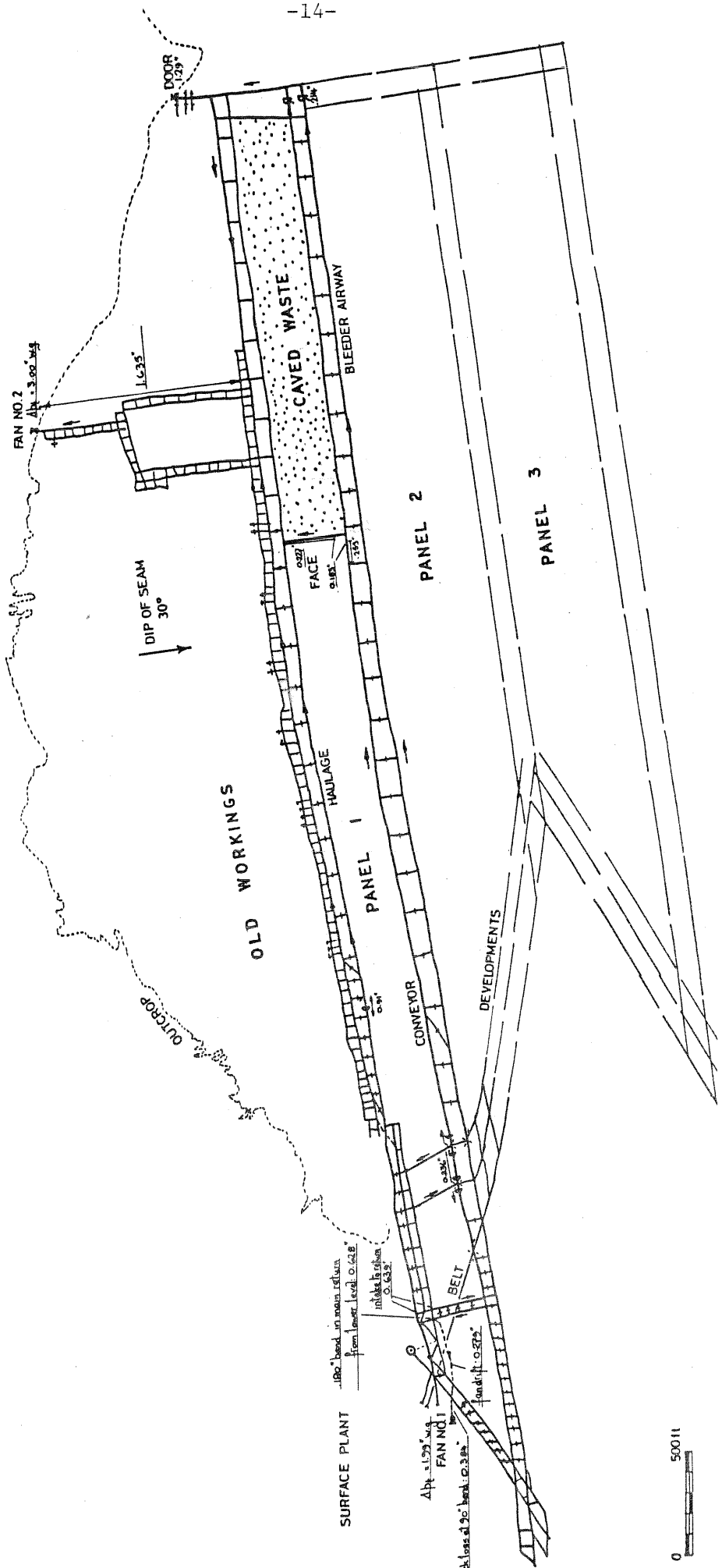

Figure 6.1 Pressure drops of significance measured during the survey.

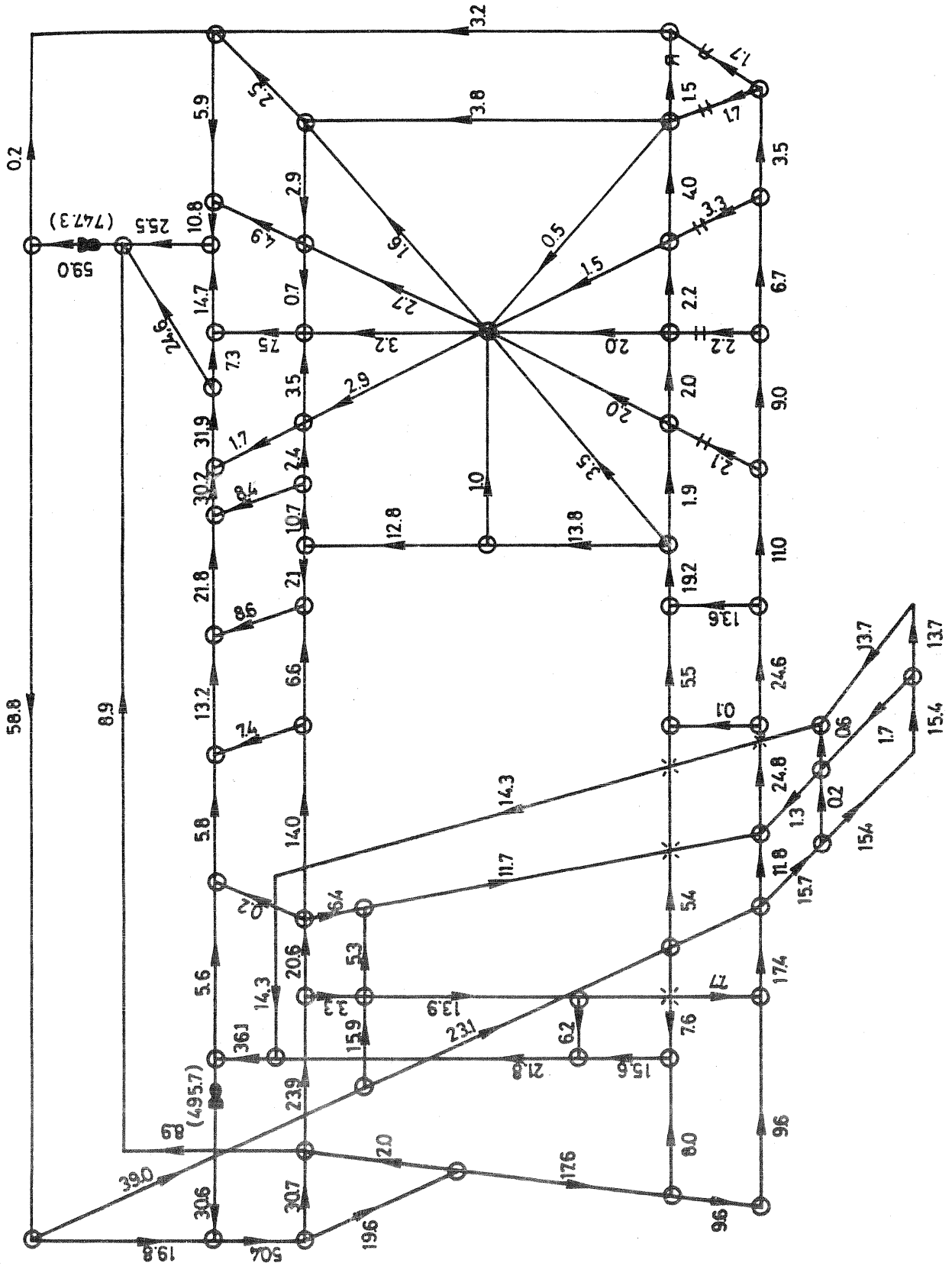

Figure 6.2 Network simulating ventilation system, shown with balanced airflows in (m^3/s).

Values of resistance for the sink branches were found by trial and error, optimizing on the correlation. The network simulation obtained, with balanced airflows, is shown on Figure (6.2). The simulation gave airflow values which correlated within 10% of the actual survey measurements.

The pressure-volume survey served to provide a picture of the ventilation infrastructure of the mine, within which the detailed investigations in the longwall panel were to be carried out. Although the survey was not as complete as would normally be required for planning the future ventilation of the mine, the correlation obtained indicated that the basic network could, indeed, be used for this purpose.

The survey indicated that whilst the longwall face and waste were well ventilated, the efficiency of the system could be improved and the operating costs reduced. Essentially, No. 2 fan provided the ventilation for the longwall face while No. 1 fan served the development area to the west. The upper level airways carried intake air, all of which leaked directly into returns. The majority of the cost of operating both fans was consumed in the fan drifts. A total pressure of 1.99 inches water gauge was measured across No. 1 fan. Of this, 1.291 inches were lost in the fan drift and associated bends. Air returning from the development area ascended to a higher level via a sharp and constricted 180° bend (consuming 0.628 inches w.g. alone) followed by a sharp 90° bend. There was a further sharp 90° bend immediately before the fan. The shock losses associated with those bends created a very high resistance to airflow and, hence, unnecesarily high fan power costs.

The airways leading up the slope to No. 2 fan were also in poor condition, giving a frictional pressure drop of 1.635 inches water gauge (out of 3.00 inches produced by the fan). Network analysis exercises indicated that improving the fan drifts would cut the fan power costs by almost 40 per cent.

7. INVESTIGATION OF THE DISTRIBUTION OF AIRFLOW ALONG A LONGWALL FACE

7.1. Significance of variations in airflow on a longwall face.

7.1.1. Variation of airflow along length of face

The variation of airflow along the length of a longwall face is of significance in the control of both methane and dust. This variation is, in turn, dependent on the type of ventilation system. Two arrangements are commonly used. The first, is termed a "bleeder system" where the caved gob region is ventilated by leakage from bleeder airways that are maintained around the gob. The second arrangement, termed the "sealed system", does not intentionally allow air to leak through or flow around the caved region. The variation in airflow along the length of the face is also a function of the consolidation of the gob.

7.1.1.1. Bleeder systems:

With this system, the pressure difference between the two bleeder airways, the bleeder intake and return, causes air to leak through the gob region. The gob region is kept at a lower pressure than the intake bleeder by the use of stoppings in crosscuts which connect the bleeder intake to the caved gob. The leakage which flows through the gob, dilutes and removes the gases accumulated in the gob. The face investigated at Snowmass operated on a bleeder system as illustrated on Figure (4.1).

The pressure difference between the bleeder return and the face line, causes air to leak from the face line into the gob. The result of this is a decrease in volume flow rate along the length of the face.

Effect of bleeder system on face gas control:

On a producing longwall face, methane is desorbed and emitted from the newly exposed face and broken coal. In addition, methane is also released in the caved gob zone behind the shields. Methane, with a specific weight of 0.56 relative to air, tends to accumulate at higher elevations, i.e. roofs of airways. On a longwall face, where frictional sparking from the shearer's cutting drums occurs frequently, ignitions and flame propagations can occur. To prevent ignition, methane must be diluted by ventilating air to concentrations below the explosive range; 5-15% by volume. Federal regulations prohibit the operation of any machinery in air containing more than 1%

methane by volume.

The objective of a bleeder type ventilation system is to keep the waste gas fringe away from the face line. The pressure difference between the face and the bleeder return, causes face line air to leak into the gob. This prevents the migration of gas from the gob zone onto the face line. This effective containment of waste gases reduces the airflow requirements along the face since only methane emitted from the exposed face and broken coal must be diluted.

Effect of bleeder system on dust control:

To this day, longwall faces have great difficulty in complying with the 1969 legislative dust regulations. The regulation threshold limit value for suspended respirable dust is 2 milligrams per cubic meter measured at the site of the operator. Suspended dust, produced from the shearer during actual cutting of the coal, must be suppressed, diluted by the ventilating air, or diverted away from the operator. Since personnel are necessarily present on the face during cutting operations, the air velocities should not be so high that larger particles remain airborne. Air velocities greater than 4.5 m/s will result in unacceptable conditions.

The decreased airflow rate at the return end of the face, caused by the bleeder system, may not be sufficient to reduce the dust concentration when the shearer is operating up wind of this location. To adjust for this, the airflow entering the face line may be increased. However, this may exacerbate the dust problem, especially if the stage loader is located on the intake end of the face. Higher velocities may entrain more respirable dust as well as the larger dust particles. Thus, for a longwall mine ventilated with a bleeder type system, the airflow distribution along the face must be balanced so that sufficient air is available to dilute dust at the return end of the face without requiring excessively high velocities at the intake end.

7.1.1.2. Closed systems:

For a closed system, all the airflow is maintained along, or close to the faceline. Relatively little air is diverted around or allowed to leak through the caved gob. Some of the air flowing along the face leaks behind the shields; however, much of this air returns back into the face line at the return end. Nevertheless, the volume flow rates remain fairly uniform along the face line. Sealing the airways leading around the caved zone will cause the gob to remain at a neutral pressure between the intake air pressure and the return air pressure.

Effect of closed system on face gas control:

With a closed system, if methane drainage is not employed, the gas will accumulate in the gob. Some of the air flowing into the face will tend to migrate into the gassy caved zone behind the shields. The return end of the face, being at a lower pressure, will tend to draw this gas laden air back into the face. The larger the pressure drop between the ends of the face or the larger the face resistance, the more air will leak behind the shields. The addition of gas laden air into the face line increases the face air flow requirments. Thus for a sealed system, from a gas control standpoint, the amount of air entering the face line must be adequate enough to dilute the methane being drawn into the face line from the waste and that emitted from the newly exposed coal surfaces.

Effect of closed system on face dust control:

Since the face airflow rates do not decrease significantly along the length of the face, as with the bleeder system, problems with varied degrees of dilution along the face, are not present. However, dust dilution is always a problem on longwall faces. The use of dust suppression sprays mounted on the shearer drum, and directional water sprays is now standard practice to assist in controlling the amount of suspended dust.

7.1.1.3. Effect of localized waste consolidation:

In retreat longwall mining, the headgate and tailgate airways immediately adjacent the waste area are allowed to cave. Due to the chain pillars next to these airways, the caving is incomplete and zones of convergence exist, leading into the gob. The extent of these zones depends on the overlying strata, seam height, the depth of the seam and the time elapsed since the face passed. The center part of the gob, on the other hand, caves more effectively and is more consolidated than the edge zones. Behind the shields, where the coverload has not yet been reattained, there exists another zone of convergence. Thus, a longwall gob is surrounded by gradients of consolidation, increasing towards its center. In terms of variation of face airflow, the convergence zone behind the shields is most important. Geologic conditions can reduce the extent of this zone and directly affect the face airflow pattern. Furthermore, consolidation behind the shields will continue through any period when the face ceases to advance or retreat.

Geologic conditions:

If the longwall face passes through a fault, the caveability of the overlying strata will change in that region. The strata may cave more effectively behind the shields and thus reduce the extent of the convergence zone. Variations in the structure of the overlying strata, weak strata and discontinuities may also alter the caveability and reduce the length of the convergence zone.

For a bleeder system, a short length of well consolidated material behind the shields may, in some cases, force leakage air back from the gob to the face line. This leakage air flows from the gob onto the face in order to bypass the highly consolidated center zone which has moved up to the back of the shields. This causes the volume flow rate to increase towards the center of the faceline, after which it decreases sharply towards the return.

For a sealed system, a consolidated convergence zone behind the shields will prevent air from leaking behind the shields and flushing accumulated gas. This will also keep the air quantity more constant along the length of the face.

Elapsed time:

During normal face travel, the convergence zone behind the shields is usually larger than those extending from the ribsides. Once mining is completed, or the face comes to a standstill, depending on the length of time, the convergence zone behind the face shortens considerably. Thus if a longwall face is down for a reasonable length of time, the gob will tend to consolidate closer to the back of the shields. This, as with the geologic factors, will affect the airflow distribution along the length of the face.

7.1.2. Airflow variations in cross-section on a longwall face.

The distribution of airflow across the width of the face is also of significance to methane and dust control. It is convenient to break the cross-section into four regions for analysis. The first being directly along the exposed face, the second, third and fourth respectively: over the armored face conveyor, over the travelling track and between the shield or chock legs. These regions are labeled A,B, C & D respectively on Figure (7.1). The optimal airflow with respect to gas and dust will be discussed for each of these regions.

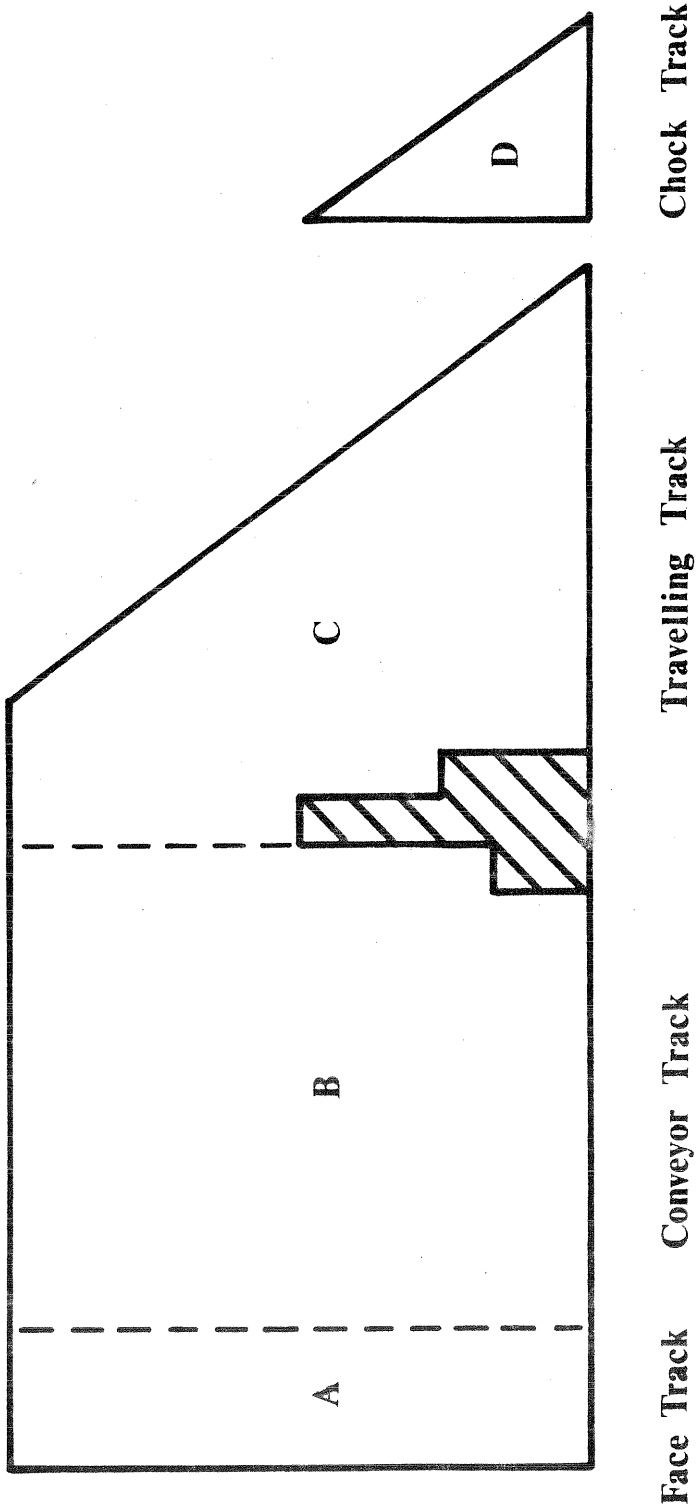

Figure 7.1 Delineation of regions in the cross-section of the longwall face.

7.1.2.1. Face track:

Conditions:

On a producing longwall face, methane is emitted during the actual cutting process from the newly exposed coal face and the fragmented coal. Frictional sparking at the machine pick point is, by far, the greatest cause of methane ignitions in modern mining. This occurs particularly when the picks strike pyrrhitic material in the seam or intersect harder strata in the roof or floor. Techniques of improving the ventilation within the cutting drum, and pick-face water flushing assist in reducing the risk. However, it is always important to maintain a good ventilating air current along the faceline to achieve rapid dilution of face-front gas.

Most of the dust produced during longwall mining results from the actual cutting of the coal rather than the breakage of the roof during shield or chock advance. Thus the largest source of dust is from the shearer during cutting.

Airflow constraints:

From a gas standpoint, the air quantity flowing next to the exposed face must be large enough to dilute the methane to well below its explosive range.

On the other hand, high velocities concentrated in this region, tend to increase the amount of dust suspended in the airstream. High velocity air, flowing over the shearer drum during cutting, tends to entrain more of the dust particles emitted from the coal cutting process.

Thus, the minimum required airflow in this region is governed by the methane emission rate, while the maximum airflow rate is limited by the dust constraint.

7.1.2.2. Conveyor track:

Conditions:

The armored face conveyor, the track through which the body of the shearer travels, transports broken coal to the stage loader. The increased surface area of the freshly broken coal enhances the desorption of methane. Thus, an increased concentration of methane is predominant along the conveyor between the shearer and the stage loader. This can cause accumulations of explosive mixture in the enclosed bottom flight track.

Fine particles of broken coal, being transported by the conveyor, may become suspended in the airflow if the relative velocity between the airflow and the conveyor is significant. The speed of the flights, the size distribution of the broken coal and the speed of shearer drum are all factors which affect the amount of suspended dust.

Airflow constraints:

As in section 7.1.2.1. the airflow in this region is constrained in quantity as well as in velocity. The airflow rate must be large enough to dilute the methane emitted from the broken coal, but should not be excessively large such that high relative velocities exist between the conveyor and the airflow.

7.1.2.3. Travelling track:

Conditions:

The travelling track is used by personnel to access the shearer, shield or chock control panels. During operation, personnel must release, advance and reset the roof support units behind the path of the shearer.

Airflow constraints:

The air flowing in this region must comply with the threshold limit values for suspended respirable dust ($2mg/m^3$) and gas (1% methane). Since this is an access way, the airflow rate must be large enough to dilute the concentration of respirable dust below this regulated value. In addition, for safety, excessively high velocities should be avoided so that large particles of dust do not remain suspended in the airstream. In general, the environmental conditions in this part of the face should be acceptable for personnel.

7.1.2.4. Chock track:

The amount of air flowing between the legs of the roof supports is a function of the clearance, the degree of consolidation behind the shields and the type of ventilation system.

If the gob is well consolidated directly behind the shields, i.e. the convergence zone is short, with either the sealed or the bleeder system, the airflow is more confined to the face line. This will cause more air to be distributed between the roof support legs than would be the case if a large convergence zone existed.

7.2. Measurements performed at the Thompson Creek No. 1 Mine, to determine the airflow distribution on the face.

7.2.1. Description of face.

Physical:

The longwall face, at the Thompson Creek No. 1 mine, measured 355 feet in length. The height of the face was about 7 feet while the width of the face varied with length. Before shutdown, the shearer had cut a 2′ deep shear 65 feet long beginning at the tailgate. The consequential change in cross-sectional area with length is illustrated on Figure (7.2).

The face was on a 30^{o} dip and advanced along the strike of the seam. The headgate airway, driven on strike, was parallel to, but down dip of the tailgate airway. The airflow was, therefore, ascentional along the face line.

Equipment:

The longwall face was equipped with the following:

- 350 ton Hemsheidt Troika shield support units
- Anderson-Boyes 500 hp - chainless shearer
- Dowty-Meco 150 hp twin outboard armored chain conveyor
- Dowty-Meco 150 hp stage loader.

At the time of the survey, the shearer was pulled away from the face for maintenance and parked at the tailgate end of the face line. Consequently, for the last 80 feet of the face line, the armored face conveyor was positioned away from the exposed face.

The shields, on the other hand, had not been advanced towards the face in this section, in order to provide better access to the shearer. Over the shearer, the shield slough plates were fully extended, while nearer to the headgate, the shield units were closer to the exposed face and the slough plates pressed vertically against the face.

Geologic conditions and effect of elapsed time:

At the time of the survey, the longwall face had been at a standstill for several weeks. Just before shut down, the face had encompassed a fault running at an angle of about 30^{o} to the face line. To maintain roof control in this region, bolts, dowels and styrofoam resin were utilized. In addition, it was apparent that the gob caved well up to the back of the shields. This was assumed to be caused by the combined effect of the fault and the standstill time.

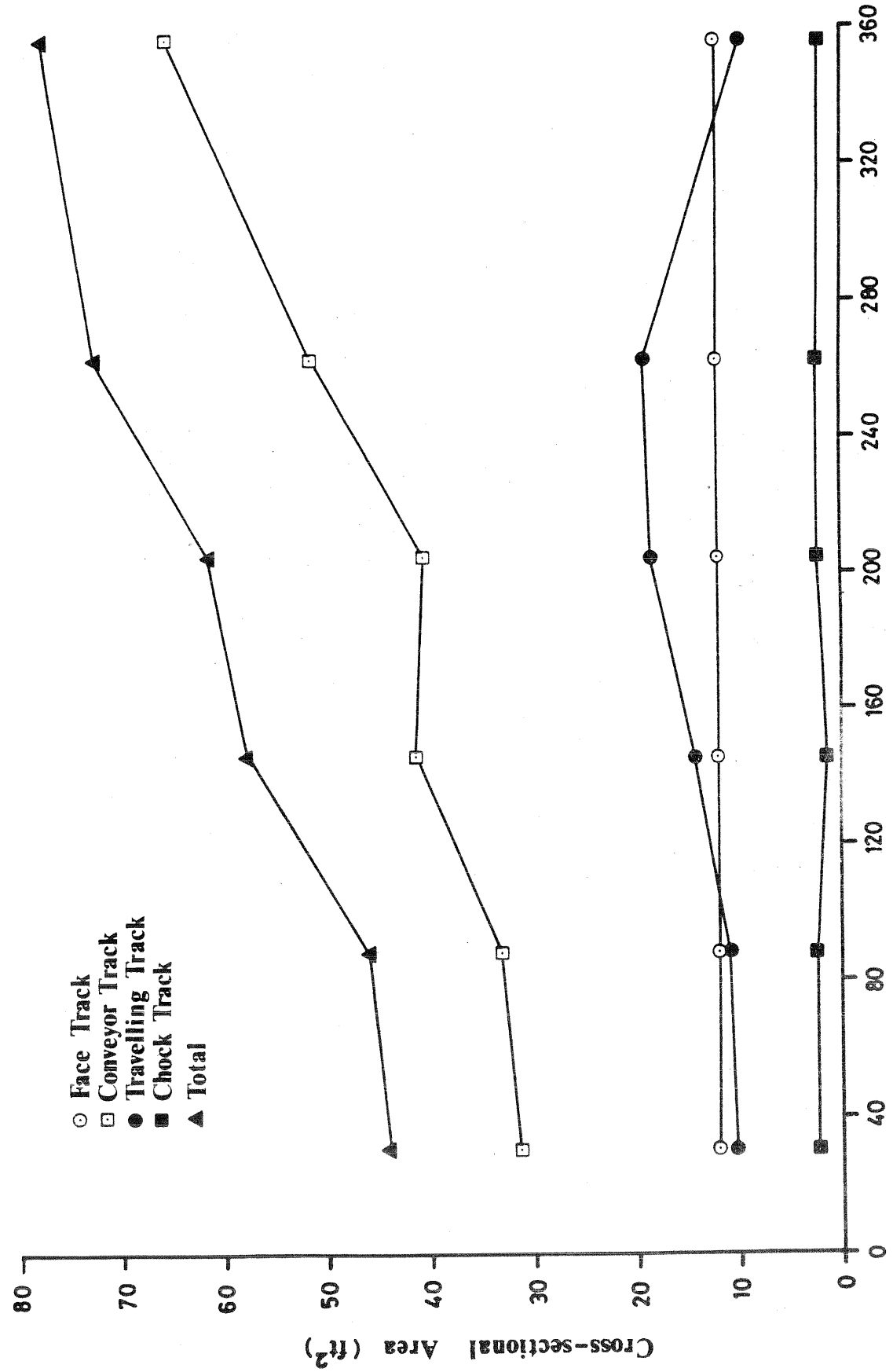

Figure 7.2 Variation of cross-sectional area along the face.

7.2.2. Description of air quantity survey along faceline.

Air quantity measurements were taken as part of the observations made to establish the variation in resistance along the face. Detailed measurements of velocity and area were taken at six cross-sections along the length of the face line. The cross-sections, measured from the headgate, were located at 30, 116, 174, 232, 290 and, at the top of the face, 355 ft.

At each cross-section, spot velocity measurements were taken with a calibrated medium-speed vane anemometer on an imaginary grid covering the cross-section. The measurements were taken with the observer downstream of the anemometer. This was accomplished by using an extension rod equipped with a swivel to keep the anemometer facing into the airstream. Depending on the size of the cross-section, 14-16 measurements were taken. Each measurement was repeated three times to check for consistency and was adjusted by a corresponding calibration correction.

Detailed cross- section dimensions were taken with a measuring tape. Each cross-section was drawn in a field book and each dimension was recorded. In addition, the location and magnitude of each velocity measurement were also recorded. A scale drawing then allowed velocity contours to be drawn. These are shown on Figures (7.3 to 7.5).

7.3. Distribution of airflow on the face

This section describes the variation in total airflow, and the distribution of this airflow, along the length of the longwall face at the Thompson Creek No. 1 mine.

7.3.1. Variation in total flow rate along face line.

Using the scale drawings (Figures (7.3-7.5)), the area between each successive pair of velocity contours was established and multiplied by the mean of the contour velocities to give the airflow occuring within that velocity range. The sum of all these gave the total volume flow rate through the cross-section. The results for each cross-section are shown in Table (7.1).

The variation in total volume flow rate with face length is shown graphically on Figure (7.6). This figure indicates that the volume flow rate increases near the center of the face line by about 10%. The volume flow rate then decreases at the return end of the face to a value equivalent to 68% of the intake quantity.

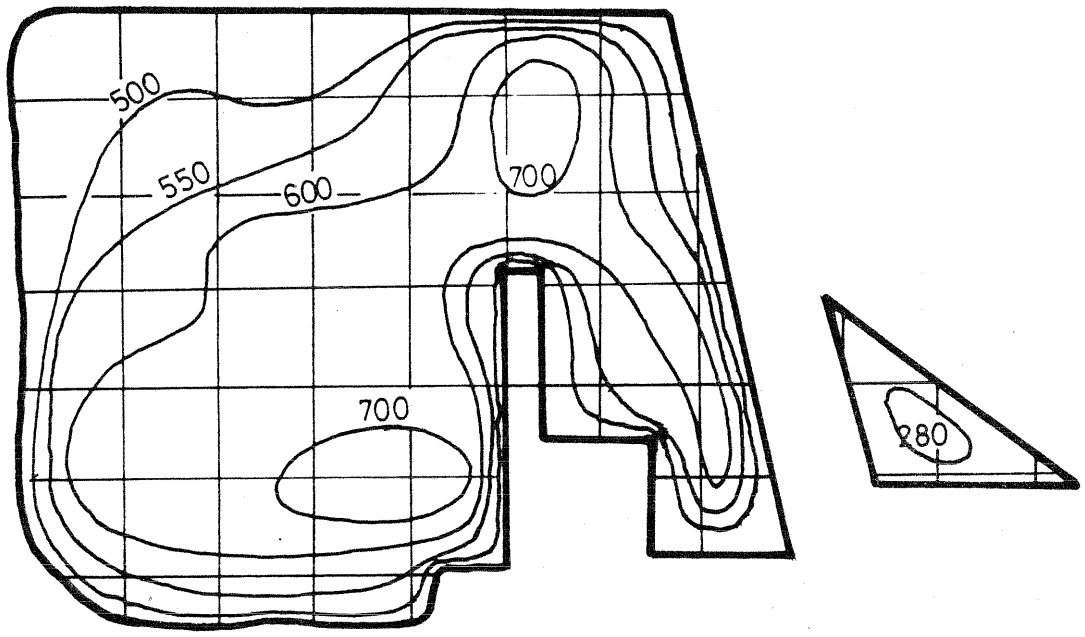

(a) 30 ft from main gate

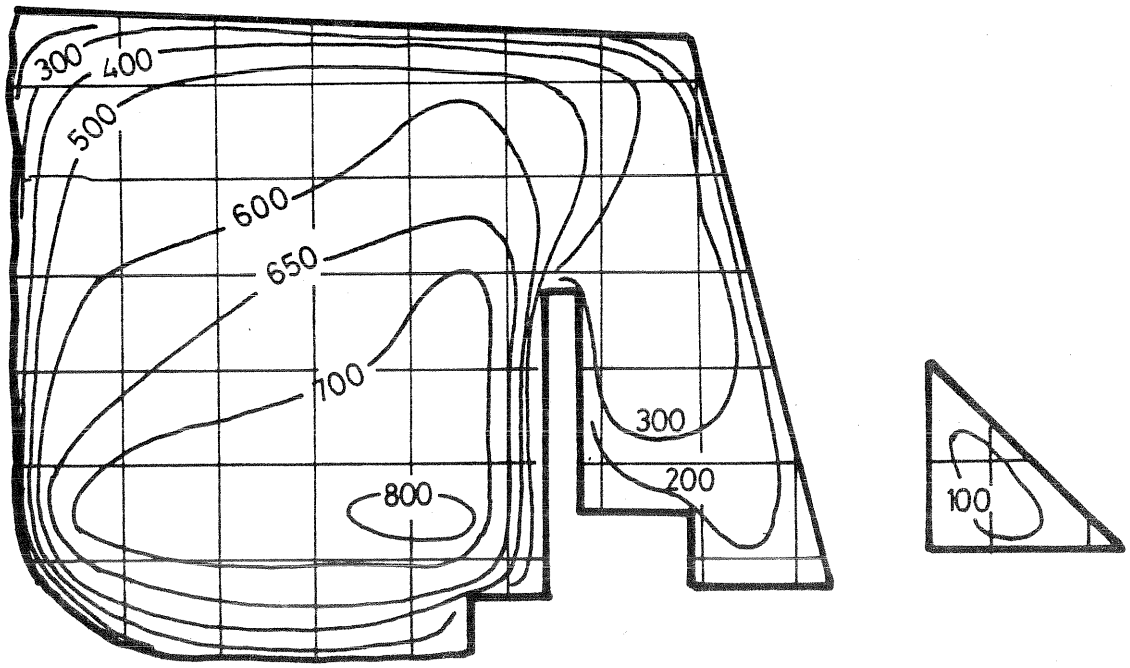

(b) 116 ft. from maingate

Figure 7.3 Velocity contours given in ft/min at cross-sections 1 and 2 along the face.

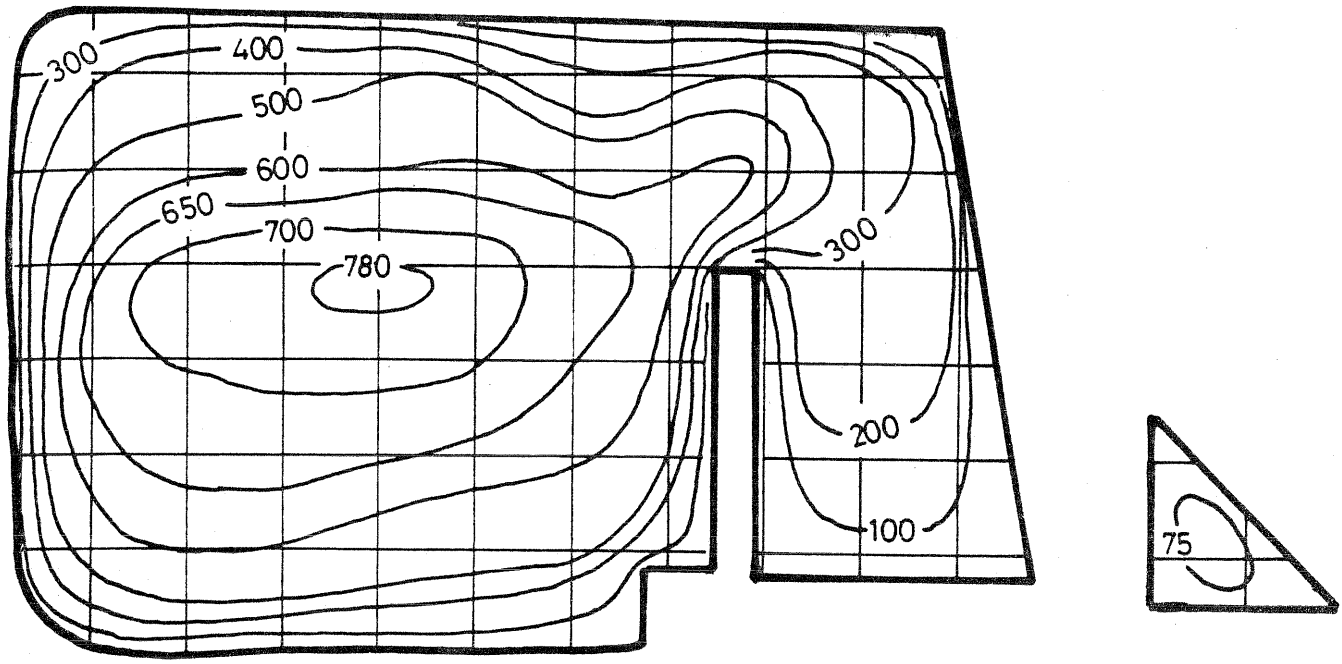

(c) 174 ft from main gate

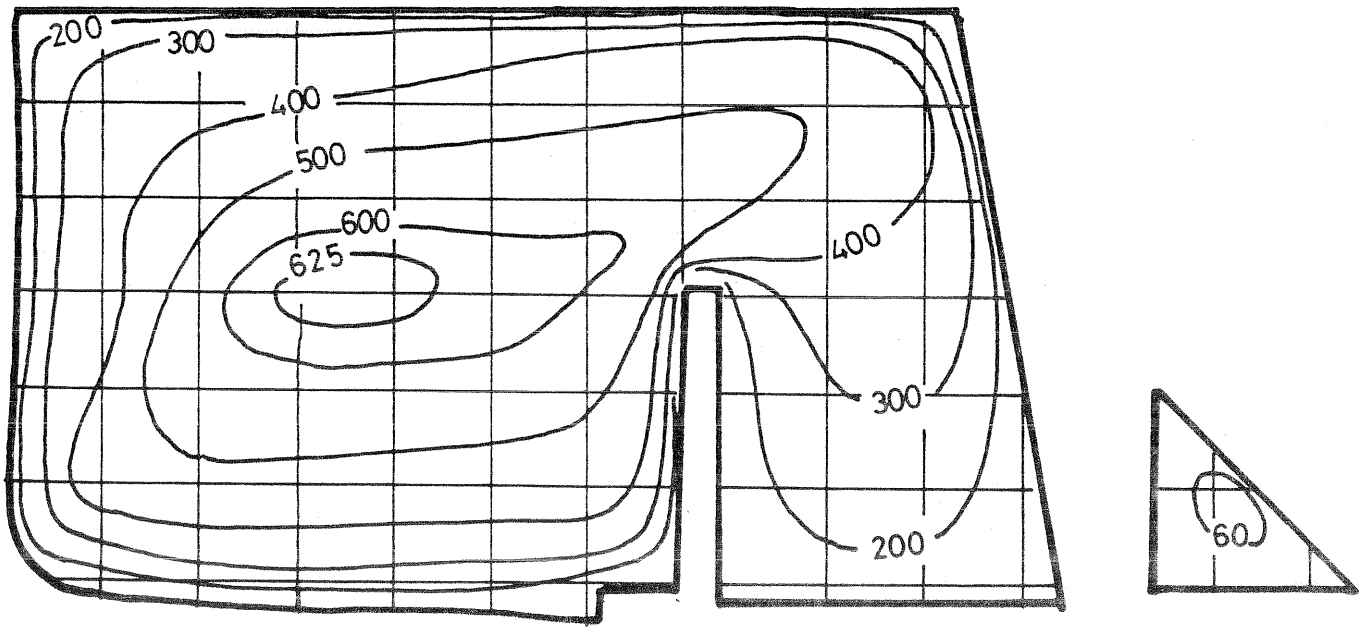

(d) 232 ft from main gate

Figure 7.4 Velocity contours given in ft/min at cross-sections 3 and 4 along the face.

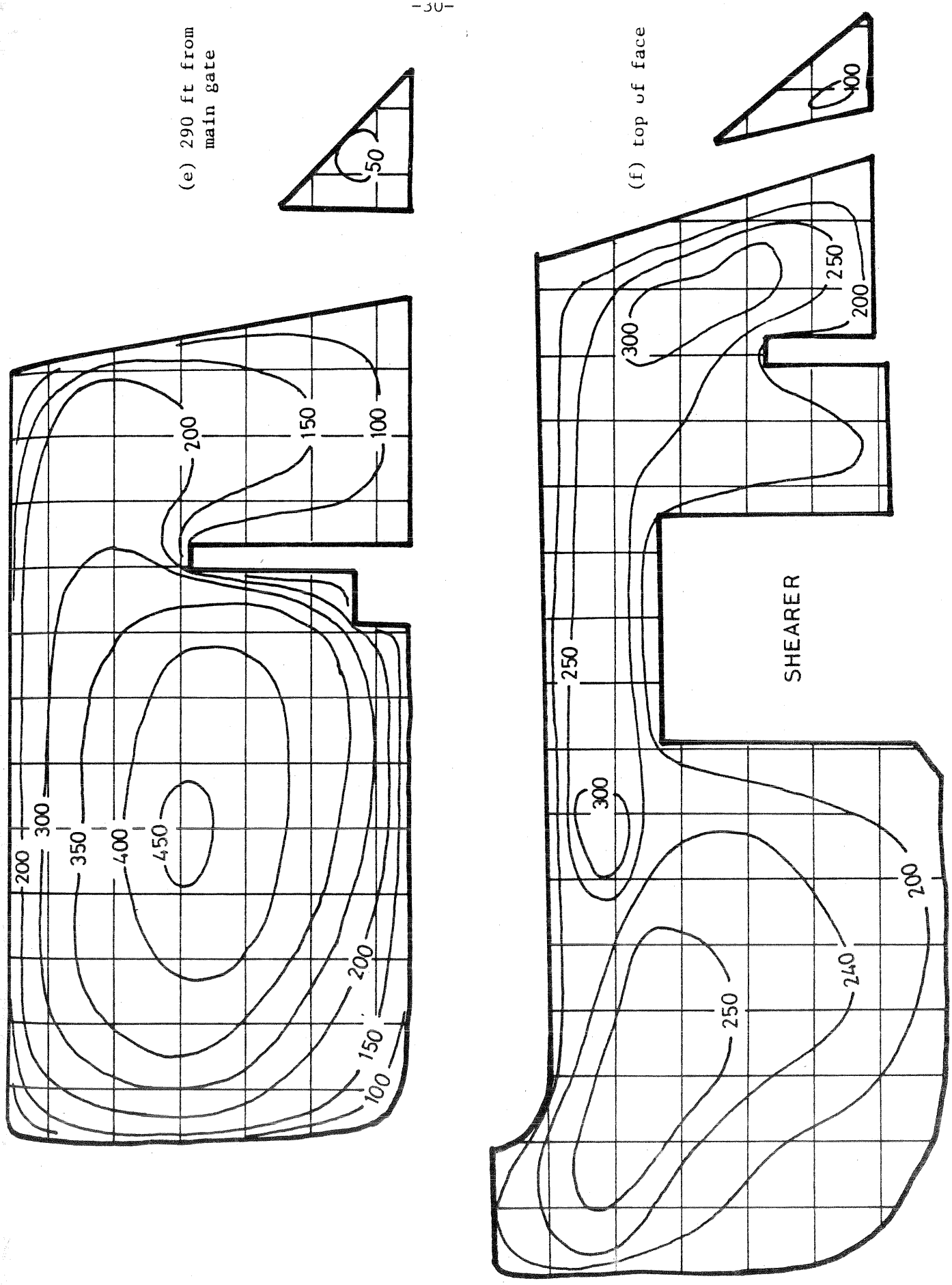

Figure 7.5 Velocity contours given in ft/min at cross-sections 5 and 6 along the face.

Mean vel. ft/min	cross-section 1			cross-section 2			cross-section 3			cross-section 4			cross-section 5			cross-section 6		
	ft^2	Q	%	ft^2	Q	%	ft^2	Q	%	ft^2	Q	%	ft^2	Q	%	ft^2	Q	%
800	2.43	1724	7.1	0.54	430	1.8												
780							0.52	406	1.5									
750				7.46	5597	23.1												
740							5.30	3918	14.6									
710																		
675				6.47	4364	18.0	7.36	4965	18.6									
650	14.00	9102	37.6															
625				6.99	4366	18.0	7.35	4592	17.1	1.03	642	2.7						
612.5										3.14	1923	8.2						
575	10.09	5799	24.0															
550				7.96	4375	18.0	10.16	5587	20.9	12.19	6703	28.5						
525	6.83	3586	14.8															
450				4.27	1922	7.9	6.61	2973	11.1	14.45	6500	27.6	0.97	434	2.2			
425													9.09	3861	20.0			
400	8.93	3572	14.8															
375													12.77	4787	24.8			
350				5.93	2076	8.6	5.86	9049	7.6	12.10	4234	18.0						
325													10.56	3433	17.8			
300																3.13	939	5.7
260																16.51	4293	26.1
250				2.87	717	3.0	5.92	1479	5.5	9.12	2281	9.7	13.86	3466	18.0			
245																10.71	2623	15.9
225																22.39	5037	30.6
200	2.00	400	1.7															
175													11.02	1928	10.0			
150				1.75	263	1.0	3.07	461	1.7	7.64	1144	4.9				22.69	3404	20.7
125													7.67	959	5.0			
80				2.00	160	0.6	3.36	261	1.0							2.00	160	1.0
75													4.70	353	1.8			
60							2.00	120	0.4									
48										2.00	96	0.4						
40													2.00	80	0.4			
Totals	44.28	24183	100.0	46.24	24270	100.0	57.51	26811	100.0	61.67	23523	100.0	72.64	19301	100.0	77.43	16456	100.0

Table 7.1 Airflow analysis of velocity contours shown on Figures (7.3-7.5). Distances are measured from the bottom of the faceline.

Figure 7.6 Variation of airflow along the face.

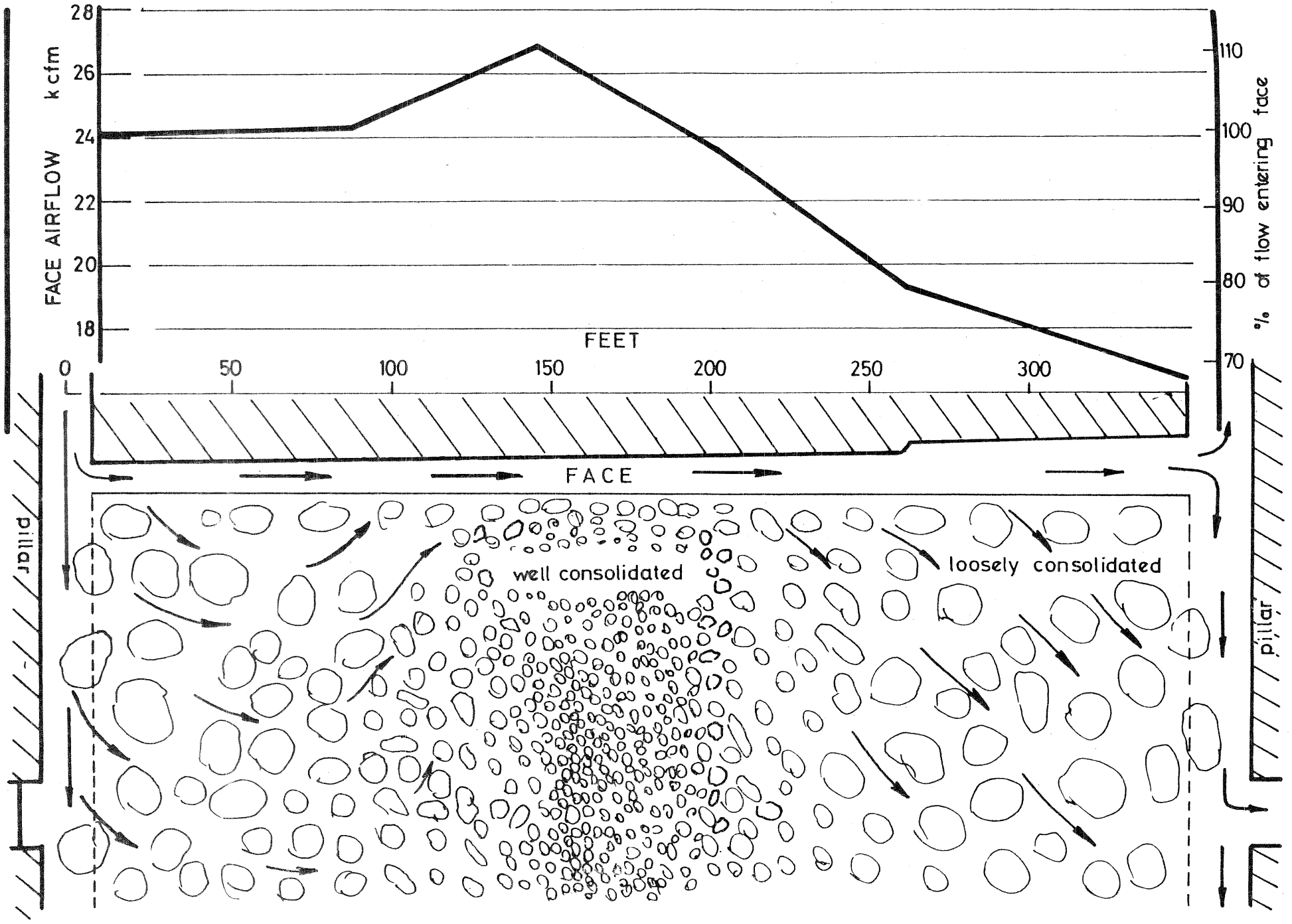

From mass conservation, if no leakage occurred along the face line, the volume flow rate would remain constant. Thus, an increase or decrease in volume flow rate indicates that leakage interactions occur between the face line and the gob.

For the longwall face at the Thompson Creek mine, air leaked from the gob into the face line beginning at about 80 feet from the intake. Progressing past the center part of the face, air leaked from the face line to the gob in increasing magnitudes.

The leakage from the gob to the face line, occuring before the center point of the face, was caused by the reduced convergence zone behind the shields. Both the fault zone and the idle time of the face caused the center of the gob to cave more effectively directly behind the shields. This forced some of the air, leaking through the gob from the bleeder intake, to flow back into the face and maneuver around this highly consolidated center zone.

The leakage from the face line to the gob, occurring along the second half of the face, was a direct consequence of the bleeder ventilation system. The bleeder return, located along the gob in the return side of the panel, drew air away from the face to keep accumulated waste gas from migrating onto the face line. Thus, the decrease in volume flow rate, observed along the second half of the face, indicated that the bleeder system was working effectively in this area.

7.3.2. Distribution of airflow in cross-section along face.

To analyze the distribution of airflow across the face, the cross-section was divided into four regions: 12 ft^2 next to the exposed face, over the armored face conveyor, over the travelling track and between the chock legs. For the distribution analysis, the air flow through each region was determined as a percentage of the total airflow at each cross-section. In addition, average velocities through each region were calculated for every cross-section along the face. (Appendix I). Values of volume flow rate, % volume flow rate and average velocity, for each region, are shown tabulated in Table (7.2) and are plotted for every measured cross-section along the face on Figures (7.7 - 7.11). Included on the distribution and the flow magnitude graphs, are averages and standard deviations from the mean.

7.3.2.1. Air distribution analysis:

The distribution of the airflow, as it travelled along the face line, may be analyzed with the aid of Figures (7.7-7.11). The following sub-sections describe the airflow distribution at each measured cross-section, the shifts in distribution along the face line and the cause of the variations.

Table 7.2

Distribution of airflow in cross-sections along face.

Location	Cross-Section	Quantity kcfm	Velocity fpm	% of total
A	1	6.39	532.7	26.25
B	1	11.7	593.5	48.07
C	1	5.71	565.1	23.46
D	1	0.54	229.8	2.22
		24.34		100.00
A	2	6.82	568.3	28.13
B	2	13.58	642.7	56.00
C	2	3.62	335.0	14.94
D	2	0.226	98.2	0.93
		24.25		100.00
A	3	6.11	508.9	22.77
B	3	17.18	586	64.03
C	3	3.41	239.85	12.72
D	3	00.13	65	00.48
		26.83		100.00
A	4	4.13	344.2	17.55
B	4	13.55	470.9	57.57
C	4	5.73	306.2	24.35
D	4	00.126	57.3	00.53
		23.54		100.00
A	5	2.73	227.08	14.14
B	5	13.3	338.9	68.89
C	5	3.18	165.5	16.48
D	5	00.095	43.2	00.49
		19.305		100.00
A	6	2.33	194.1	14.16
B	6	11.6	217.5	70.47
C	6	2.34	236.9	14.22
D	6	00.19	86.3	01.15
		16.46		100.00

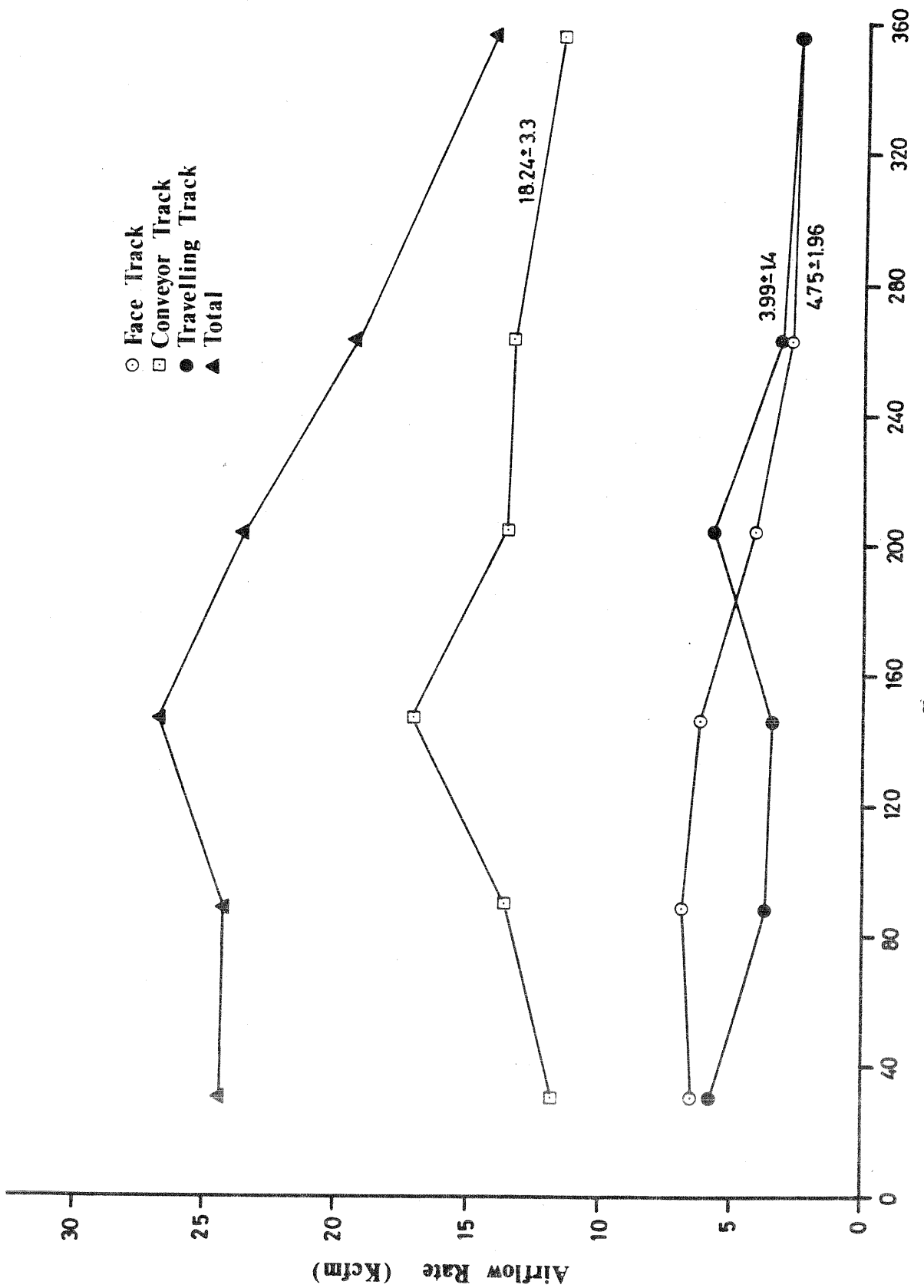

Figure 7.7 Airflow in face track, conveyor track, travelling track and entire cross-section, as a function of face length.

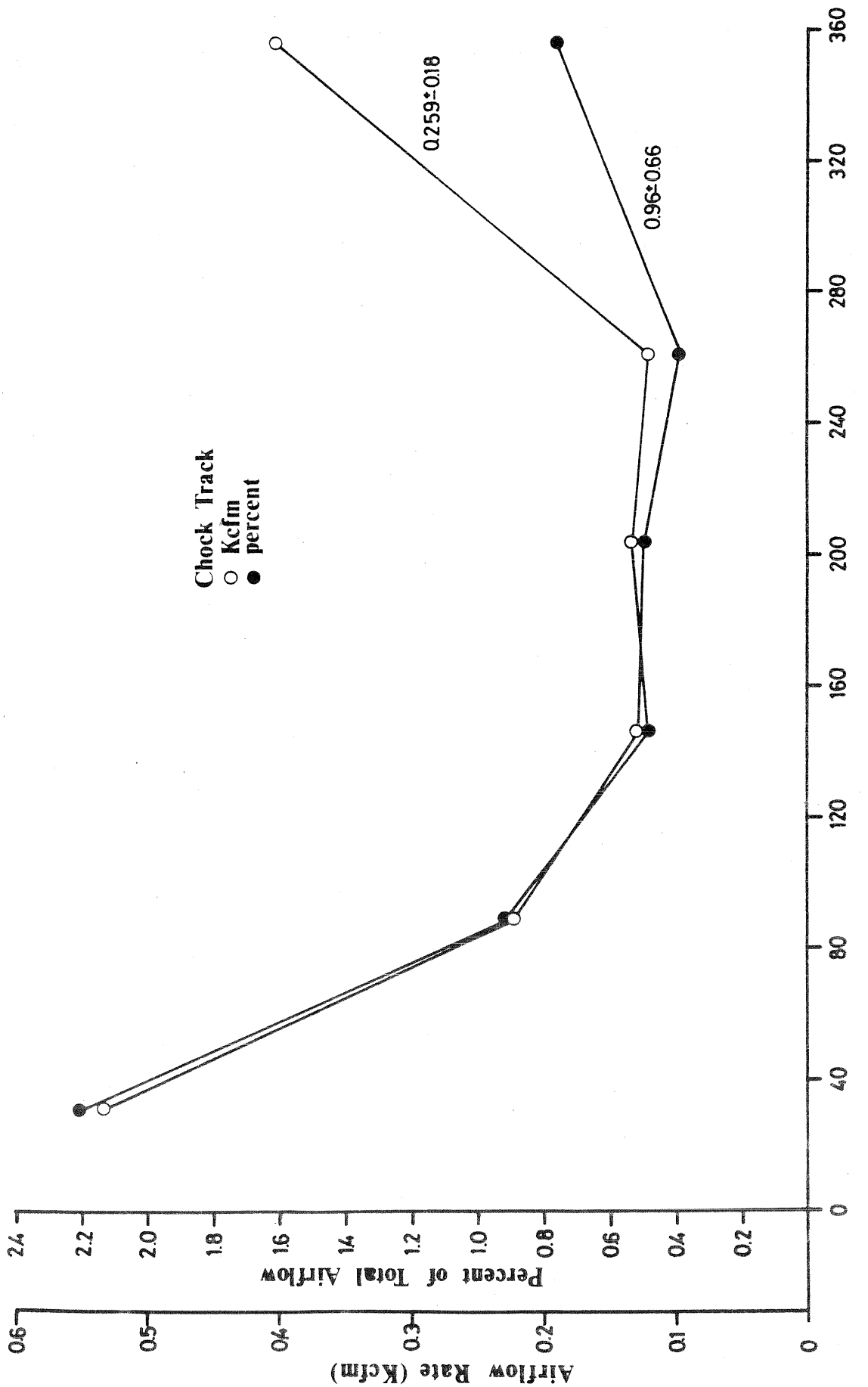

Figure 7.8 Airflow rate and percent of total air flowing in the chock track.

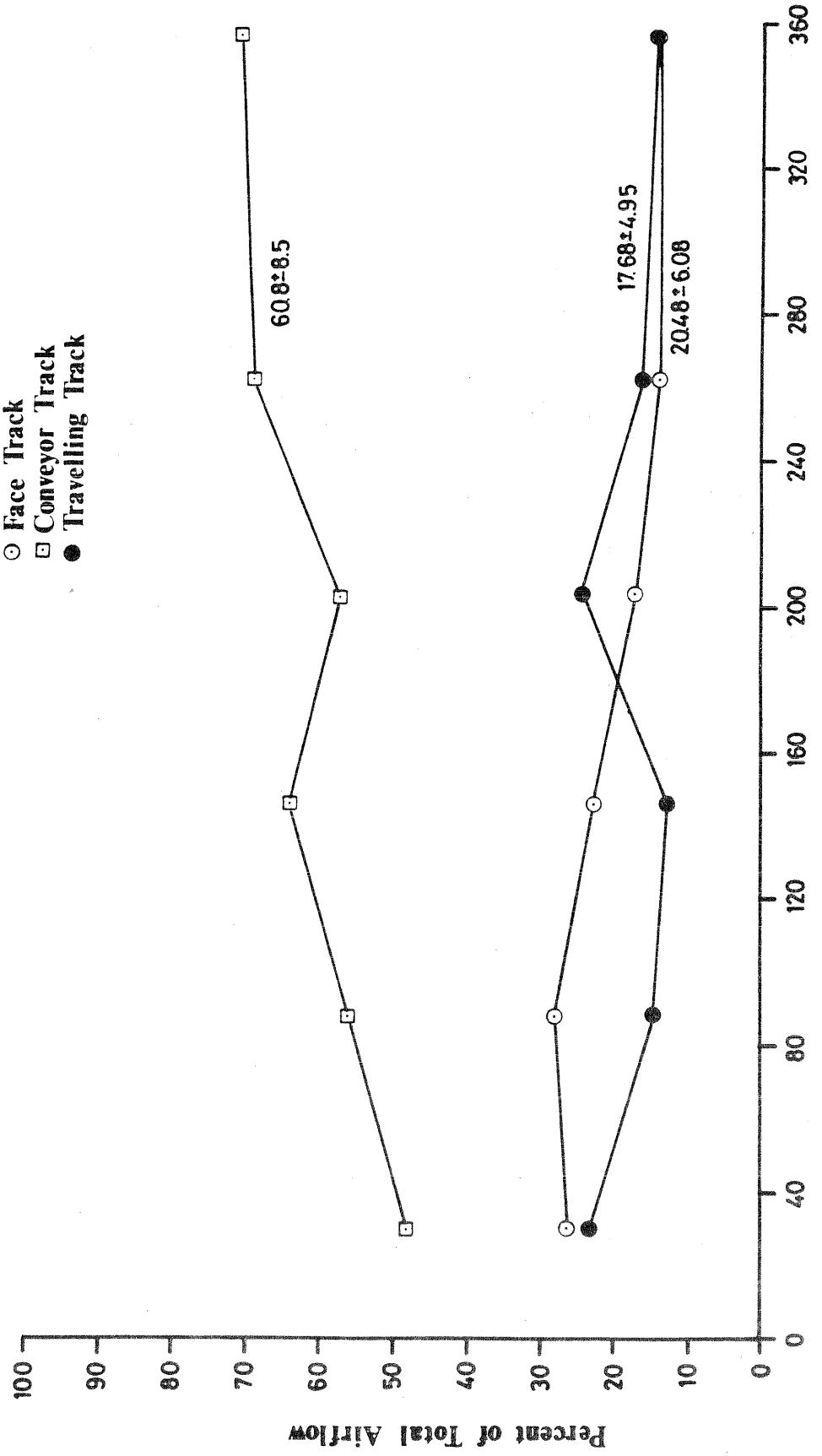

Figure 7.9 Percent of total air flowing in face track, conveyor track and travelling track.

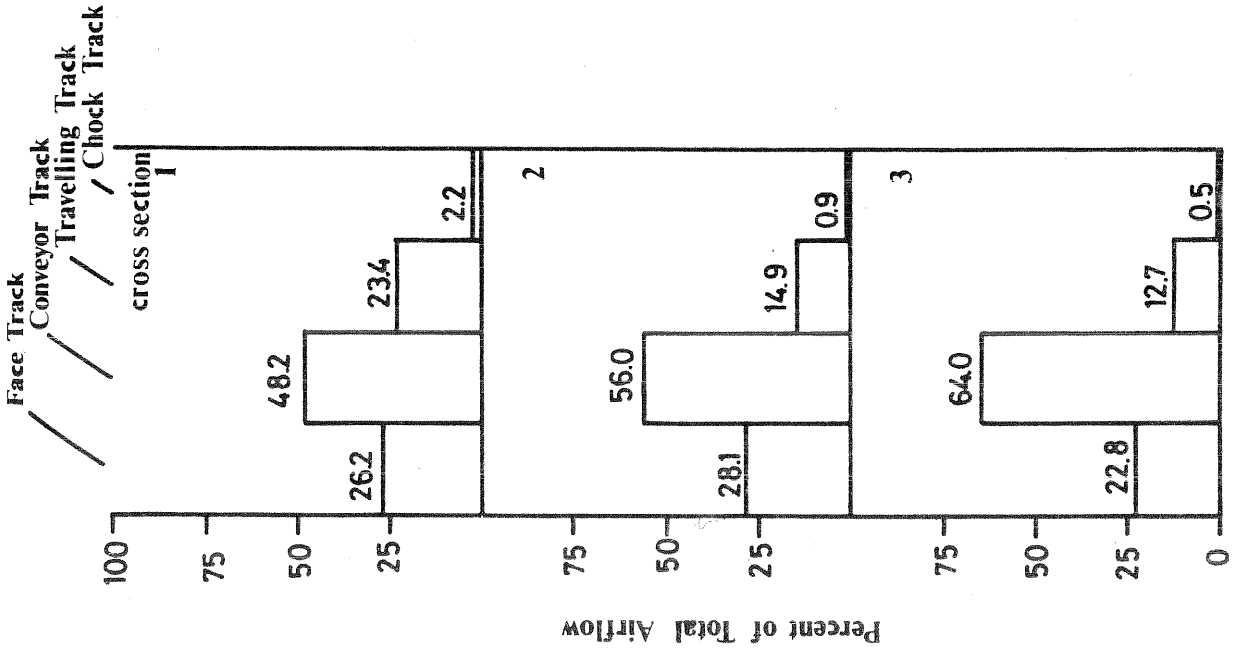

Figure 7.10 Histograms showing airflow distribution at each measured cross-section.

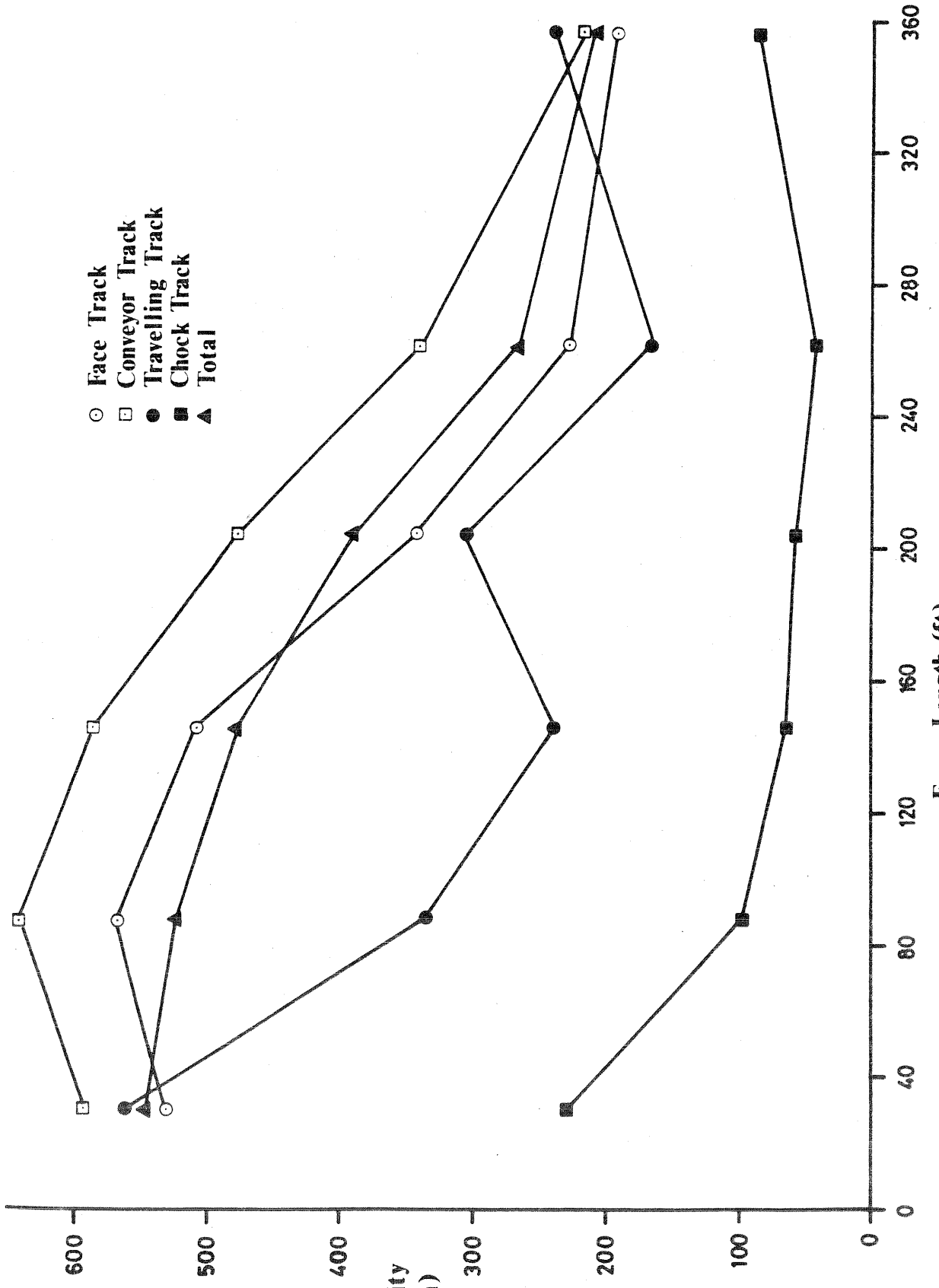

Figure 7.11 Variation of average velocity, for each cross-sectional region, with face length.

Cross Section 1, 30 Feet from Maingate

Near the maingate, as illustrated in Figure (7.10) for cross-section 1, the airflow is distributed symmetrically about the armored face conveyor. About fifty percent of the air flows directly over the armored face conveyor, while the other fifty is distributed fairly evenly over the travelling track and next to the face. The 2.2% flowing between the shield legs is negligible relative to that flowing in the other regions. However, compared to the other measured cross-sections, this 2.2% is quite high. This trend is seen on Figure (7.8), where the percentage of air flowing in the region decreases steadily, levels out and then increases towards the end of the face line.

Cross-Section 2, 116 feet from Maingate

At cross-section 2, located 116 feet from the main gate, the airflow is no longer symmetrically distributed over the armored face conveyor but tends more towards the face. This skewed distribution is shown on Figure (7.10). The increase in percentage of air flowing next to the face and over the armored face conveyor, and the subsequent decrease of that over the travelling track, between cross sections 1 and 2, is evident on Figure 7.9.

This shift in distribution, between the first two measured cross-sections, is also evident from the velocity profiles; Figure (7.3). The velocity contours, for cross-section 1, are widely distributed. The contours are centered around two peak velocity zones located over the armored face conveyor and over the travelling track. The result of this is a more symmetrical distribution of airflow in the cross-section. On the other hand, for cross- section 2, the velocity contours are centered around a single peak velocity zone, located directly over the armored face conveyor. This causes the airflow to exhibit a much more localized type of distribution as indicated on Figure (7.10).

Cross-section 3, 174 feet from Maingate

At this location, the airflow distribution, shown on Figure (7.10) is still skewed towards the face and is even more localized over the armored face conveyor. From Figure (7.7), the increase in flow over the armored face conveyor, between cross-sections 2 and 3, coincides well with the increase in total flow between these cross sections. It is interesting to note that the amount of air flowing near the face and over the travelling track, remains fairly constant between cross- sections 2 and 3. This indicates that the additional

air, leakage air in this case, is distributed mostly to the region over the armored face conveyor while the proportion of air between the travelling track and the region near the face, remains constant.

Cross-section 4, 232 feet from Maingate

The airflow distribution at this cross-section, unlike that at the previous three cross-sections, is skewed towards the gob. This shift of air flow toward the travelling track, is seen on Figure (7.10) and (7.9). Figure (7.9) shows distinctly the transfer of flow from the conveyor track to the travelling track between cross-sections 3 and 4.

Thus far, proceeding from the headgate end of the faceline, the airflow distribution has changed from symmetrical, to skewed toward the face and then after 232 feet, it has changed to skewed towards the gob. These skewed distributions are caused mainly by the changes in the cross-sectional area of the travelling track (Figure 7.2), but may also be influenced by the pressure differences between the gob and the face line.

At cross-section 4, the pressure in the adjacent gob, must have been less than the pressure on the face line. This pressure difference caused air to leak from the face line into the gob which in turn drew the airflow distribution towards the gob. This may have contributed towards the skewed distribution seen on Figure (7.10).

Cross-sections 5 and 6, 290 & 350 feet from Maingate

In both these cross-sections, the airflow was concentrated heavily in the armored face conveyer region, but was distributed fairly evenly in the region near the face and over the travelling track; Figure (7.10).

The total airflow, on the other hand, still decreased between cross-section 5 and 6 due to leakage from the face into the gob. However, the symmetrical distribution of the air at these cross-sections was most probably caused by the greater cross-sectional area combining with the reduced airflow to give significantly lower velocities.

7.3.2.2. Conclusions derived from analysis:

Based on the Thompson Creek No. 1 mine analysis, the following conclusions, regarding airflow distribution on a longwall face of a mine ventilated with a bleeder system, can be drawn.

- More than 50 percent of the air flowing along a face is distributed in the region over the armored face conveyor.

- The percentages of air flowing over the travelling track and near the face are subject to variations, but on the average remain fairly constant along the face line.

- The variations in distribution are affected by changes in cross-sectional area and pressure gradients between the gob and the face line. These pressure gradients are a direct consequence of the conditions in the gob. Since the gob at the Thompson Creek No. 1 mine was well consolidated closely behind the shields around the center of the face these pressure gradients were relatively large. With a uniform cross-section and fault free conditions, pressure gradients between the face line and the gob, would be smaller and thus the air distribution would vary less along the length of the face.

- The variations in total volume flow rate are caused by leakage air which is also a function of the conditions in the caved gob region as well as the pressure differentials that exist between the face and the bleeder airways.

- The percentage of air flowing between the legs of shield roof support units is negligible relative to the air flowing in other regions.

8. LONGWALL FACE RESISTANCE

8.1. Background

One of the vital sets of data required for the analysis of mine ventilation networks, and for the prediction of airflows in projected layouts, is the resistance, R, of each branch in the network. This is used in the general law

$$p = RQ^n \qquad (8.1)$$

in order to quantify the relationship between the air volume flow, Q, and the frictional pressure drop, p, along the airway. The logarithmic index, n, is normally 2 for fully turbulent airflow and reduces to unity at laminar flow. Section 9 of this report confirms that the Square Law (n=2) holds for the longwall face investigated at the Snowmass Mine.

For existing flow paths, and where the airflows and pressure drops are sufficiently high for sensible measurement, the most reliable means of ascertaining resistance is to measure p and Q, then, assuming the Square Law, the resistance is given by

$$R = p/Q^2$$

In the case of planned, but as yet unconstructed airways, or where airflows are too low for dependable measurements, the resistance may be calculated from

$$R = \frac{k\ L\ O}{52A^3} \qquad (8.2)$$

where k = friction factor ($\times 10^{10}$ lbf min^2/ft^4)
L = length (ft)
O = perimeter (ft)
and A = cross sectional area (ft^2)

Whilst the literature contains lists of k factors for various types of shafts and airways, there is very little data available to assist in assessing the resistances of longwall faces. There are two reasons for this. First, it is normally difficult on an operating longwall to make the measurements required to establish a reliable value of resistance to airflow or k factors. Second, the resistance of a longwall is caused not only by the face itself but also by shock losses at face ends and constrictions at machine sites.

• This section of the report employs British Imperial Units owing to the large amount of observed data involved, all of which was obtained from instruments calibrated in those units.

During the field observations at Snowmass, detailed measurements on the longwall face allowed the components of resistance to be identified and quantified. This section of the report describes the measurements taken to establish face resistance, the analysis of that data, and proposes a method of evaluating the resistance of other longwall faces.

8.2. Experimental Procedure

Over the lower half of the face length at Snowmass, the armored flexible conveyor was pushed close to the coal face and the conveyor jacks fully retracted. The distance from the coal front to the front legs of the chocks varied between 7.5 and 10 ft. Face conditions were good. About half way along the face, however, resin grout injection had been used to stabilize the ground around a small fault in the seam. Above that point, the face had become wider due to sloughing from the coal front. The uneven surface left on the face combined with the broken coal to give an aerodynamically rougher flowpath. The shearer was parked at the upper end of the face (tailgate) where the width of the face had increased to 14 ft.

The test commenced by erecting a brattice in the lower bleeder airway (Fig. 4.1) and opening the brattice in the maingate leading to the face. These steps were taken to produce a relatively high airflow along the face line and, hence, to improve the accuracy of airflow and pressure drop measurements. More than 50 per cent of the air supplied to the panel still entered the caved area from the lower bleeder airways. Nevertheless, as a safety precaution one of the team patrolled the cross-cuts at the top edge of the caved waste throughout the day, monitoring methane concentrations. Most of these cross-cuts showed 0.1 or 0.2 per cent methane. Higher concentrations were found towards the starting-off line of the face. The methane readings and their locations are shown on Figure (10.2). There was no significant increase in gas concentration in any one cross-cut during the day.

Stations A1 through A10 were set up at locations indicated on Figure (8.1). The face was divided into 58 ft. lengths with shorter increments where the face widened and across the shearer. Additional lengths of 70 ft. in the conveyor road and 58 ft. in the upper haulage road were included in order to determine the resistance of these airways close to the face ends.

Airflows were measured at midpoints between stations by the "point traverse" method. This involved taking anemometer readings at a number of points on a grid covering the cross-section of the measuring station. The readings enabled velocity contours to be established in a manner similar to those illustrated in Section 7.2. These, in turn, were used to determine the volume flow of air.

The frictional pressure drops between stations were determined by

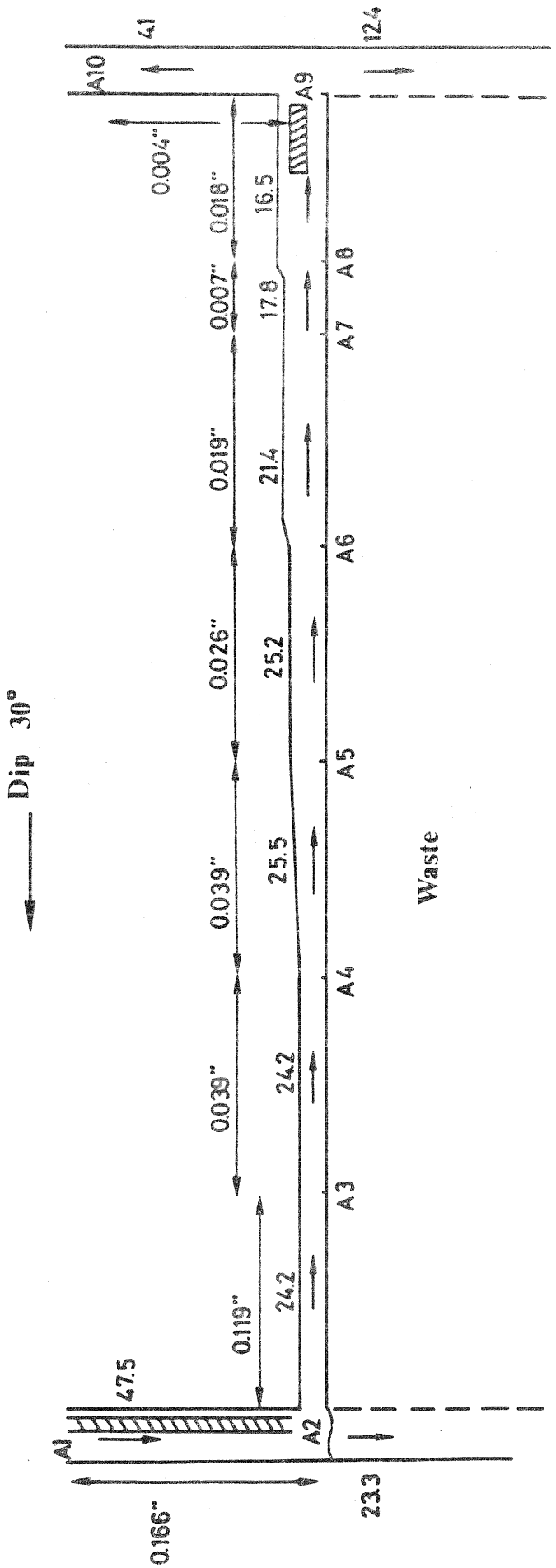

Figure 8.1 Location of stations and measured airflows (kcfm) and pressure drops (inches of water) at each station.

the gauge and tube technique. A length of 1/8 inch internal diameter plastic tubing was laid out between each pair of consecutive stations in turn. The ends of the tubing were each attached to the total head connections of a 2 ft pitot tube. A 0 to 0.25 inch water gauge magnehelic diaphragm gauge was connected into the line in order to measure the pressure difference between the two pitot tubes.

The pressure tubing was suspended from roof supports and tested for pressure integrity at each setting. The pitot tubes were held facing into the airflow. Care was taken to prevent the bodies of the observers from affecting the readings, a precaution that is particularly important in the cramped confines of a longwall face. The observers holding the pitot tubes lay flat on their backs on the face conveyor during each reading and traversed the pitot tubes slowly over the central part of the cross-section, but maintaining the orientation of the pitot head into the airflow. This technique avoided spurious readings arising from any anomolous local turbulence.

For each reading, the magnehelic gauge observer sited himself between a pair of chocks, well out of the main airstream - again in order not to affect the airflow or associated pressure drop. The pressure gauge was observed until a stable reading was established. All anemometer and magnehelic readings were corrected according to the relevant calibration.

8.3. Test Results

The measured pressure drops and corresponding airflows are shown in Table 8.1. Pressure drops are given in thousandths of an inch of water gauge (milli inch w.g.) and airflows in thousands of cubic feet per minute (kcfm). The corresponding resistances, calculated from the square law have units of

$$R = \frac{p}{Q^2} \quad \frac{\text{milli in. w.g.}}{(\text{kcfm})^2} \quad \text{or} \quad \frac{(\text{in.w.g.}) \times 10^{-3}}{(\text{ft}^3/\text{min})^2 \times 10^6}$$

$$= \frac{(\text{in.w.g.})}{\text{ft}^6} \ \text{min}^2 \times 10^{-9} \qquad (8.3)$$

This is sometimes called the Practical Unit (P.U.) of mine resistance as it derives directly from the square law without the need for any multiplying constant.

Station From	To	Length ft	Pr. Dp. m.in.w.g.	Airflow kcfm	Resistance P.U.	Resistance P.U./ft	Comments
A1	A2	70	166	47.523	0.0735	0.00105	Stageloader & Electrics
A2	A3	58	119	24.181	0.2035	0.00351	Maingate end of face
A3	A4	58	39	24.230	0.0664	0.00114	
A4	A5	58	39	25.536	0.0598	0.00103	
A5	A6	58	26	25.170	0.0410	0.00071	
A6	A7	58	19	21.415	0.0414	0.00071	
A7	A8	20	7	17.797	0.0221	0.00111	Face widens
A8	A9	45	18	16.452	0.0665	0.00148	Shearer
A9	A10	58	4	4.120	0.2356	0.00406	Tailgate

Table 8.1. Resistances on the longwall face

In order to compare resistances for the various sections of the face, Table 8.1. also gives the resistances in P.U. per foot length. These values are further illustrated on Figures (8.2a) and (8.2b). The peaks of resistance at the face ends show very clearly. These arise from the concentration of equipment causing obstruction to the airflow, and from the shock loss as the airflow changed direction at the junctions of airway and face.

The larger cross-sectional area through the upper half of the face is revealed as a lower resistance per unit length. The slight shock loss as the face widens in section A7-A8 shows as a small increase in resistance. There is a further rise due to the presence of the shearer at the upper end of the face, but this is not so great as would normally be expected from such a major obstruction. The reason for this was that the face was much wider and the cross-sectional area considerably larger at the shearer than along the rest of the face (see also Figure 7.5).

The cumulative increase in resistance from a point 70 ft. outbye the maingate end of the face to a point 58 ft. outbye the tailgate end was 0.81 P.U. A summary of the breakdown is given in Table 8.2.

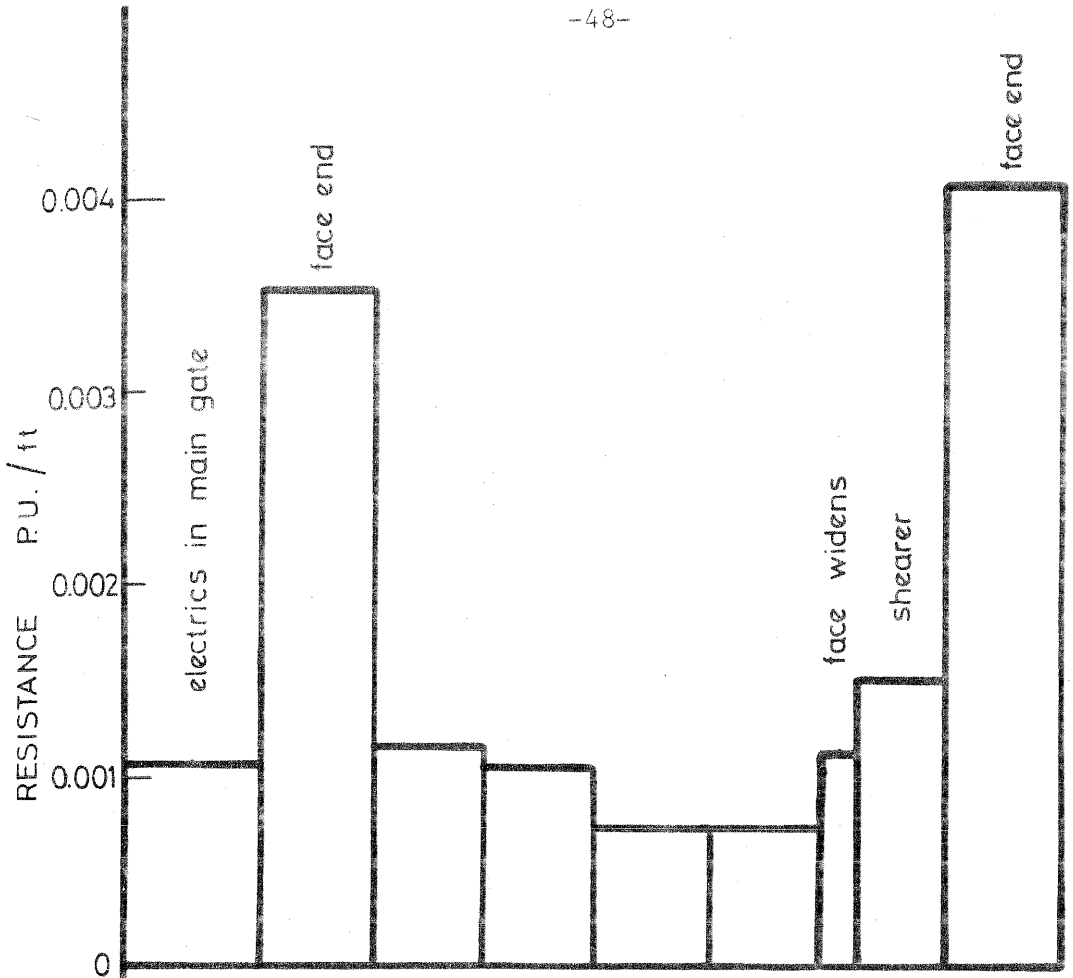

Figure 8.2a

Variation of resistance along the face.

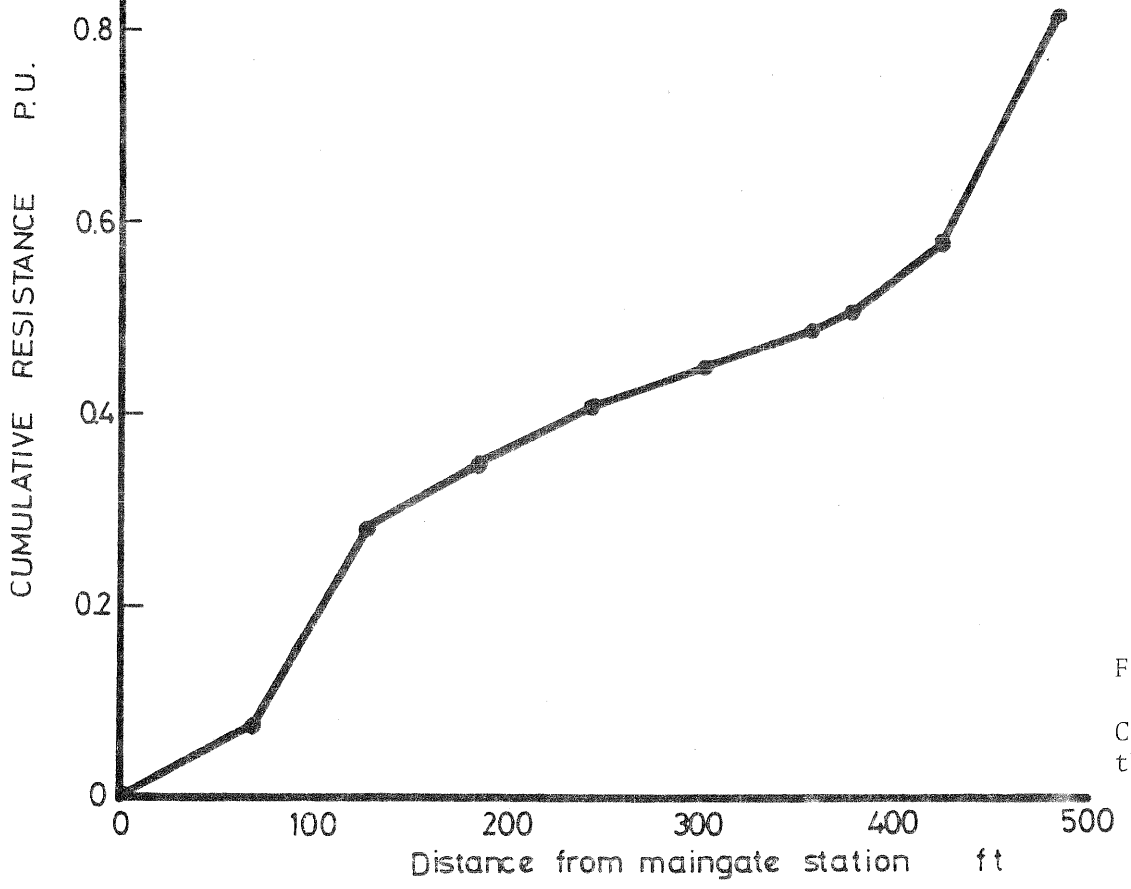

Figure 8.2b

Cumulative resistance through the face.

	Resistance P.U.	Percentage of total
Stage loader/electrics	0.0735	9.1
Face ends and tailgate	0.4391	54.2
Face line	0.2972	36.7
	0.8091	100.0

Table 8.2. Summary of components of face resistance

8.4. Estimation of the Resistance of a Longwall Face

The results given in the previous section show that more than half the total resistance occurs at the face ends. It is clear that previous practices of estimating the resistance of a longwall face simply as a function of length and height could give misleading results. Shock losses must be assessed separately and the appropriate resistance combined with the face line resistance.

In this section of the report a more detailed analysis of the Snowmass face resistance is undertaken and a method is proposed for the estimation of the resistance of other longwall faces. This involves assessing the resistance of (i) the unobstructed face line (ii) face ends and (iii) shearer or other power-loader.

8.4.1 Face line friction factors:

The four 58ft sections between stations A3 and A7 (Figure 8.1) represented an unobstructed face line bounded by the shield supports, the armored conveyor and the coal face. The upper half of this 232 ft length had a greater cross-sectional area but rougher conditions due to sloughing of the coal face.

The resistance of any airway may be expressed in American Units as

$$R = \frac{k\ L\ O}{5.2\ A^3} \qquad \frac{lbf\ min^2}{ft^4}\ \frac{ft\ \ ft}{ft^6}\ \frac{ft^2(in.w.g.)}{lbf} \qquad (8.4)$$

where k = friction factor ($lbf\ min^2/ft^4$)
L = length (ft)
O = Perimeter (ft)
A = cross-sectional area (ft^2)

and 5.2 = Pressure Conversion Factor from lbf/ft^2 to inches of water

$$= \frac{62.4}{12} \quad \frac{lbf}{(ft^3 \text{ of water})} \quad \frac{ft}{inches}$$

$$= 5.2 \ \frac{lbf}{ft^2} \text{ per inch w.g.}$$

In this system of units, numerical values of the friction factor are very small and lists of k values given in the literature are normally multiplied by the factor 10^{10}. Following this conversion, the units of R become

$$\frac{(in.w.g.)\ min^2}{ft^6} \times 10^{-10}$$

It will be noted that this differs by a factor of 10 from the resistances (P.U.) calculated from the observed airflows and pressure drops (eqn. 8.3). This also explains the difference between equations (8.2) and (8.4).*

In order to calculate k factors from the measured resistances (P.U.), the relationship becomes

$$k = \frac{R \times 5.2 \times A^3}{L \times O} \times 10 \ \frac{lbf\ min^2}{ft^4} \times 10^{10} \qquad (8.5)$$

Table 8.3. gives the k values calculated from equation 8.5 and also in SI units (kg/m^3), where

$$k = \frac{(lbf\ min^2)}{ft^4} \times \frac{4.4482 \times 60^2}{(0.3048)^4} = \frac{Ns^2}{m^4} \text{ or } \frac{kg}{m^3}$$

Hence k (American Units x 1.855×10^6) = k (SI)

---

* The confusion arising from the use of British Imperial Units in mine ventilation is well illustrated in this analysis. Such difficulties are eliminated entirely in the SI where no conversion factors are required.

Section	Length ft	Q kcfm	p milli. in.w.g.	A ft^2	O ft	R P.U.	k factors $\frac{lbf\ min^2 x 10^{10}}{ft^4}$	$\frac{kg}{m^3}$
A3-A4	58	24.230	39	46.24	31.5	0.0664	187	0.0347
A4-A5	58	25.536	39	57.41	37.0	0.0598	274	0.0509
A5-A6	58	25.170	26	67.67	36.0	0.0410	316	0.0587
A6-A7	58	21.415	19	72.64	41.0	0.0414	347	0.0644

Table 8.3. Calculation of friction factors for four consecutive lengths of face.

Two points emerge from the k factors calculated for the longwall face. First, the values are considerably higher than those listed in the literature for shafts, airways or slopes. This is a direct and inevitable consequence of the aerodynamic drag caused by the powered supports added to the high d/D values of the roof beams, conveyor structure and chocks (where d is the distance protruded into the airway and D is the hydraulic mean diameter of the face). The rubbing surfaces along a mechanized longwall face are aerodynamically much "rougher" than other airways underground.

Second, the measured k factors increase along the face line. This is entirely in accord with the deteriorating appearance of the face through and above the fault.

8.4.2. Prediction of face-line resistance:

The longwall face at Snowmass varied in cross-sectional area, perimeter and surface roughness. This variability has proved to be advantageous to this project as it has given ranges of friction factors and resistances that may be used to estimate face-line resistances of other longwalls.

Three friction factors have been chosen, to represent (i) good (ii) normal and (iii) rough conditions for a longwall face equipped with power supports. The values are given in Table 8.4.

$\frac{lbf\ min^2 x10^{10}}{ft^4}$	$\frac{kg}{m^3}$	Condition
200	0.0371	Good
275	0.0510	Normal
350	0.0649	Rough

Table 8.4. k values for a mechanized longwall face.

The resistance of a face-line may be estimated by choosing a k value from Table 8.4 and using one of the following two equations:

American Units

$$R = \frac{k\ L\ O}{52\ A^3} \qquad P.U. \left\{\frac{milli.in.w.g.}{(kcfm)^2}\right\} \qquad (8.6)$$

where k is the value read directly from Table 8.4 in $lbf\ min^2 x10^{10}/ft^4$

L = length (ft)
O = perimeter (ft)
A = cross-sectional area (ft^2)

S.I. Units

In the more rational SI system, no constants are necssary and the equation is simply

$$R = \frac{k\ L\ O}{A^3} \qquad Ns^2/m^8$$

where k is read from Table 8.4 (kg/m^3)
L = length (m)
O = perimeter (m)
and A = cross-sectional area (m^2)

In these calculations, A should be taken as the full cross sectional area available for airflow including open flow paths between chock legs. In the majority of modern installations of power supports, there will be relatively little flow between the chock legs. The perimeter, O, may be taken as a line that traverses the coal face, the conveyor structure (including spill plates), the front of the chocks and the underside of the roof beams.

Example

A mechanized longwall is 350 ft. long, the cross-sectional area is 60 ft^2 and the perimeter is 40 ft. Using an average condition k factor of 275 (American Units), the face line resistance is

$$R_f = \frac{275 \times 350 \times 40}{52 \quad (60)^3} = 0.343 \text{ P.U.}$$

At a mean airflow of 20 kcfm (20,000 cfm) this will give a pressure-drop along the face-line of

$$p = R_f \, Q^2 = 0.343 \times 20^2 = 137 \text{ milli inches w.g.}$$

or 0.137 inches w.g.

8.4.3. Nomograms for rapid estimation of face-line resistance:

In order to provide a rapid means of estimating face-line resistances three nomograms have been constructed to represent good, normal and rough conditions. These are reproduced on Figures 8.3, 8.4 and 8.5 and give the face line resistance per 100 ft for any given cross-sectional area and perimeter.

8.4.4. Face Ends:

The ends of longwall faces differ considerably in the resistance they offer to airflow. This is due to variations in equipment, geometry and roof supports. The shock losses that occur when an airstream is required to change direction are often described in terms of 'velocity heads':

$$P_{sh} = X\rho \frac{u^2}{2g} \qquad \frac{lbf}{ft^3} \; \frac{ft^2}{s^2} \; \frac{s^2}{ft} = \frac{lbf}{ft^2}$$

$$\text{or} \quad X\rho \frac{u^2 \times 1000}{5.2 \times 2g} \text{ milli inches. w.g.} \qquad (8.7)$$

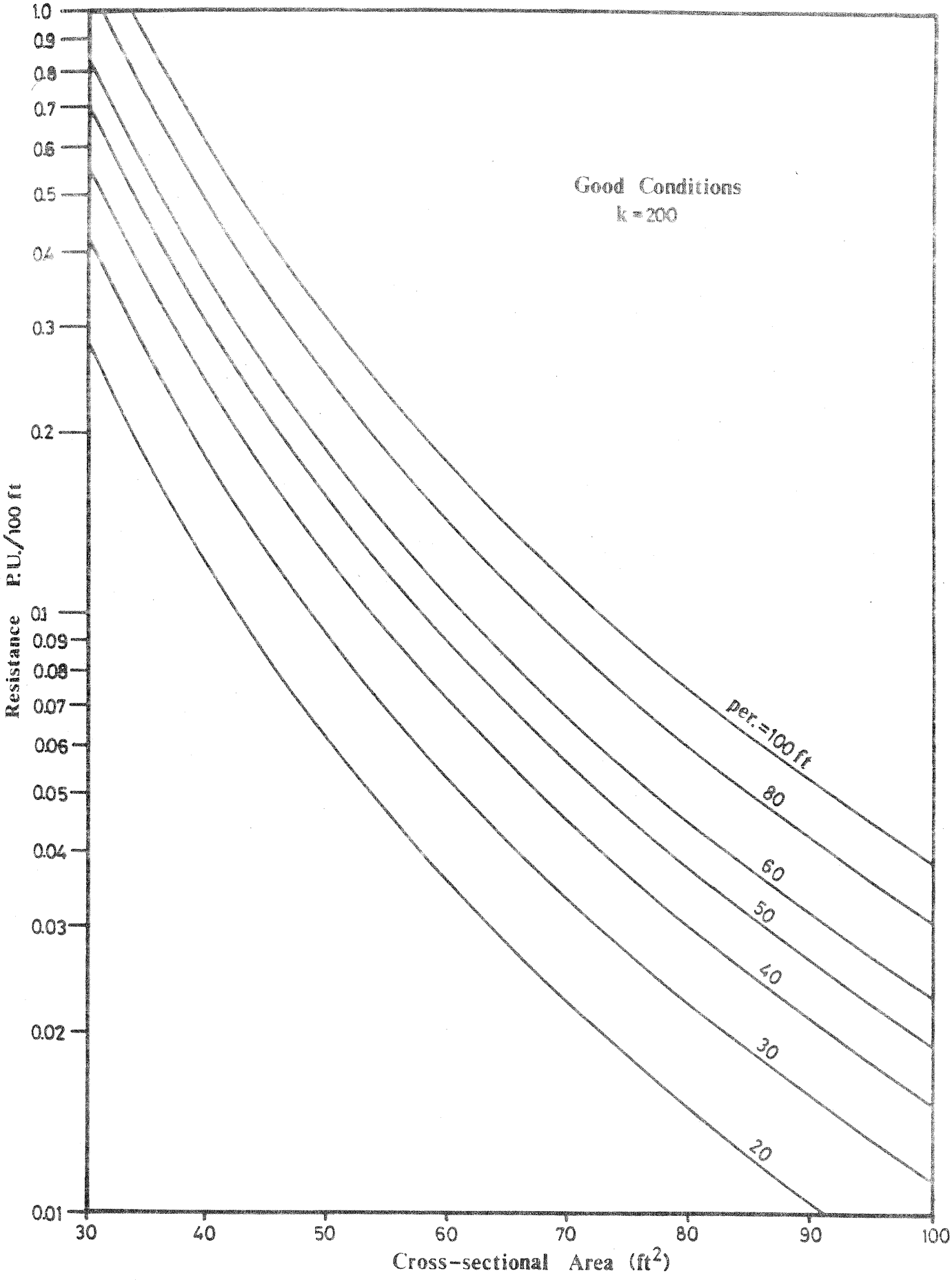

Figure 8.3 Nomogram used to determine face line resistance for good airway conditions.

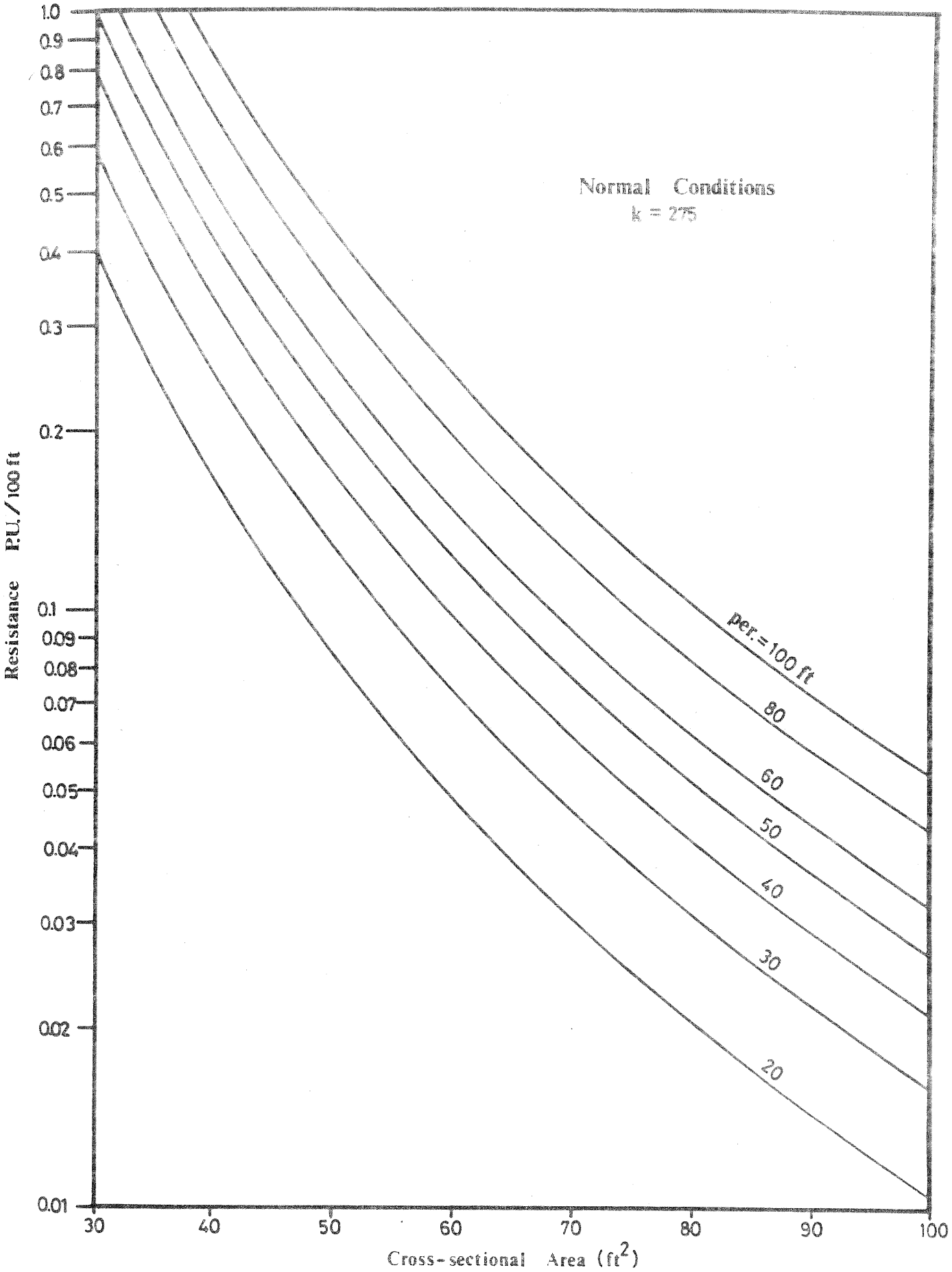

Figure 8.4 Nomogram used to determine face line resistance for normal airway conditions.

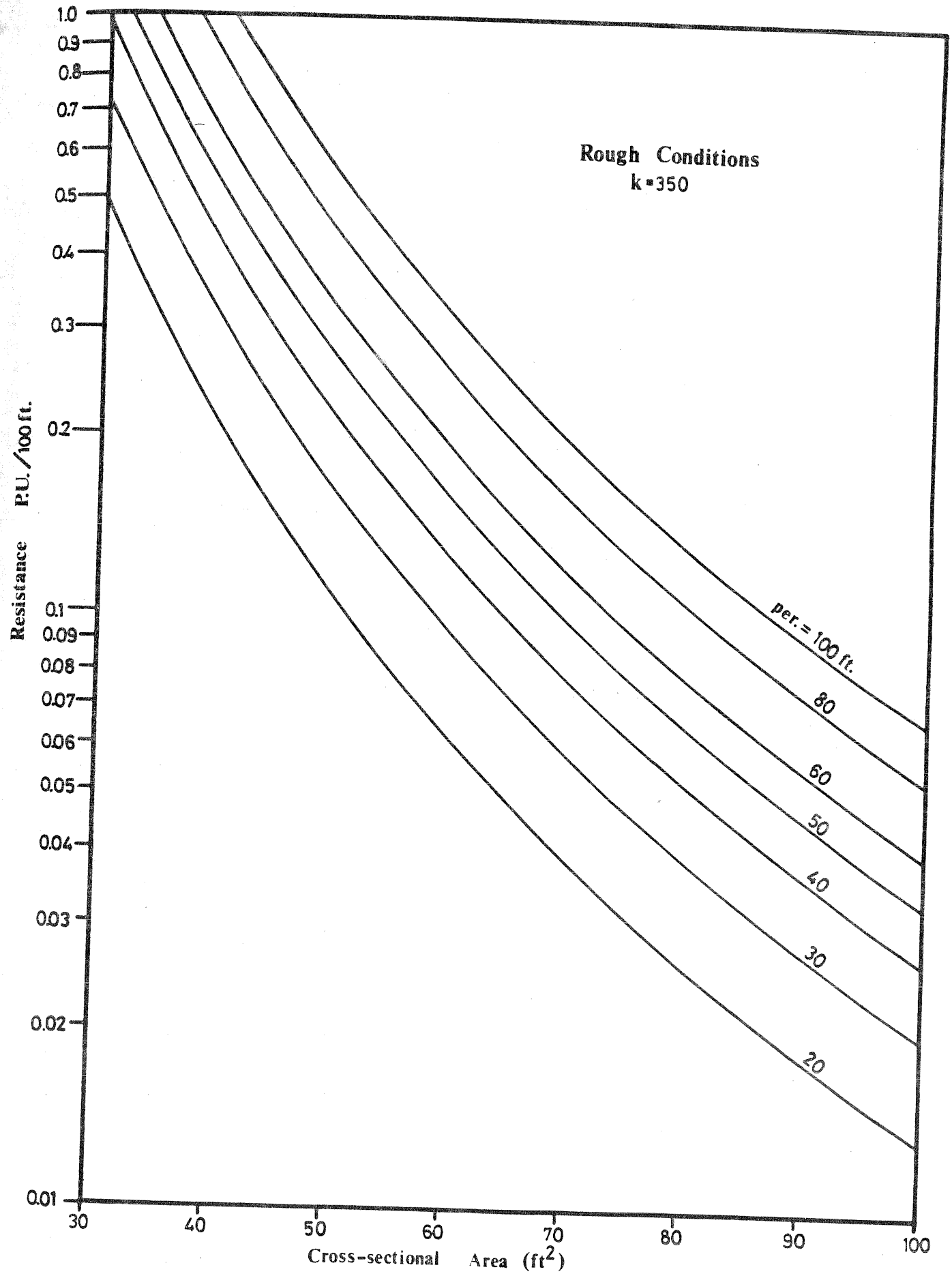

Figure 8.5 Nomogram used to determine face line resistance for rough airway conditions.

where X = Shock loss factor
ρ = air density (lbf/ft3)
u = air velocity (ft/s)
and g = gravitational acceleration (32.2ft/s^2)

Rewriting the equation in terms of a volume flow, Q kilo ft^3/min where

$$Q = u \times 60 \times A/1000 \tag{8.8}$$

$$P_{sh} = \frac{X \rho}{5.2 \times 2g} \quad \frac{Q^2 \times 10^9}{60^2 A^2}$$

Taking a standard value of 0.075 lbf/ft^3 for air density gives

$$P_{sh} = \frac{62.21}{A^2} \times Q^2 \tag{8.9}$$

This may be written in the form of a square law as

$$P_{sh} = R_{sh} \; Q^2 \tag{8.10}$$

where the shock resistance is

$$R_{sh} = \frac{62.21}{A^2} \quad X \quad \text{P.U.} \tag{8.11}$$

In all these analyses, A has been taken to be the cross-sectional area of the unobstructed face.

It then remains to determine the shock loss factor for the often constricted conditions at a face end. The literature pertaining to both mine ventilation and the heating and ventilating industry contains lists of loss factors for many types of duct configurations. At the junction of an airway with a longwall face, there are at least three identifiable causes of shock loss; namely, (i) the sudden change in flow direction as the airflow turns into the face-line, (ii) the cross-sectional area of the face will usually be different to that of the airway, particularly at the face end - hence there will be a shock loss due to the sudden contraction, and (iii) there will normally be a concentration of equipment at the face end resulting in a further obstruction loss. Each of these matters is further examined below with suggested means of estimating the corresponding shock loss factors.

Bend:

For a sharp 90° bend, the shock loss factor is approximately 1.4. This drops rapidly as the radius of curvature increases. However, in the case of a junction between an airway and a longwall face, the turn will invariably be sharp and, in the great majority of cases very close to 90°. Hence, the value of $X_b = 1.4$ for the bend will be used for all such junctions.

Contraction:

At the sudden contraction as the air enters the face - line, the recommended shock loss factor is

$$X_c = \left\{\frac{1}{C_c} - 1\right\}^2 \qquad (8.12)$$

where the coefficient of contraction, C_c, depends upon the geometry of the face end. However, the effect of the contraction is fairly small compared with that of the bend and obstructions from equipment. A mean value of 0.7 for C_c is suggested, giving

$$X_c = \left\{\frac{1}{0.7} - 1\right\}^2 = 0.184 \qquad (8.13)$$

Obstruction:

In many cases, the entry to the face-line will be heavily obstructed by the face conveyor gearhead and transfer point. The shock loss is dependent upon the cross-sectional area of the face and how much of this is filled with equipment. Hence, in this case, there is no single value of shock loss factor that is generally applicable. The "obstruction formula" that may be employed is:

$$X_{ob} = \left\{\frac{A}{C_c(A-a)} - 1\right\}^2 \qquad (8.14)$$

where A = the full cross-sectional area of the face (ft^2 or m^2)
a = the cross-sectional area that is obstructed (ft^2 or m^2)
C_c = coefficient of contraction (take as 0.7)

Total shock loss factor at face-end:

The three shock loss factors X_b, X_c and X_{ob} are not independent. Shock losses may interfere one with another and it is possible that the integrated effect may be less than the sum of the individual components. However, a simple addition of the three shock loss factors gives a result which is in sensible agreement with the measurements made at Snowmass. It is suggested, therefore that the overall face-end shock loss is computed as

$$X_{fe} = X_b + X_c + X_{ob} \qquad (8.15)$$

8.4.5. Correlation with Snowmass intake face end:

At the intake end of the Snowmass face, the cross-sectional area of the face was 44 ft^2 of which 20 ft^2 were obstructed by the gear head of the conveyor. This combined with the transfer point on to the gate conveyor, causing considerable contraction of the airflow at the face-end. The high air velocity and excessive turbulence were all too obvious. The shock loss factors estimated from the relationships given above were

bend	X_b	$= 1.4$
contraction	X_c	$= 0.184$
obstruction	X_{ob}	$= \left\{ \frac{44}{0.7(44-20)} - 1 \right\}^2 = 2.621$

Total shock loss factor at intake end

$$Xint = 1.4 + 0.184 + 2.621 = 4.205$$

Equation 8.11 gives the equivalent resistance to be

$$\frac{62.21}{442} \times 4.205 = 0.135 \text{ P.U.}$$

Table 8.1 gives the total resistance of the first 58ft of the face (section A2 to A3, including the face end) to be 0.2035 P.U. Through this section, the cross-sectional area was 44 ft^2, the perimeter 31ft and the frictional factor 187 ($\times 10^{-10}$ lbf.min $^2/ft^4$), similar to that of section A3-A4 (see Table 8.3).

Hence the resistance of this section of face line without the shock losses would be

$$R = \frac{k\,L\,O}{52\,A^3} = \frac{187 \times 58 \times 31}{52\,(44)^3} = 0.076 \text{ P.U.} \qquad (8.6)$$

The equivalent resistance due to the shock losses is then given as the difference between the measured total resistance and that due to the 58 ft of face-line, i.e.

$$0.2035 - 0.076 = 0.128 \text{ P.U.}$$

This differs from the computed resistance of 0.135 P.U. by only 0.007 P.U., or 5 per cent. This is considered to be a satisfactory correlation.

8.4.6. Shearer:

The power loading machinery offers additional resistance to airflow on a longwall face. The pressure losses occur because of two distinct effects. First, wake losses occur at the downstream end of the shearer as the higher velocity airstream through the restricted area around the body of the machine is projected into the lower velocity downstream. Second, the increased velocity in the restricted zone along the shearer causes enhanced frictional losses in this area.

It is possible to calculate the theoretical shock loss caused by a symmetrical obstruction to airflow in a straight mine airway. However, such calculations give results which are less than half the losses measured across a shearer on a longwall face. This was also the case at Snowmass. The reasons for such discrepancies arise from the over-simplifications necessary for a theoretical treatment. In practice, the resistance offered by a power-loader depends not only upon the dimensions of the machine and those of the face, but also upon:

- the position of the shearer within the cross-section.
- the location of the machine along the face, particularly if in proximity to the face ends and also with respect to positions of open flow paths in the waste behind the chocks.
- whether the machine is moving and, if so, in which direction relative to the airflow.
- the position and air-deflecting capabilities of water sprays.
- the position of the operator.
- the orientation of the cutting drums and any deflecting plates that may be fitted.
- the local friction (k) factor of the longwall.

One further indirect factor associated with a producing unit is the depth of broken coal on the face conveyor and its direction of travel relative to the airflow.

With such a diversity of variables, it is not surprising that a theoretical treatment based on a simplified geometry yields unsatisfactory results. An empirical method is, therefore, suggested and is based on the Snowmass measurements. However, it is also suggested that further investigations on a range of longwall faces are required to provide design data for shock losses across power-loaders. Table 8.1 shows that over the 45 ft long section, A8-A9, containing the shearer, the measured resistance was 0.0665 P.U. Figure 7.5 shows the cross-section at the position of the shearer body. The mean cross-sectional area of the face between stations A8 and A9 was 80 ft^2. The perimeter of the face cross-section, not including the shearer was 46 ft.

The resistance of the 45 ft. section, in the absence of the shearer is given by equation (8.6)

$$R = \frac{k\ L\ O}{52\ A^3}$$

Using the value of $k = 347$ lbf min^2/ft^4 for the upper part of the face (Table 8.3) gives

$$R = \frac{347 \times 45 \times 46}{52 \times (80)^3} = 0.0270 \text{ P.U.}$$

for the unobstructed face. Hence, the effective resistance of the shearer is

$$R_{shear} = 0.0665 - 0.0270 = 0.0395 \text{ P.U.}$$

The shock loss factor for the shearer is given by equation 8.11

$$X_{shear} = \frac{R_{shear}\ A^2}{62.21} = \frac{0.0395 \times 80^2}{62.21} = 4.06$$

On the basis of this result, it is suggested that an estimate may be made of the resistance of a longwall shearer by assuming a shock loss factor of 4.

8.4.7. Caved Area:

The overall resistance of a longwall face will decrease considerably if there are open areas available for airflow in the waste zone behind the chocks. For planning purposes, however, the resistance of the face should be estimated on the basis of the conveyor being at its closest position to the coal front, the chocks fully advanced and the waste area caved up to the rear of the chocks. This situation will give the smallest cross-sectional area and highest resistance offered by the longwall under normal operating conditions.

8.5. Summary of Procedure for Estimating Face Resistance

1. Determine the length, L, mean cross-sectional area, A, and perimeter, O, of the face and estimate a friction factor, k, from Table 8.4. Then determine face-line resistance, R_f, from Figures 8.3, 8.4 or 8.5, or from equation 8.6

$$R_f = \frac{k\ L\ O}{52\ A^3} \text{ P.U.} \left[\frac{\text{milli in.w.g.}}{(\text{kcfm})^2}\right] \qquad (8.6)$$

2. For each face-end, determine the following shock loss factors where applicable.

Sharp right angled bend, $X_b = 1.4$
Sudden contraction at intake end, $X_c = 0.184$
Face-end obstruction, $X_{ob} = \left[\frac{A}{0.7(A-a)} - 1\right]^2$

where A = full cross-sectional area of face
a = cross-section of obstruction facing the airflow

[For the majority of longwall faces in the United States, the height of the face is the same as that of the gateroads. For this reason, no allowance need be made for an expansion loss at the return end unless there is a concentration of equipment at this location.]

3. Use a shock loss factor of $X_{shear} = 4$ for each shearer on the face.

4. Sum all shock loss factors to give X_{tot}

5. Determine the equivalent resistance of the shock losses.

$$R_{sh} = \frac{62.21}{A^2} X_{tot} \quad \text{(gives R in P.U. if A is in ft}^2\text{)}$$

6. Determine the full face resistance

$$R = R_f + R_{sh}$$

7. The resistances of the main gate and tail gate should be determined separately from

$$R = \frac{k\ L\ O}{52\ A^3}$$

using values of friction factor, k, appropriate to the conditions expected, and taking into account the location of equipment close to the face.

8.6. Worked Example of Estimating Face Resistance

A mechanized longwall face has the following planned specifications.

Length:	350 ft.
Cross-sectional area with chocks forward	60 ft^2.
Corresponding perimeter	40 ft.

The intake face end will have the cross-sectional area reduced by 35 ft^2 due to a conveyor transfer point. There is no additional equipment at the return face end. The face is at right angles to both main and tail gates. There is one shearer on the face.
Compute the face resistance and the frictional pressure drop at an airflow of 30,000 cfm.

Procedure:

1. Assuming normal conditions for powered supports, ($k = 275 \times 10^{-10}$ $lbf.min^2/ft^4$) the face-line resistance may be determined from either

$$R_f = \frac{k\,L\,O}{52\,A^3} = \frac{275 \times 350 \times 40}{52 \times (60)^3} = 0.3428 \text{ P.U.}$$

or

read from Figure 8.4: at A = 60ft^2 and perimeter = 40 ft, the nomogram gives a resistance of 0.098 P.U. per 100 ft.

Hence $R_f = 0.098 \times \frac{350}{100} = 0.343$ P.U.

2. At intake face-end, shock loss factors are

bend $X_b = 1.4$
contraction $X = 0.184$
obstruction $X_{ob} = \left\{ \frac{60}{0.7\,(60-25)} - 1 \right\}^2 = 2.10$

Total shock loss factor at intake

$$X_{int} = 1.4 + 0.184 + 2.10 = 3.684$$

3. At return end, only the sharp bend contributes a significant shock loss, hence

$$X_{ret} = 1.4$$

4. Shearer shock loss factor

$$X_{shear} = 4.0$$

5. Total of shock loss factors

$$X_{tot} = 3.684 + 1.4 + 4.0 = 9.084$$

6. Equivalent resistance for shock losses

$$R_{sh} = \frac{62.21}{60^2} \times 9.084 = 0.157 \text{ P.U.}$$

7. Full face resistance

$$R = R_f + R_{sh} = 0.343 + 0.157 = 0.500 \text{ P.U.}$$

8. The frictional pressure drop across the face at an airflow of 30,000 cfm (Q = 30 kcfm) is given as

$$p = R\,Q2 = 0.5 \times 302 = 450 \text{ milli in. w.g.}$$
or 0.45 inches w.g.

9. INVESTIGATION OF THE LAW OF AIRFLOW ON A LONGWALL FACE

9.1. Introduction

The great majority of mine ventilation planning exercises are conducted on the assumption that the frictional loss in total pressure, p, varies with the square of the airflow, Q^2, in mine airways. The constant of proportionality, R, is known as the resistance of the airway. The resulting equation

$$p = RQ^2$$

is often referred to as the Square Law of mine ventilation.

The square law has a firm theoretical basis as described in the following section. However, that theory, together with some practical considerations, leave a doubt concerning the applicability of the square law to longwall faces. Consequently, several authorities have questioned the validity of the square law for air flowing along a longwall face.

In order to determine the law of airflow from practical observations it is necessary to measure the frictional pressure drops and corresponding airflows over as wide a range of air quantities as possible. This has been done on numerous occasions for intake and return airways, across regulators, bends, junctions and other obstructions. Unfortunately, it is seldom practicable to vary airflows and monitor the corresponding pressure drops on an operational longwall face. The availability of a fully equipped standing face at the Thompson Creek No. 1 mine gave a rare opportunity to carry out the experiment.

This chapter of the report gives the background to the square law, describes the test that was carried out on the longwall face, and highlights the very convincing result that was achieved.

9.2. Background to the Square Law

Based on the work of Antoine de Chezy (1718-98) and Henri Darcy (1830-58) in France, equations relating head loss to velocity were developed for water flow, initially for open channels then for pipes. The modern version of the Chezy Darcy pipe equation is

$$h = \frac{4 f L u^2}{2 g d} \qquad (9.1)$$

where h = head loss in meters of fluid,
f = friction coefficient depending upon the roughness of the pipe lining (dimensionless)
L = length of pipe (m)
u = fluid velocity (m/s)
g = gravitational acceleration (9.81 m/s^2)
and d = pipe diameter

[Some authorities write the equation as $\lambda Lu^2/2gd$ where $\lambda = 4f$]

During the 1850's, a mine agent named John Job Atkinson conducted experimental work on the airflows in mines in the north of England [2]. He found that the pressure difference required to promote an airflow through a mine roadway was proportional to the square of the velocity, the length and perimeter of the airway, and inversely proportional to the cross-sectional area. He also discovered that the pressure difference also varied with the condition of the airway lining.

Atkinson was influenced by the work of the French hydraulic engineers and there was a clear parallel between his findings and the Chezy Darcy equation. He modified this equation in two ways in order to adapt it for mine airways.

First, he replaced the head loss, h, by the frictional pressure drop, p,

$$p = \rho g h \qquad (9.2)$$

where p = frictional pressure drop (N/m^2 or Pa)
and ρ = air density (kg/m^3)

The Chezy Darcy equation then becomes

$$p = \frac{4 \rho f L u^2}{2 d} \qquad (9.3)$$

Second, in order to make the equation applicable to non-circular airways, the diameter d was taken as the hydraulic mean diameter i.e.

$$d = \frac{4A}{O}$$

where A = cross-sectional area (m^2)
and O = perimeter (m)

Then

$$p = \frac{4 \rho f L u^2}{2} \quad \frac{O}{4A}$$

The term L x O is the internal rubbing surface, s (m^2), of the airway. Hence

$$p = \frac{\rho f}{2} \frac{s}{A} u^2$$

This may be written as

$$p = \frac{ksu^2}{A} \qquad \text{(Atkinson's equation)} \qquad (9.4)$$

where the friction factor $k = \frac{\rho f}{2}$ kg/m^3 (9.5)

The friction factor, k, commonly used as an indication of the roughness of the airway surfaces is, therefore, dependent upon the air density. Tables of k in the literature are based upon a standard value of air density (1.2 kg/m^3 or 0.075 lbf/ft^3). Where high accuracy is warranted, standardized values of k may be corrected to actual densities

$$k_{act} = \left(k_{stand} \times \frac{\rho_{act}}{\rho_{stand}} \right) \qquad (9.6)$$

where the subscripts 'act' and 'stand' refer to actual and standard conditions respectively.

Referring back to Atkinson's equation (9.4), the air velocity u may be expressed in terms of volume flowrate, Q

$$Q = u \times A \quad (m^3/s) \qquad (9.7)$$

giving

$$p = \frac{k\, s\, Q^2}{A^3} \qquad (9.8)$$

Furthermore, for any given airway, known values exist for friction factor, k, rubbing surface, s, and cross-sectional area, A. Hence equation (9.8) may be re-written as

$$p = RQ^2 \qquad \text{The Square Law} \qquad (9.9)$$

where

$$R = ks/A^3 \quad Ns^2/m^8 \tag{9.10}$$

and is known as the 'resistance' of the airway.

The concept of airway resistance, and the Square Law are of fundamental importance in mine ventilation planning. All current techniques of predicting airflow distributions, whether manual or by computer programs, require a knowledge of airway resistances and utilize the square law for main airflow routes.

9.3 Deviations from the Square Law

The conventional application of the Square Law (9.9) assumes that for a given airway of fixed geometry and surface roughness, the resistance, R, remains a fixed constant of proportionality between p and Q^2. There are three reasons for questioning the invariability of R and the accuracy of the square law, even when the geometry of the airway is fixed.

9.3.1 Effect of air density

Equation (9.10) shows that resistance, R, is a function of the friction factor k. This, in turn, depends upon the air density (equation (9.5)). Combining these two equations gives

$$R = \frac{\rho f}{2} \frac{s}{A^3} \quad Ns^2/m^8 \tag{9.11}$$

showing that the resistance of an airway depends not only upon lining and geometry but also upon the density of air flowing through it. For this reason, some authorities prefer to use a 'rational resistance', r, [3] where

$$r = \frac{R}{\rho} \quad m^{-4} \tag{9.12}$$

The units of r indicate that it now depends solely upon geometry. The square law then becomes

$$p = r \rho Q^2 \tag{9.13}$$

Where air density varies by more than 5 per cent in a mine ventilation system, this latter version of the square law allows such variation to be taken into account. A 5 percent variation in air density approximates to a depth below surface of 550 m (1800ft). Fortunately, most coal mines in the United States are shallower than this and changes in air density are of secondary importance. In these circumstances the corresponding correction to the square law may be neglected for most practical purposes.

9.3.2. Effect of flow regime:

If a fluid flows sufficiently slowly through any pipe or channel, the streamlines will be almost parallel to each other. This is known as laminar flow. The resistance to flow is caused by viscous friction or shear between layers moving at different velocities. At higher velocities, the streamlines no longer remain stable and parallel, but break up into vortices or eddy currents. This is known as turbulent flow and, because of the additional shear effect of the vortices, the resistance is considerably higher than in laminar flow.

The total energy of an airflow is made up of mechanical energy (kinetic, potential and "pressure" energy) and thermal (internal) energy. The effect of shear resistance within the airflow is to increase the thermal energy at the expense of mechanical energy. This is manifested as a measurable "frictional pressure drop" along the airway and shows as a loss of total pressure (static pressure plus velocity pressure). The frictional pressure drop is the same p as that used in the square law.

The background and derivation of the square law given in the previous section was based entirely upon turbulent flow. If the airflow does not remain fully turbulent then the square law, with a constant value of resistance for a given airway, will break down.

Osborne Reynolds, in the 1890's discovered that the flow in pipes was laminar provided that the value of

$$Re = \frac{\rho u d}{\mu} \qquad (9.14)$$

did not exceed approximately 2500.

Re is a dimensionless number (Reynold's number) and μ is the dynamic viscosity of the fluid (Ns/m^2). At higher Reynold's numbers, the flow becomes turbulent.

For mine airways, the Reynolds Number at which turbulent flow is fully established depends upon the friction factor as shown on Figure 9.1. This diagram also shows the limiting Reynolds' Numbers for the strict application of the square law. However, with the exception of smooth concrete or steel lined shafts which contain no fittings, deviations from the square law are likely to be small in airways with Reynold's Numbers exceeding 40,000.

An approximation to the Reynold's Number in a mine airway is given by

$$Re = 270{,}000 \frac{Q}{O}$$

where Q = airflow in m^3/s

and O = perimeter in m

Example:

In a 4 x 2 m airway, the perimeter O = 12m. At a limiting Reynolds Number of 40,000, the airflow is

$$Q = \frac{40{,}000}{270{,}000} \times 12 = 1.78 \ m^3/s$$

or a velocity of $u = \frac{Q}{A} = \frac{1.78}{8} = 0.22$ m/s (44 ft/min)

While most ventilation air routes have airflows which maintain turbulent flow, some fall into the transitional region between laminar flow and fully developed turbulence. In cases where leakage of air occurs through caved areas, worked out zones or through permeable strata the flow may be completely laminar. This is further investigated in Section 10 of the report (Leakage through gob areas).

Where deviations from the square law exist then there are two ways of handling the situation. First, a $p = m Q^2$ relationship may be retained where m is no longer a constant value of resistance but

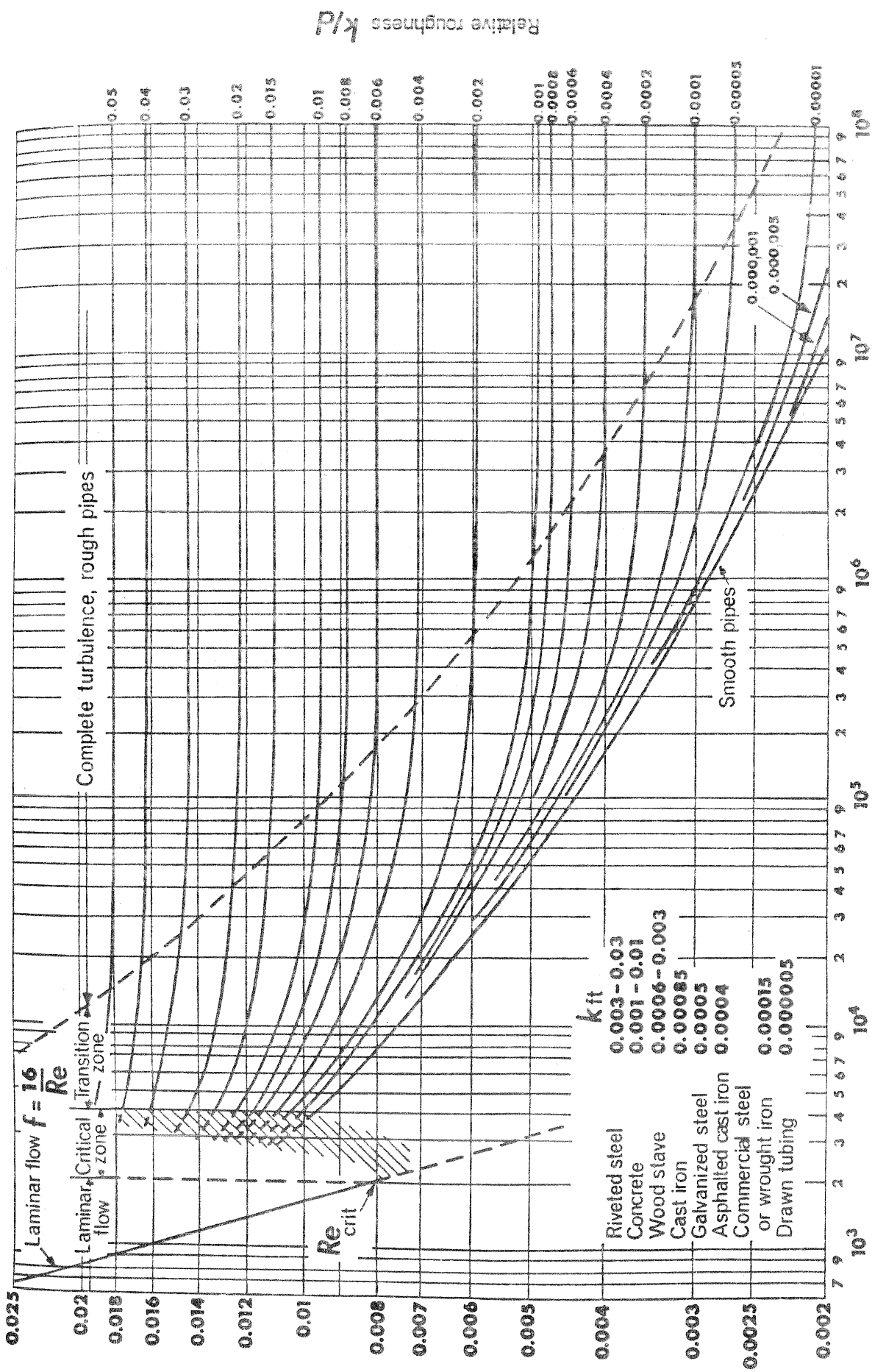

Figure 9.1 Moody diagram. (Mechanics of Fluids, B.S.Massey Van Nostrand)

varies with Reynold's Number along the appropriate curve on Figure 9.1. Second, the method that is often preferred in mine ventilation, is to express the pressure - volume relationsip as

$$p = R' Q^n$$

where n = 1 for laminar flow and 2 for fully developed turbulence.

Unfortunately the parameter R' is also a complex function of n, Q, the physical properties of the air and the airway geometry. In mine ventilation computer programs that take Reynold's Number into account, the problem is simplified by assuming that airflow in each branch is either laminar

$$p = R_L Q \qquad (9.15)$$

or turbulent

$$p = R Q^2$$

In contrast to the variable parameter R', the relationship between the laminar resistance, R_L, and the normal turbulent resistance, R, is definable. For laminar flow, Poiseuille's equation applies. For a circular passage, this may be stated as

$$Q = \frac{p \pi r^4}{8 \mu L} \qquad (9.16)$$

where r = radius (m)

This may be expressed as

$$p = \frac{8 \mu L}{\pi r^2 . r^2} Q = \frac{8 \mu L \pi}{A^2} Q$$

Hence $$R_L = \frac{8 \mu L \pi}{A^2} \qquad (9.17)$$

Inserting the value for air viscosity at 20°C, $\mu = 18 \times 10^{-6}$ Ns/m^2 gives

$$R_L = 0.4524 \times 10^{-3} \frac{L}{A^2} \quad \frac{Ns}{m^5} \qquad (9.18)$$

where L = length of airway (m)
A = cross-sectional area (m^2)

Comparing this with the turbulent resistance (equation 9.10)

$$R = \frac{k\ L\ O}{A^3}$$

illustrates that whilst the normal turbulent resistance depends upon surface roughness and shape, the laminar resistance is independent of these parameters.

It is convenient to express the relationship between the two resistances as a ratio.

$$\frac{R}{R_L} = \frac{k\ L\ O}{A^3} \quad \frac{A^2}{8\ \mu\ L\ \pi} \quad \frac{s}{m^3} \qquad (9.19)$$

$$= \frac{k\ O}{8\ \mu\pi\ A}$$

$$= \frac{2210\ k\ O}{A} \quad \frac{s}{m^3} \qquad (9.20)$$

Example

A 4 x 2m airway, 100m long has a friction factor of 0.012 kg/m^3.

Turbulent resistance

$$R = \frac{k\ L\ O}{A^3}$$

$$= \frac{0.012 \times 100 \times 12}{8^3} = 0.028125\ Ns^2/m^8$$

Laminar resistance

$$R_L = 0.4524 \times 10^{-3} \frac{L}{A^2}$$

$$= 0.4524 \times 10^{-3} \times \frac{100}{8^2} = 0.000\ 7069 \quad Ns/m^5$$

Ratio $\frac{R}{R_L} = \frac{0.028\ 125}{0.000\ 7069} = 39.78$

or $\frac{R}{R_L} = 2210 \frac{k0}{A}$

$$= 2210 \times \frac{0.012}{8} \times 12 = 39.78 \quad s/m^3$$

Thus, in this typical example the resistance to turbulent flow is nearly 40 times greater than that for laminar flow.

Note that the laminar resistance for a pipe or airway is different from that of a porous medium where, neglecting compressibility of the air

$$R_L = \frac{\mu L}{KA}$$

K = Liquid permeability of the medium (m^2)

9.3.3 Effect of free standing obstructions:

The Atkinson friction factor, k, and its more fundamental companion, the Chezy Darcy coefficient of friction, f, arise from a combination of turbulent eddies and viscous shear. In turbulent airflow, the energy required to maintain the vortices is far greater than that needed to overcome viscous shear.

The degree of turbulence is affected to a major extent by the roughness of the airway walls. Hence, so also is the friction factor, or coefficient of friction (Fig (9.1)).

It is to be expected that any cause of additional turbulence, such as bends, junctions or obstructions in the airway would result in

an increase in resistance but remain consistent with the square law. However, the evolution of the square law has been based on wall-type roughness and not upon free standing obstructions.

The aerodynamic drag, D, on a free standing obstruction in a fluid stream is given by

$$D = C_D \; A \; \frac{\rho u^2}{2} \qquad N \qquad (9.21)$$

where C_D = Coefficient of drag, dependent upon the shape of the body and A = Projected area perpendicular to the direction of flow. This is clearly a "square law" type of relationship. However, if a row of closely spaced obstructions exists, such as a line of props or chocks on a longwall face, then aerodynamic interference occurs within the turbulent vortices between sets of supports. This reduces aerodynamic drag but effectively decreases the cross-sectional area available for flow. In such cases the only effective means of testing the validity of the square law is by experiment.

9.4. Experimental Test Underground

The face airflow test at Snowmass consisted of measuring the frictional pressure drop along the full length of the face and over a range of airflows.

9.4.1 Pressure measurements:

The positions of the instruments are shown on Figure 9.2. A calibrated 0 to 0.25 inch w.g. magnehelic gauge was sited on the longwall face about 100 ft from the intake end. A single length of strong 1/8 inch i.d. plastic tubing was extended throughout the length of the face, tied to the roof beams of the powered supports and tested for leaks. The magnehelic gauge was levelled to its calibration position, checked for zero adjustment and connected into the pressure tubing as illustrated on Figure 9.2.

Pitot static tubes were connected to the pressure tubing at both ends of the longwall face. Initially the facing ends of the pitot tubes were oriented towards the airflow. However, cramped conditions around the conveyor transfer point at the intake end of the face caused excessive turbulence and instability of the magnehelic readings. The problem was overcome by attaching the pressure lines to the side (static) tappings of the pitot tubes and, in addition, by wrapping several layers of loose muslin around the static pressure holes on the stems of the pitot tubes. This device ensured that static pressures only were transmitted from the face ends to the magnehelic gauge. The ensuing readings were very stable.

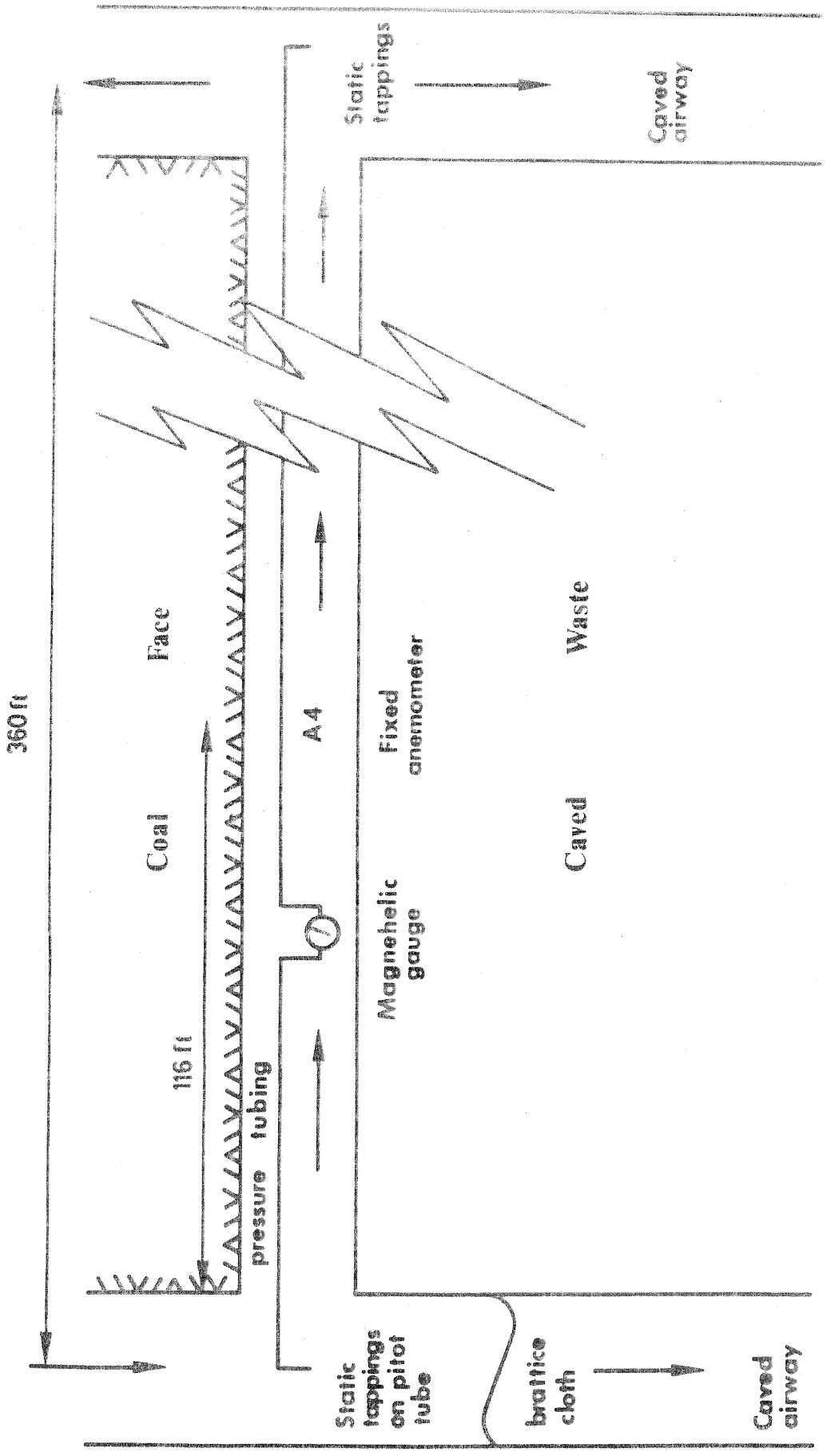

Figure 9.2 Position of instruments for square law test on a longwall face.

9.4.2. Airflow measurements

An airflow measuring station was selected at a site where face conditions were good, with uniform cross section and sufficiently far from the intake end to be free of face entry shock effects. The station is shown as A4 on Figure 9.2.

A number of careful traverses were made using a calibrated, medium speed Davis anemometer. The traverses were conducted with the anemometer on an extension rod and maintained facing directly into the airflow. The body of the observer was kept out of the main airflow and downstream from the instrument. There was no other activity anywhere in the mine. The stability of the airflow conditions was reflected by the anemometer traverses yielding mean air velocities within the range 552 ft/min ± 2 per cent.

The anemometer was then located in a fixed position about 18 inches below the roof beams and over the center of the armored face conveyor. This was a position of relatively flat velocity gradient over the cross-section (ref. Figure (7.3) for velocity contours at this station). The instrument was fastened securely by tie wires so that it remained facing directly down the 30deg. slope of the face. Readings were taken by an observer located downstream, out of the airstream and without ever touching the anemometer. Repeated observations of the fixed anemometer gave a spot velocity in the range 755 ft/min ± 0.5 per cent. The fixed point correction to convert the spot reading to mean velocity was therefore

$$\frac{552}{755} = 0.731 \pm 2\ 1/2 \text{ per cent}$$

It was assumed that the fixed point correction remained constant throughout the test.

Wet and dry bulb temperatures were recorded from a sling hygrometer at the intake end of the face. These were utilized, together with an absolute air pressure corrected from a mine surface reading, to determine the density of the air.

9.4.3. Experimental procedure

The test commenced by closing the regulator at the inbye end of the lower bleeder airway (Figure (4.1)) and erecting an additional brattice cloth in the same airway just inbye the position of the faceline. A further brattice cloth was erected to minimize air

leakage into the caved airway at the bottom of the face. This work was carried out in order to commence the test with the maximum airflow on the face. Readings were taken on the anemometer and the maghehelic gauge.

The face airflow was reduced in stages by

(a) progressively dismantling the temporary stoppings
(b) re-opening the bleeder airway regulator, and
(c) erecting a brattice cloth in the conveyor (intake) airway between the last open cross-cut and the face.

At each stage, observations of air velocity and faceline pressure drop were made on the anemometer and magnehelic gauge respectively. The magnehelic gauge was very responsive and reached stability quickly following a change in airflow. Indeed, the gauge was used during the course of the experiment to direct the progressive building and dismantling of the temporary stopping.

The readings were both tabulated and graphed as they were collected, and showed a stable pattern. About midway through the test the main fans stopped for about 5 minutes due to a temporary power failure. The airflow on the face stagnated (and actually drifted very slowly in the reverse direction). Both anemometer and pressure gauge indicated zero readings through this period. Following restoration of the main fan power, both instruments reverted to their previous readings, again indicating the stability and repeatability of the observations.

The test terminated by returning all brattice cloths to their normal position and taking further readings of air velocity and pressure drop.

9.4.4. Results

The observed results are listed in Table 9.1 in the units recorded by the instruments, i.e. Imperial units. The pressure drop and air velocity readings have been corrected according to the calibrations of the relevant instruments.

The cross-sectional area at the airflow measuring station was 46.225 ft^2. Hence the airflow was calculated as

$$Q = u_{mean} \times 46.225 \qquad ft^3/min$$

where u_{mean} = spot velocity x 0.731

The frictional pressure drop, p, refers to the loss of <u>total</u> head due to the irreversible transfer of mechanical energy to heat energy by turbulence and viscous shear within the airflow

Spot velocity u ft/min	Mean velocity u_{mean} = u x 0.731 ft/min	Airflow Q = $0.046225 u_{mean}$ k ft^3/min	Frict.pr.dp. (static) p_{st} milli.in.wg.	Velocity head correction h_v milli.in.w.g.	Fric.pr.dp. (total) $p = p_{st}+h_v$ milli.in.w.g.	log Q	log p
795	581.1	26.86	163	21.4	184	3.291	5.217
785	573.8	26.52	172	20.9	193	3.278	5.262
733	535.8	24.77	146	18 2	164	3.210	5.101
719	525.6	24.30	133.5	17.5	151	3.190	5.018
677	494.9	22.88	116	15.6	132	3.130	4.879
613	448.1	20.71	101.5	12.7	114	3.031	4.738
583	426.2	19.70	87	11.5	99	2.981	4.590
527.5	385.6	17.82	69.6	9.4	79	2.880	4.370
477	348.7	16.12	62.6	7.7	70	2.780	4.253
390.5	285.5	13.20	39.4	5.2	45	2.580	3.797
728	532.2	24.60	137	18.0	155	3.203	5.043
787	575.3	26.59	150.6	21.0	172	3.281	5.145
758	554.1	25.61	146	19.5	165	3.243	5.109

Table 9.1 Summary of results obtained in total face airflow test.

$$p_t = p_v + p_s$$

where p_t = total head
p_v = velocity head
and p_s = static head

It will be recalled that in order to obtain stable readings, the static tappings on the pitot tubes were employed.

$$p = p_{t1} - p_{t2} = (p_{s1} + p_{v1}) - (p_{s2} + p_{v2})$$

where subscripts 1 and 2 refer to the intake and return ends of the face respectively or,

$$p = (p_{s1} - p_{s2}) + (p_{v1} - p_{v2}) \qquad (9.22)$$

The difference in static pressures $(p_{s1} - p_{s2})$ was indicated by the magnehelic gauge leaving the difference in velocity heads to be applied as a correction.

The pitot tube at the top of the face was sited close to the roadway side facing into the airflow. Most of the flow was diverted into the caved side of the haulage road some 15 ft lower down, assisted by the presence of the shearer. The air velocity at the upper pitot tube was, therefore, low and the kinetic energy correction, p_{v2}, negligible. However, the situation at the bottom of the face was very different. Air conditions here were blustery. Attempts were made to monitor the air velocity around the pitot tube but the high turbulence gave excessive fluctuations on the instruments. For this reason, the mean velocities recorded at the anemometer station were used as representative of the kinetic energy of the air entering the bottom of the face. The validity of this assumption was verified by the continuity of airflow through the lower part of the face. (Section 10)

In the SI system, the velocity head is given simply as

$$p_v = \rho_a \frac{u^2}{2} \qquad \frac{kg\ m^2}{m^3\ s^2} = \frac{N}{m^2}$$

However, the irrational constants inherent in the Imperial system give the velocity head as

$$h_v = \left(\frac{\rho_a}{\rho_w} \cdot \left(\frac{u}{60} \right)^2 \cdot \frac{12}{2g} \times 1000 \right) \text{ milli-inches w.g.}$$

where ρ_a = density of air (lbf/ft^3)
ρ_w = density of water (lbf/ft^3)
u = mean air velocity (ft/min)
g = gravitational acceleration (ft/s^2)

Values of ρ_w = 62.4 lbf/ft^3 and g = 32.2 ft/s^2 were employed, giving,

$$h_v = \left(\rho \cdot \left(\frac{u}{1097} \right)^2 \quad \times 1000 \right) \quad \text{milli-inches w.g.}$$

The air density, ρ_a, was determined from psychrometric measurement (barometric pressure, wet and dry bulb temperatures) and remained close to the standard value of 0.075 lbf/ft^3.

9.4.5 Analysis of results

9.4.5.1. Test of the Square Law

Assuming a general law of airflow gives the relationship between frictional pressure drop, p, and airflow, Q as

$$p = R\, Q^n \qquad (9.23)$$

The primary purpose of this part of the project was to determine the value of the index, n, for the longwall face at Snowmass.

Taking logs gives

$$\log p = \log R + n \log Q \qquad (9.24)$$

A plot of log p against log Q will give n as the slope and log r as the intercept. Figure (9.3) shows the plotted points with a line fitted by linear regression.

The first observation on this graph is that it is, indeed, linear. There is no evidence of the curvature that would indicate a variation in n over the range considered. Secondly, the scatter of points is less than that usually expected in mine ventilation observations. The coefficient of correlation (in the range 0 through 1) is 0.9984. This result authenticates the experimental techniques that were employed.

The slope of the line on Figure 9.3 is 1.987, giving the law of airflow for the face to be

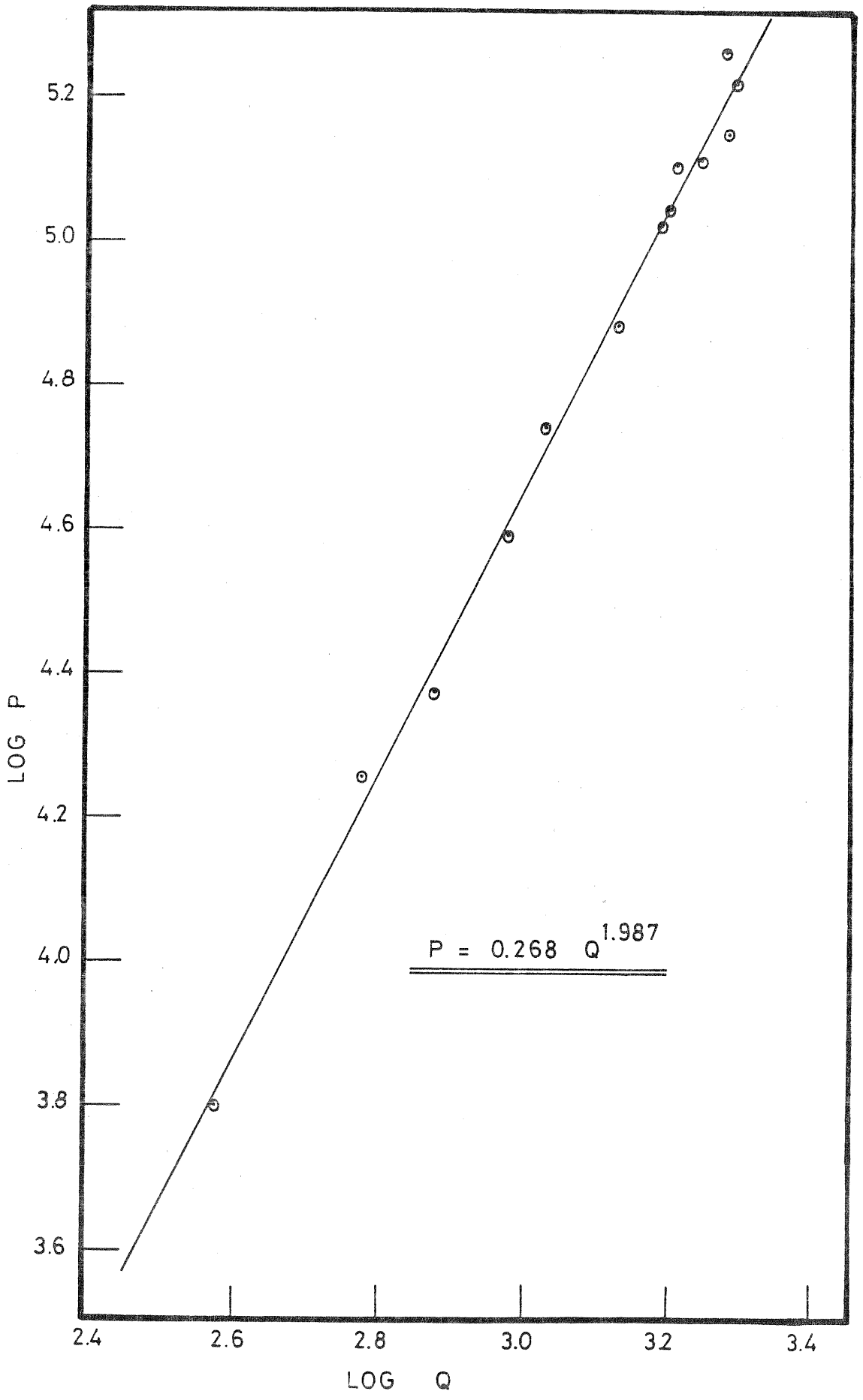

Figure 9.3 Pressure drop - airflow relationship on the longwall face.

$$p = R\,Q^{1.987}$$

The index varies from the theoretical value of 2 by only 0.65 per cent. This result is a very convincing verification of the square law for this longwall face.

9.4.5.2. Faceline resistance

Equation (9.24) shows that the intercept of the line on Figure 9.3 is log R. This gives a value of 0.268 P.U. for R, the equivalent resistance of the faceline. This is not quite the same as the true resistance of the faceline given in Section 8. as 0.2972 P.U.

During the square law test, the face airflow was measured accurately, but at one position only (station A4). However, at any moment in time, the airflow varied along the faceline due to leakage from and to the caved area. The extent of the variation is shown on Figure 7.6. From this diagram it is seen that the faceline may be divided into four sections and a mean airflow assigned to each section.

The full face pressure drop, p, measured during the square law test may be re-written as

$$p = R_1 Q_1^2 + R_2 Q_2^2 + R_3 Q_3^2 + R_4 Q_4^2 \qquad 9.25)$$

where the subscripts refer to the four sections of face.
This equation may be re-written as

$$p = R_1(C_1 Q_1)^2 + R_2(C_2 Q_1)^2 + R_3 (C_3 Q_1)^2 + R_4 (C_4 Q_1)^2$$

where $C_x = Q_x/Q_1$

Then

$$p = (R_1C_1^2 + R_2C_2^2 + R_3C_3^2 + R_4C_4^2)Q_1^2$$

It is the value of

$$R = (R_1C_1^2 + R_2C_2^2 + R_3C_3^2 + R_4C_4^2)$$

that is given by the intercept on Figure 9.3, while the true resistance of 0.2972 P.U. given in Section 8 is $R_1 + R_2 + R_3 + R_4$.

In order to check the consistency between
(i) the face resistance observations (Section 8)
(ii) the airflow law test, and
(iii) the face airflow distribution test (Section 7)
the section resistances and corresponding mean airflows have been collated from Tables 8.1 and 7.1 in order to calculate the values of C and RC^2. The results are given in Table 9.2.

Section	Mean airflow (from Table 7.1) Q (kcfm)	$C = Q/Q_1$	Actual Resistance (from Table 8.1) R (P.U.)	RC^2 P.U.
1 A3-A4	24.226	1	0.0664	0.0664
2 A4-A5	25.541	1.0543	0.0598	0.0665
3 A5-A7	23.212	0.9581	0.0824	0.0756
4 A7-A9	17.894	0.7386	0.0886	0.0483
			0.2972	0.2568

Table 9.2. Calculation of faceline equivalent resistance.

The equivalent resistance of the faceline, taking into account the variation in airflow along the face is calculated in Table 9.2 to be 0.2568 P.U. This compares with a value of 0.268 P.U. given by the intercept on Figure 9.3. The difference between the two results is 4.2 per cent. This is considered to be an excellent correlation involving data from three independent sets of observations on the longwall face.

10. LEAKAGE THROUGH CAVED WASTE

10.1. Significance of Gob Ventilation.

In standard triple entry longwall retreat mining, gob ventilation is performed by allowing the intact second and/or third entry ways to remain open. These airways can then be used as bleeder entries for gob ventilation and, if desired, as access ways.

The air pressure difference between the intake and return bleeder entries will cause air to leak through the gob. Stoppings constructed in the cross cuts on the intake side of the gob minimize this leakage, while open crosscuts on the exhaust side provide the outlets. The stoppings are located on the intake side so that the gob is maintained at a reduced pressure. This encourages any air leakage to flow from the face into the gob rather than vice versa and, hence, prevent the migration of accumulated gas onto the face.

Air leaking through the gob will reduce ventilating efficiency and, in susceptible mines, provoke spontaneous combustion. On the other hand, gob ventilation dilutes and removes accumulations of methane that would otherwise occur in the waste and which might cause emissions into the face line.

10.1.1. Loss of Ventilating Efficiency due to Leakage.

Leakage of air into a ventilated longwall gob is found to occur (as shown on Figure (10.1)): along the stoppings in the crosscuts on the intake side of the gob, (b) at the junction between the intake airway and the face line and (c) along the longwall face, through the shields. This leakage of air contributes to a loss in ventilation efficiency.

Ventilation efficiency is a measure which relates the air quantity reaching the face with the total air quantity provided. For a single longwall district, the ventilating efficiency may be computed as the percentage of the volume of air entering the face relative to the volume of air entering the district. Thus an efficient longwall ventilation system will allow the minimum amount of air to flow around or through the gob. This will keep the mine intake airflow requirement at a minimum. A subsequent reduction in the total required mine airflow may* result in a significant drop in fan operating costs. This is shown by the following relationships which assume that the total mine resistance remains constant.

* This is not always the case. See Reference [4]

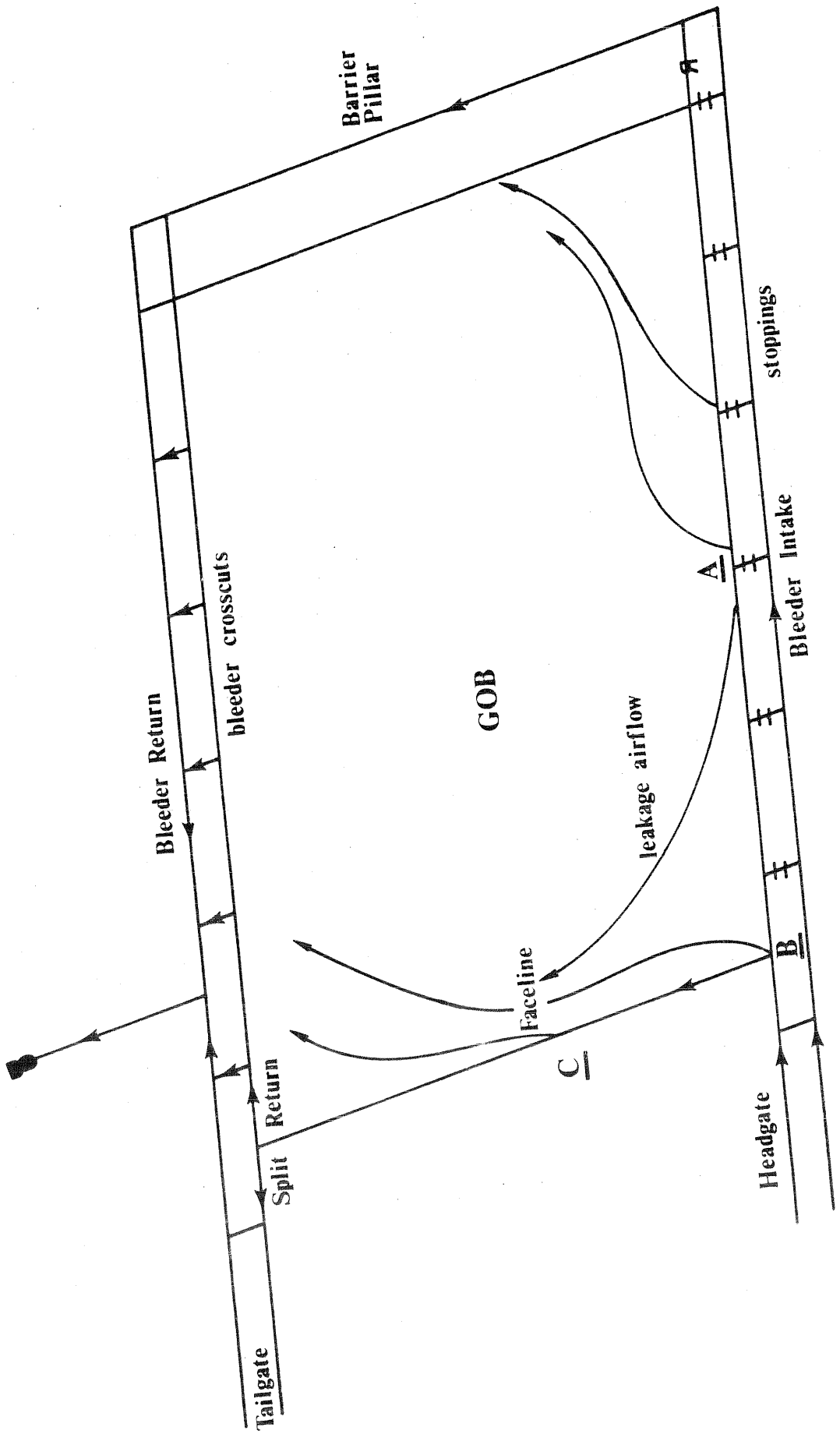

Figure 10.1 Location of leakage airflows into the longwall gob.

Assuming the square law:

$$P_{tot} = R_{tot}\, Q_{tot}^2 \qquad (10.1)$$

where: P_{tot} = Total pressure drop through mine (N/m^2)
R_{tot} = Total resistance of mine ventilation network (Ns^2/m^8)
Q_{tot} = Total volume flow rate provided by fan (m^3/s)

and since:

$$P = P_{tot}\, Q_{tot} \qquad (10.2)$$

where: P = air power required (watts)

then from (10.1) and (10.2):

$$P = R_{tot}\, Q_{tot}^3$$

but:

$$P \propto OC$$

where: OC = operating costs ($/yr)

then: $OC \propto R_{tot}\, Q_{tot}^3 = P$

now if Q_{tot} is decreased by ΔQ the new operating cost would be:

$$OC^1 \propto P \cdot \left\{\frac{Q_{tot} - \Delta Q}{Q_{tot}}\right\}^3$$

where OC^1 = reduced operating cost

Thus, the reduced operating cost is proportional to the cube of the new volume flow rate as a fraction of the original volume flow rate. Hence, from an economic viewpoint, it is evident that a ventilation system with the least amount of leakage or diverted air flow is an optimal system.

In many instances however, diverted and deliberate leakage airflow quantities are required to dilute methane emissions.

10.1.2. Methane Dilution

High concentrations of methane may be present in gob regions of longwall mines. The methane is either desorbed from the broken coal left in the gob, or is released from roof or floor sources following caving and relaxation of stress in the adjacent strata.

Due to the buoyancy of methane (specific weight 0.56 relative to air) accumulations of the gas tend to occur at higher elevations, for example at the roof of airways, at the top of ascentional - descentional airways and in airways up dip from a source. For a longwall face advancing or retreating along the strike of a dipping

seam, increased gas concentrations in the upper bleeder airway are common.

In gassy longwall situations, especially with dipping seams, gob ventilation is required if the face line is to be unaffected by waste area gas. The total leakage which flows through the gob dilutes the methane while the leakage from the face maintains the gas fringe within the caved area. The diverted air, which flows around the gob to the bleeder return, dilutes the gas emerging from the bleeder crosscuts to a value below the mandatory concentration limit. Federal regulations limit the methane concentration of the air flowing through the bleeder crosscuts to 2.0%. The air quantity flowing through the bleeder return must then be sufficient to dilute this to below 1.0% by volume.

In case of large methane accumulation in the gob and where spontaneous combustion is a problem, methane drainage should be employed.

10.1.3. Spontaneous Combustion

In longwall mines susceptible to spontaneous combustion, i.e. particularly in mines producing low rank coal, the velocity of the air leaking through the gob is important. Spontaneous combustion requires large surface areas of oxydizable material, and insufficient airflow to remove heat at the rate at which it is produced. These requirements are easily met in shadow areas of ventilated longwall gobs. Therefore to prevent spontaneous combustion from occurring, the appearance of a stationary critical zone in the gob should be avoided. This is best accomplished by rapid face advance [5].

Fortunately, at Snowmass, high concentrations of methane were not apparent and the coal was not liable to spontaneous combustion.

10.2. Survey of leakage through caved area at the Thompson Creek No. 1 Mine

During the field study, a separate survey was taken to determine the amount of air leakage through the caved waste region. Air quantities were determined at each opening connecting the gob to the bleeder airways.

10.2.1. Description of Leakage Survey Methods

At each crosscut or opening to the gob, the survey team measured the air velocity and the cross-sectional area. The product of these gave the volume-flow rate.

10.2.1.1. Velocity measurements:

The methods used to measure leakage air velocity depended on its magnitude. For relatively high velocities, calibrated vane anemometers and the moving traverse method were employed. Where the velocity was not uniform in cross section but still measurable by anemometer, a grid traverse was conducted. Where low velocity leakage occurred through a small uniform opening in a stopping, single spot measurements were taken using the aneomometer. When the air velocity was too low to be measured with anemometers, chemical smoke tubes were utilized. The smoke was timed as it travelled a known distance within the airstream. More accurate methods to measure slow moving air, such as the brattice window technique, were not utilized due to the large number of stopppings and time constraints. Velocity measurements were repeated at each site until three consistent values were obtained. These values were averaged and the appropriate calibration corrections were applied.

10.2.1.2. Area measurements:

Cross-sectional area measurements were taken immediately following each set of velocity determinations by means of a measuring tape. Since most of the cross-cuts were of fairly uniform shape, two horizontal and three vertical measurements were sufficient.

10.2.2. Survey Procedure

10.2.2.1. Bleeder Return Crosscuts:

All the bleeder return cross-cuts were open and accessible. The leakage air velocities were sufficiently high to allow moving traverses with the vane anemometers. All traverses were performed using a anemometer rod with the operator down wind of the instrument, and at least four meters into the crosscut. This prevented the measurements from being affected by turbulence, eddy currents and air reversal produced from end effects and airway obstructions. In addition to velocity and area measurements, methane concentrations were also determined. The resulting air quantities and the methane concentrations are shown on Fig. (10.2).

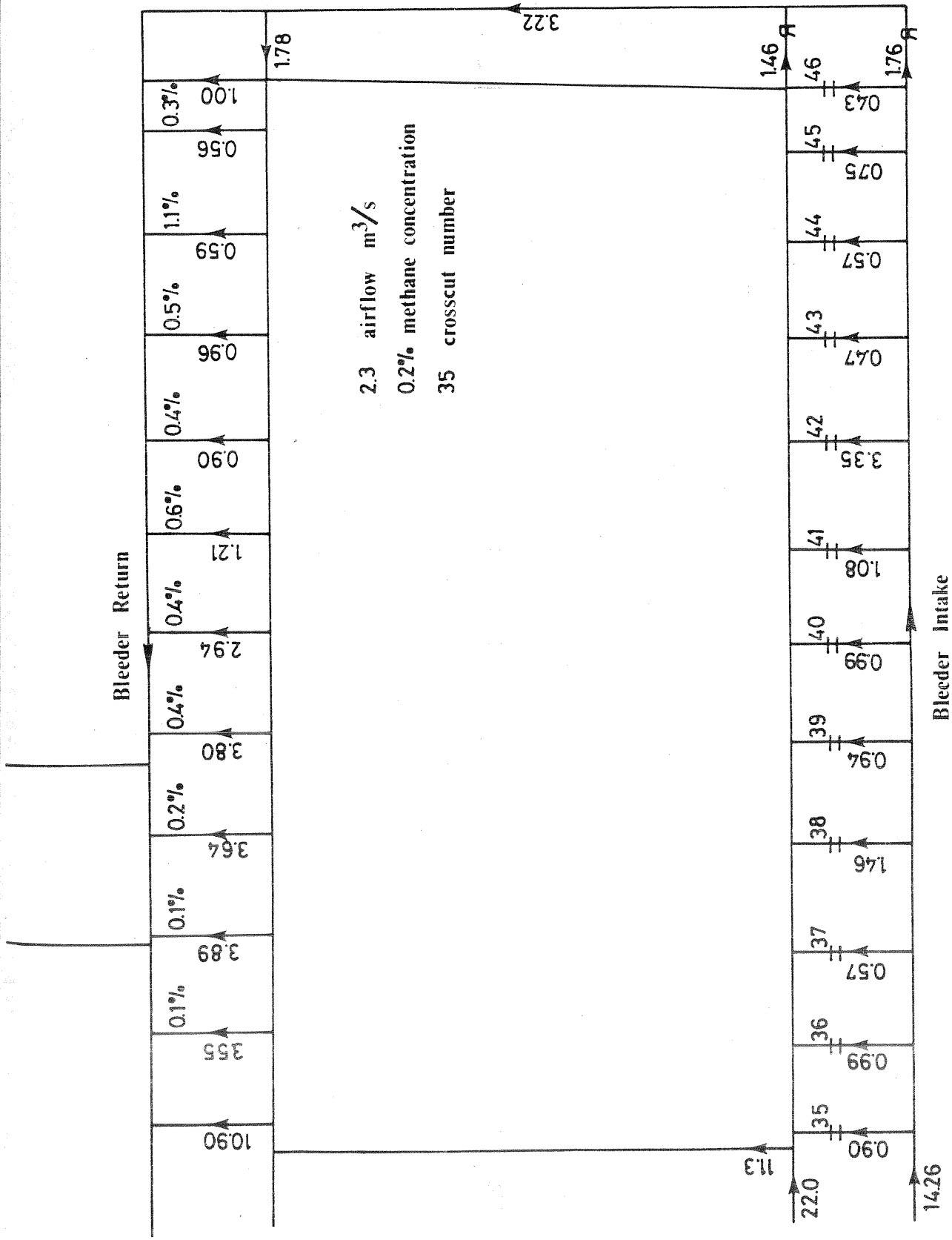

Figure 10.2 Leakage airflows and methane concentrations in crosscuts adjoining caved area.

10.2.2.2. Bleeder intake crosscuts:

Of the twelve crosscuts leading into the gob from the bleeder intake, ten contained intact masonary stoppings while the stoppings in two of the crosscuts, No. 38 and 42, (Fig. 10.2) were broken. These stoppings were, however, temporarily repaired with brattice cloth.

The leakage through the brattice stoppings was significant enough to allow the use of the vane anemometer. An anemometer traverse was also conducted at crosscut 41. The significantly higher flow rates obtained at these crosscuts can be seen on Fig. (10.2).

Due to sufficient but non-uniform air flow through crosscut 45, the spot traverse method was employed. The leakages through crosscuts 36, 43 and 46 on the other hand, were determined by spot anemometer measurements at holes in the stoppings. Dangerous roof conditions and running water prevented any form of measurement and required the estimation of the leakage through crosscut 37.

Smoke tubes were utilized to measure the velocity of the leakage flow through crosscuts 35, 39, 40 and 44. The time taken for smoke to travel between two fixed marks was measured by stopwatch, the upstream mark being at least six meters from the point of emission. The volume flow rates obtained from the velocity and area measurements are listed on Figure (10.2).

It is interesting to note that of the total air provided to the longwall district, around 24 m^3/s or about 60% leaked through the longwall gob.

10.3 Modelling the Caved Waste

This section of the report deals with computer network modelling of longwall ventilation systems. Reasons for requiring gob network models, the types of models presently used and improved models are discussed in detail.

10.3.1. Purpose of Modelling

It is important to be able to simulate ventilation systems of longwall gobs for the following reasons:

- the amount of air used for gob ventilation may be a significant portion of the air supplied to the longwall district and hence affects the economics and efficiency of the ventilation system.

- the gob ventilation system plays an important role in the control of environmental conditions in the mine, particularly for gas emissions and in seams liable to spontaneous combustion.

- to improve the accuracy of ventilation network simulation programs used in mine planning.

The results obtained from the survey conducted at the Thompson Creek No. 1 mine indicate that a substantial amount of air is used for a gob bleeder ventilation system. Most of this air leaks directly into the gob. Thus, to simulate the gob ventilation system realistically, any realistic model must account for this significant amount of leakage airflow.

An accurate simulation of the gob can be performed with a properly designed model. The criteria for a representative model are:

- The model must be able to describe accurately the leakage flow patterns present in a longwall gob.

- The model must be able to simulate the leakage from the bleeder intake way and the face line.

An ideal model, on the other hand, would comply with the above criteria , but, in addition, would be simple enough to be utilized by mine ventilation planners employing a network analysis program. Developing a model of this type was the objective of this part of the investigation.

10.3.2. Methods of Modelling Gob Areas

Present methods of modelling gob areas either neglect leakage through the gob or represent it by a few leakage branches. In this section, these current methods are described prior to discussing more complex, improved models. These improved models include a conventional finite element model along with two new models developed from the analysis of the Thompson Creek survey.

The two new models, termed the "difference" and the "simplified representative resistance" (SRR) model, were designed to give results

similar to a finite element model. Like a finite element model, the new models consider the gob as a permeable medium of varied consolidation. On the other hand, unlike the finite element model, the new models utilize representative branches, i.e. branches that represent a known volume of the medium, to simulate the leakage through gob regions. In addition, these new models were designed to be utilized with conventional network analysis programs.

The "SRR" model is a simplification of the "difference" model and was designed specifically for incorporation into an existing network analysis program. A finite element model, which is difficult to combine with conventional network analysis programs, was not developed with the Thompson Creek data.

10.3.2.1. Simple modelling methods:

When modelling longwall ventilation systems, ventilation planners frequently neglect the leakage through the gob. Gob bleeder systems are simulated by considering the intake bleeder and the bleeder return only. All the air which leaks through the gob is assumed to flow around the gob. The volume flow rate then remains constant along the face.

Several limitations are apparent with this oversimplified model. Since the leakage through the gob region is not considered, the effects of the gob on the total ventilation requirement for the mine (in terms of decreased resistance and the fan duties required) and the environmental effects are not simulated realistically.

Such a model should not be used for detailed analysis but may be employed when several longwall districts are modelled together within an overall network analysis of a mine. This will give an acceptable approximation to airflows in the main airways but may be considerably in error on, or close to, each face.

Another modelling method used by ventilation planners to simulate longwall gob ventilation systems, is the equivalent resistance method. In this case, the practice is to construct branches leading from the bleeder airways to a common center node as shown on Figure (10.3). These leakage branches are usually oriented fairly symmetrically around the gob. Resistance values are ascribed to these branches such that they represent the total gob resistance.

This method, unlike the pevious one, does consider leakage through the caved region. Since representative resistances can be ascribed to the gob leakage branches, a realistic leakage quantity can be simulated. On the other hand, the leakage flow paths do not represent airflow through defined regions of the gob. Thus, this model cannot describe the airflow patterns which occur within a longwall gob. This model should be used only for a simplified simulation, where only the magnitude of leakage need be considered. To simulate the quantitity, as well as the path and distribution of the leakage through a gob, an improved modelling method must be used.

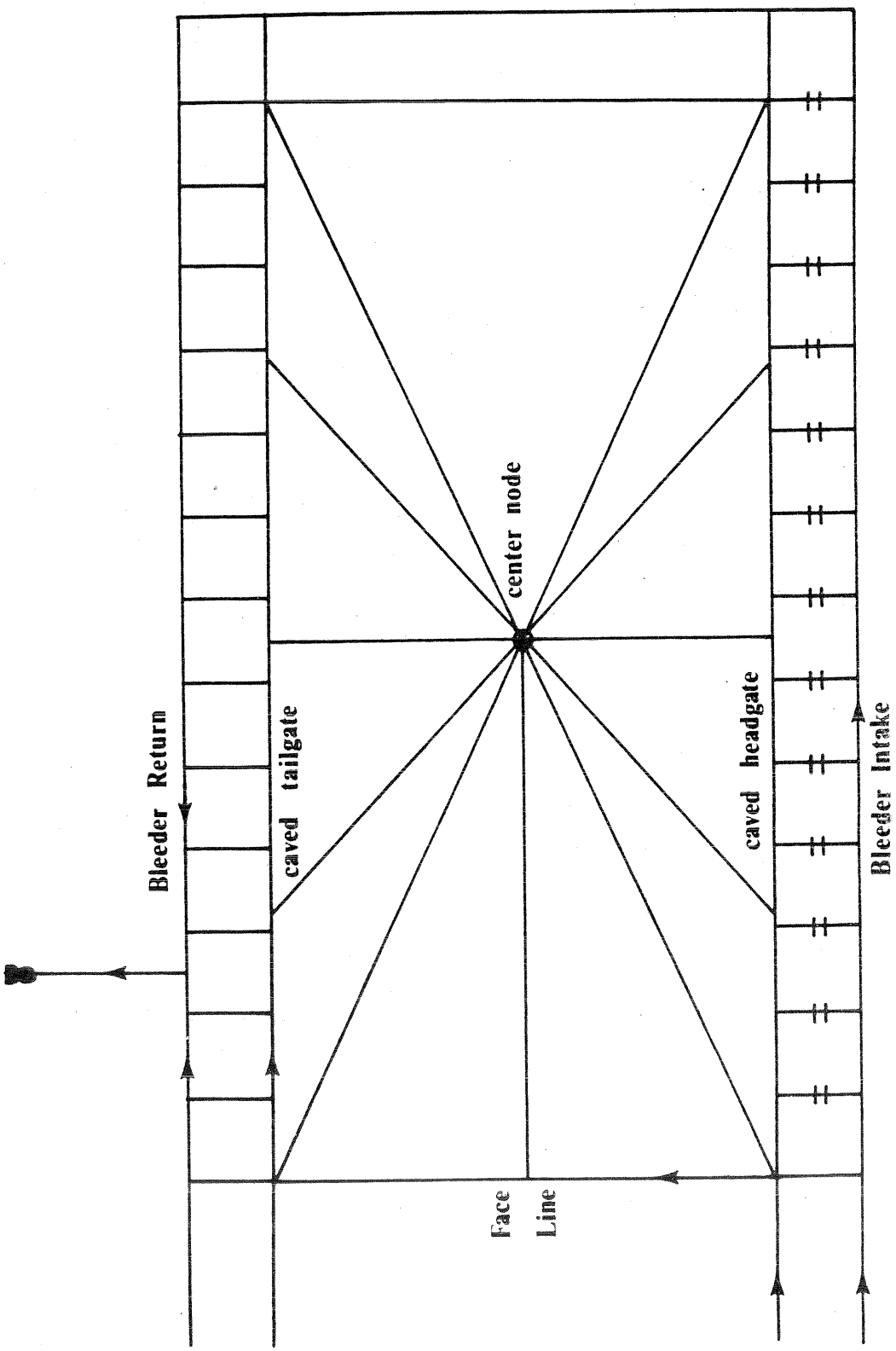

Figure 10.3 Equivalent resistance method used to model leakage through the gob.

10.3.2.2. Basis for improved gob models:

The caved gob region can be described as a porous medium of variable grain size and consolidation. Since the gob region is not an airway, representative resistances, (resistance of a known volume of the gob), may be used. When the leakage flows are in the turbulent regime, an equivalent turbulent resistance must be estimated. On the other hand, if the leakage air falls in the laminar flow regime, laminar resistance can be calculated from the permeability. Thus the type of resistance depends on the flow regime of the leakage air. All the improved methods, the finite element model, the difference model and the SRR model, are based on the assumption that the leakage flows are all in the laminar flow regime.

Flow regime:

For an airway, velocity, size and roughness are the main factors affecting the airflow regime. The airflow regime is represented by the dimensionless Reynolds number,

$$Re = uD/\nu$$

where : Re = Reynolds number based on hydraulic diameter of airway
u = Center line velocity (m/s)
ν = kinematic viscosity of fluid (m^2)

and

$D = 4A/O$
= hydraulic diameter of airway (m)
O = perimeter of airway (m)
A = flow area of airway (m^2)

With non circular airways, the transition Reynolds number is found to be around 2300. Flows with Reynolds numbers greater than 40,000 may be considered to be turbulent, while flows with Reynolds numbers less than 2300 are considered laminar (Section 9.3.2.). A variable range of Reynolds numbers exists, where the flow transforms from laminar to turbulent or vice versa. This region of the flow regime is termed the transitional zone and its range is a function of surface roughness, bends, disturbances and the direction of the flow transformation.

To determine the flow regime for leakage through a porous medium, the Reynolds number must be evaluated with external flow considerations.

The airflow through a porous medium is considered to be in the laminar flow regime when the Reynolds number, based on average particle size, is less than 1.[6]

Turbulent flow equation - Turbulent resistance

The general flow equation relating frictional pressure drop to volume flow rate is:

$$p = RQ^n \qquad (10.4)$$

where: p = frictional pressure drop
Q = volume flow rate (m^3/s)

and n, the exponent, ranges between 1 and 2 depending on the flow regime. For fully developed turbulent flow, n is equal to 2, thus:

$$p = RQ^2$$

where: R = Turbulent resistance $\left(\frac{Ns^2}{m^8}\right)$

For mine airways, the turbulent resistance is a function of the geometry, surface roughness and length of the airway.

$$R = \frac{k\,l\,O}{A^3} \qquad (10.5)$$

where: R = turbulent resistance $\left(\frac{Ns^2}{m^8}\right)$

k = airway friction factor (kg/m^3)
l = length of airway (m)
O = perimeter of airway (m)
A = cross-sectional area of airway (m^2)

On the other hand, for a flowpath representing turbulent flow through a volume of material, the turbulent resistance cannot be calculated as above. The turbulent resistance must be equivalent to the combined resistances of the many small flow paths through the medium. Since this cannot be easily calculated, an estimated equivalent resistance is chosen.

Laminar flow equation - laminar resistance

For laminar flow, the exponent n, of equation (10.4), is taken as unity. Thus the laminar flow equation is linear:

$$p = R_L Q$$

where: p = frictional pressure drop (Pa)
R_L = laminar resistance (Ns/m^5)
Q = volume flow rate (m^3/s)

Laminar resistance, for flow through a permeable medium, is a function of the geometry and permeability of the medium, as well as the fluid properties.

From Darcy's equation for flow through a permeable bed, neglecting the compressibility of air:

$$Q = \frac{k A p}{\mu L}$$

where: Q = volume flow rate (m^3/s)
k = liquid permeability of medium (m^2)
μ = dynamic viscos ity (Ns/m^2)
A = cross-sectional area (m^2)
p = pressure drop (Pa)
L = length of bed (m)

upon rearranging:

$$p = (\mu L/kA)Q$$

hence:

$$R_L = (\mu L/kA) \qquad (10.6)$$

For network analysis, it is convenient to model laminar airflows through porous regions, such as caved gobs, by representative laminar resistance branches. These branches are assigned resistance values corresponding to the resistance of the volume of medium represented. The following example illustrates the determination of the flow regime and the calculation of a representative resistance for a permeable region.

Example

A porous volume of dimension 150 x 150 x 4 meters and of liquid permeability 2 x 10^{-7} m^2 is represented by an airway as shown on the following Figure .

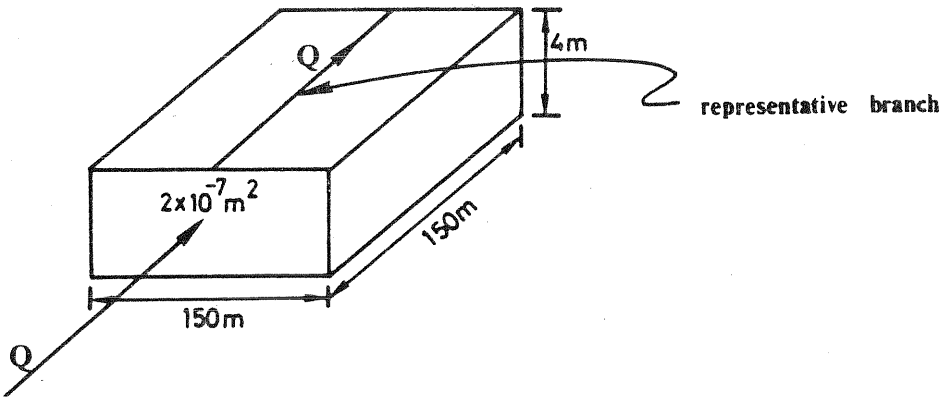

D = average particle diameter-.015m
Q = volume flow rate - 0.5 m^3/s
ρ = density of air-1.2 kg/m^3
k = permeability-2 x 10^{-7} m^2
A = cross-sectional area-$600m^2$
μ = dynamic viscosity of air-1.84 x 10^{-5} Ns/m^2

(1) To find velocity:

using the volume - flow relation

$$Q = u A$$

where: Q = volume flow rate (m^3/s)
u = velocity (m/s)

rearranging and substituting from the data given:

$$u = Q/A$$

$$u = 0.5/(150 \times 4) \ \frac{m^3}{s} \cdot \frac{1}{m} \ \frac{1}{m}$$

$$u = .00083 \text{ m/s}$$

(2) To find the Reynolds number:
using equation (10.3)

$$Re = uD/\nu$$

where: ν , the kinematic viscosity is equal to : μ/ρ

$$\nu = \mu/\rho = \frac{1.8 \times 10^{-5}}{1.2} \ \frac{Ns}{m^2} \cdot \frac{m^3}{kg}$$

$$= 1.53 \times 10^{-5} \ Ns \ m/kg = (m^2/sec)$$

then:

$$Re = \frac{(.00083)\cdot(.015)}{(1.53 \times 10^{-5})} \quad (m).(\frac{m}{s}).(\frac{s}{m^2})$$

$$= 0.814 \text{ which is less than 1.}$$

Flow is, therefore, laminar.

(3) To find resistance of representative airway:

Since airflow is laminar, equation (10.6) is used:

$$R_L = \mu L/kA$$

$$= \frac{(1.84 \times 10^{-5})\cdot(150)}{(2 \times 10^{-7}) \cdot (150x4)} \quad \frac{(Ns)}{(m^2)} \cdot (m) \cdot (\frac{1}{m^2}).(\frac{1}{m^2})$$

$$= 23.00 \quad \frac{Ns}{m^5}$$

Using representative branches to model airflow through a permeable medium has its limitations, in that the airflow patterns are confined by the branches themselves. A finite element model, on the other hand, does not suffer from this disadvantage since it does not utilize representative branches.

10.3.2.3. Finite element modelling:

Although a finite element analysis was not performed, the design procedure, the output expected and the disadvantages of a finite element gob model will be discussed.

Description

The flexibilities allowed in constructing finite element grids enables various degrees of accuracy to be obtained. For a longwall gob, the size and distribution of the elements should be chosen such that the important zones are detailed. An ideal element pattern would have small elements concentrated behind the face line and along the bleeder airways where most of the leakage occurs. Larger elements would be located at the center of the gob where less flow pattern detail is required.

Each element in the grid should be assigned a permeability depending on its location relative to the redistributed vertical stress. As shown in Figure (10.4), the redistributed vertical stress over a longwall gob is dome shaped. Vertical stress gradients exist,

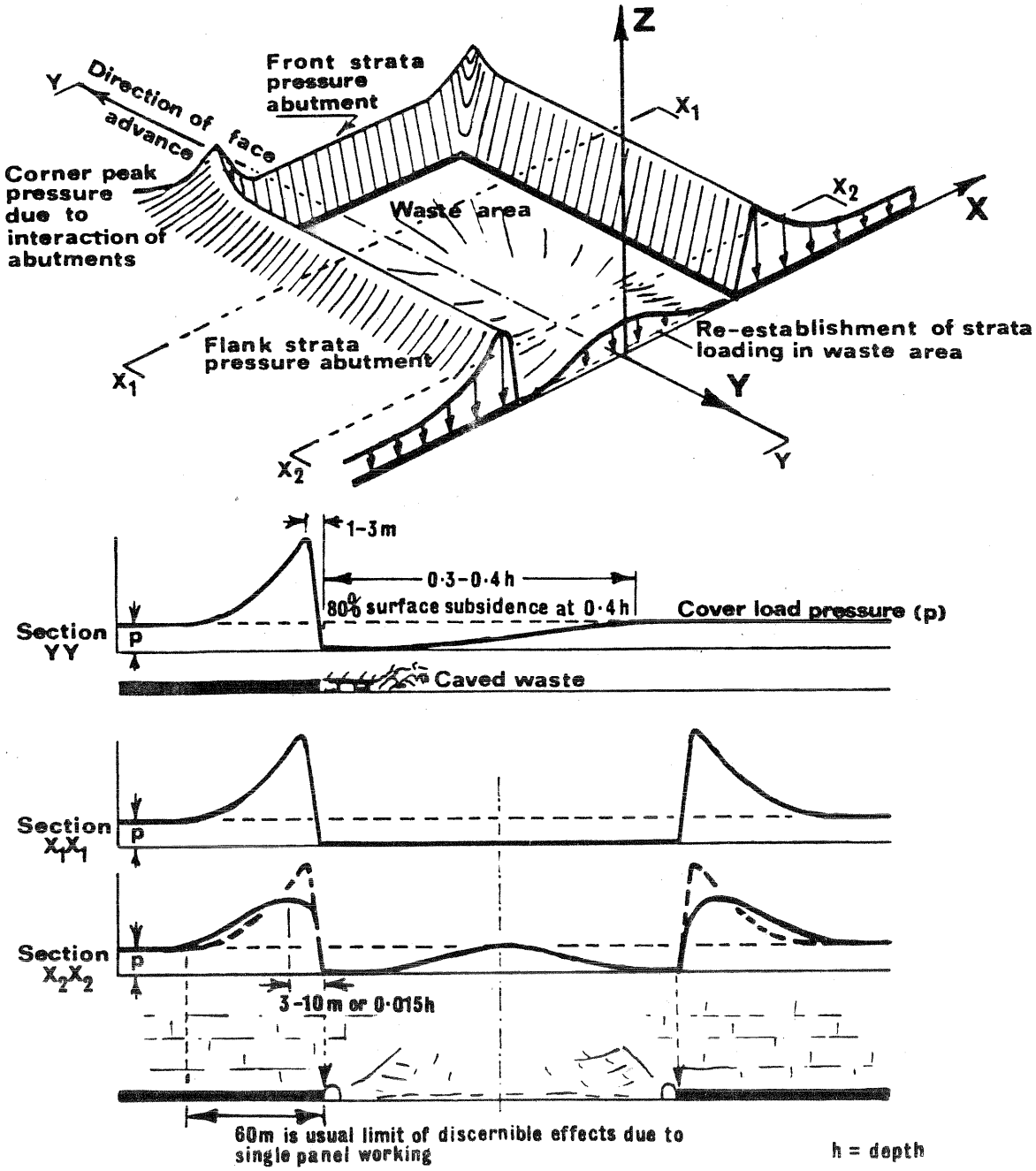

Figure 10.4 Redistribution of vertical stress over longwall gob.[7]

initiating at the gob edges and proceeding to the center. The permeability is a function of the consolidation of the medium and this is directly proportional to the redistributed vertical stress. Thus the elements should be assigned low permeability values at the gob center, and increasingly larger permeability values toward the gob edges. The next step in the design procedure requires the definition of the boundary conditions.

All four boundary conditions, required for a steady state, two dimensional finite element analysis, are of the same type. As shown on Figure (10.4), the caved airways immediately surrounding the gob are subjected to a relaxed stress zone. Thus, these airways do not cave completely but remain open enough to lead leakage airflow around the caved gob region. The air velocity in these airways is assumed to be high enough to be in the turbulent region and thus obey the square law. From the square law and reference pressures, the pressure distributions along these boundries can be represented as functions of position. The pressure distribution fuction will then define the pressure of each element node along the boundaries.

Output from a finite element model.

After successive iterations to obtain the steady state solution, the computer program will have determined the pressure at each element node and the air velocity at the center of each element. Constructing velocity contours will reveal the final airflow patterns represented.

This model will give an accurate simulation of the airflow pattern and the airflow quantities leaking into the gob. It relates the airflow pattern to the stress distribution and does not confine airflow to representative branches. In other words, this model simulates the leakage by considering the actual physical conditions present in a gob region. This method is by far the best if a very detailed and accurate gob model is to be devised. A model of such detail may be required to research into, for instance, the effect of gob ventilation on spontaneous combustion or methane migration in the caved area.

Limitations

The finite element model has its drawbacks, in that it requires a great deal of computer memory and run time. This makes it impracticable to incorporate finite element techniques into an iterative network analysis program and, in any case, such detailed results are not required for most ventilation planning purposes. If this is the case, a simpler "difference" type of analysis can be used in conjunction with a conventional network analysis program to obtain results of adequate scope and accuracy.

10.3.2.4. Difference model:

The difference model, developed during this investigation, combines a satisfactory simulation of leakage patterns in the gob with the speed and convenience of a ventilation network analysis program. The major difference between this model, and the finite element model, is that here, representative airways are utilized. By distributing these airways plentifully and symmetrically throughout the gob, and by assigning permeabilities related to the stress conditions, the results can approximate those from a finite element model.

Description

As with the finite element model, the difference model utilizes an element grid. Elements of known dimension should be constructed, as rectangles, with equal dimensions for simplicity; but may be of various sizes. Due to the use of representative flow paths which confine the airflow, a large number of elements will be required to approximate the finite element solution. Thus the more elements used, the more detailed the solution. Each of these elements should be assigned values of permeability according to the redistributed vertical stress.

Airways representing the airflow through each element should be constructed diagonally through each rectangular element as shown on Figure (10.5). Each branch is then assigned a resistance computed from the laminar resistance equation; (eqn.(10.6)). The permeability of the element, the element dimensions and the permeable cross-sectional area are the main parameters controlling these resistances. The increased vertical stress at the center of the gob decreases the permeability of the broken zone. This creates a high resistance dome along the center of the gob.

High resistances should also be assigned to the branches leading from the face line. These are required to represent the sealing effect of the longwall shields. The shields help to confine the air to the face line and thus act much like the stoppings in the bleeder intake airway.

The airways around the gob, i.e. the caved head and tailgate airways, contain turbulent airflow and should be assigned turbulent resistances.

Output from Difference Model

With the use of a ventilation network program, modified to accommodate laminar airflows, a balanced network model of the gob can be obtained. The program will determine the volume flow rate and the

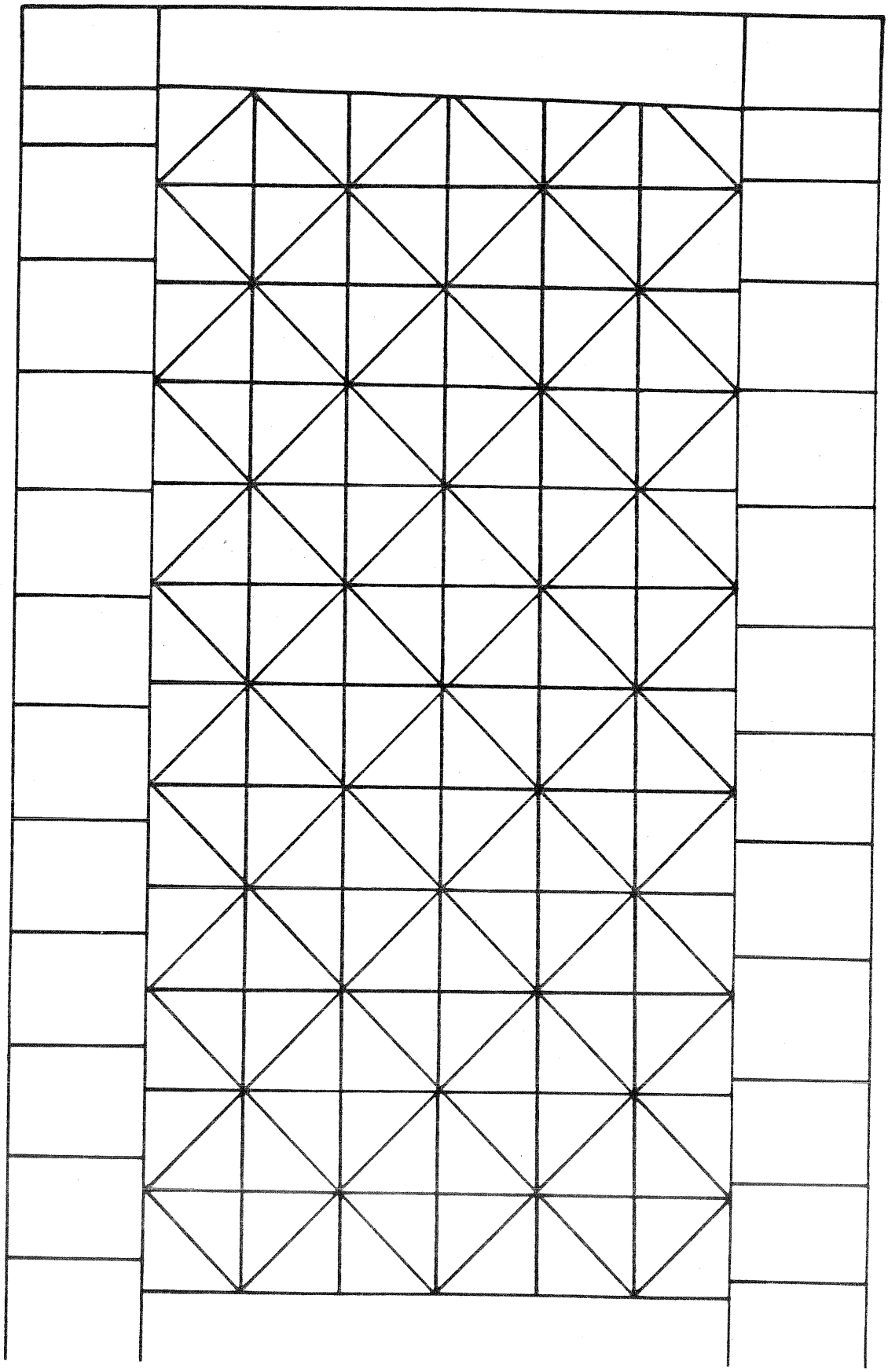

Figure 10.5 Representative branches constructed through rectangular elements for Difference model.

pressure drop through each representative branch in the gob. From these values the leakage airflow pattern can be visualized and drawn.

This type of model can be used, if enough elements are implemented, as a substitute for a finite element solution. The model utilizes the same flow equations and represents the stress conditions in a similar fashion. The degree of correlation with the finite element model is, however, a function of the number of elements.

Limitations

The detail involved in this model may not be desired by the ventilation planner. However, a simpler model, designed from the airflow patterns obtained from the difference model, may prove to be adequate.

10.3.2.5. Simplified Representative Resistance Model:

The simplified representative resistance (SRR) model, a simpler version of the difference model, is designed to be used by ventilation planners to describe the leakage characteristics of longwall gobs simply but with acceptable accuracy. The object of this model is to be able to obtain results similar to the complex element model by utilizing fewer branches.

The stress distribution pattern over the gob region suggested the type of model that could be designed. The resulting airflow patterns could be visualized since they are direct functions of the permeability of the medium. The permeability, on the other hand is related to the consolidation of the medium and is governed by the redistributed stress.

Description

From the stress distribution, Fig. (10.4), it is evident that most of the leakage air will flow around the consolidated center of the gob. The flow will be concentrated in the convergence zones behind the shields and along the bleeder airways. The SRR model allows these concentrated airflows to be represented by branches connecting elliptically around the center gob zone as shown on Figure (10.6). The relatively small amount of leakage that occurs through the highly consolidated center is not neglected but represented by high resistance branches. The number of leakage airways leading to the gob should be equal and symmetrical on opposite sides. This assumes that since the stress distribution is symmetrical, the airflow distribution can also be represented symmetrically.

Since fewer leakage airways are used, they now each represent a larger area. The laminar resistances must be adjusted to correspond to their representative areas. High resistance values are still

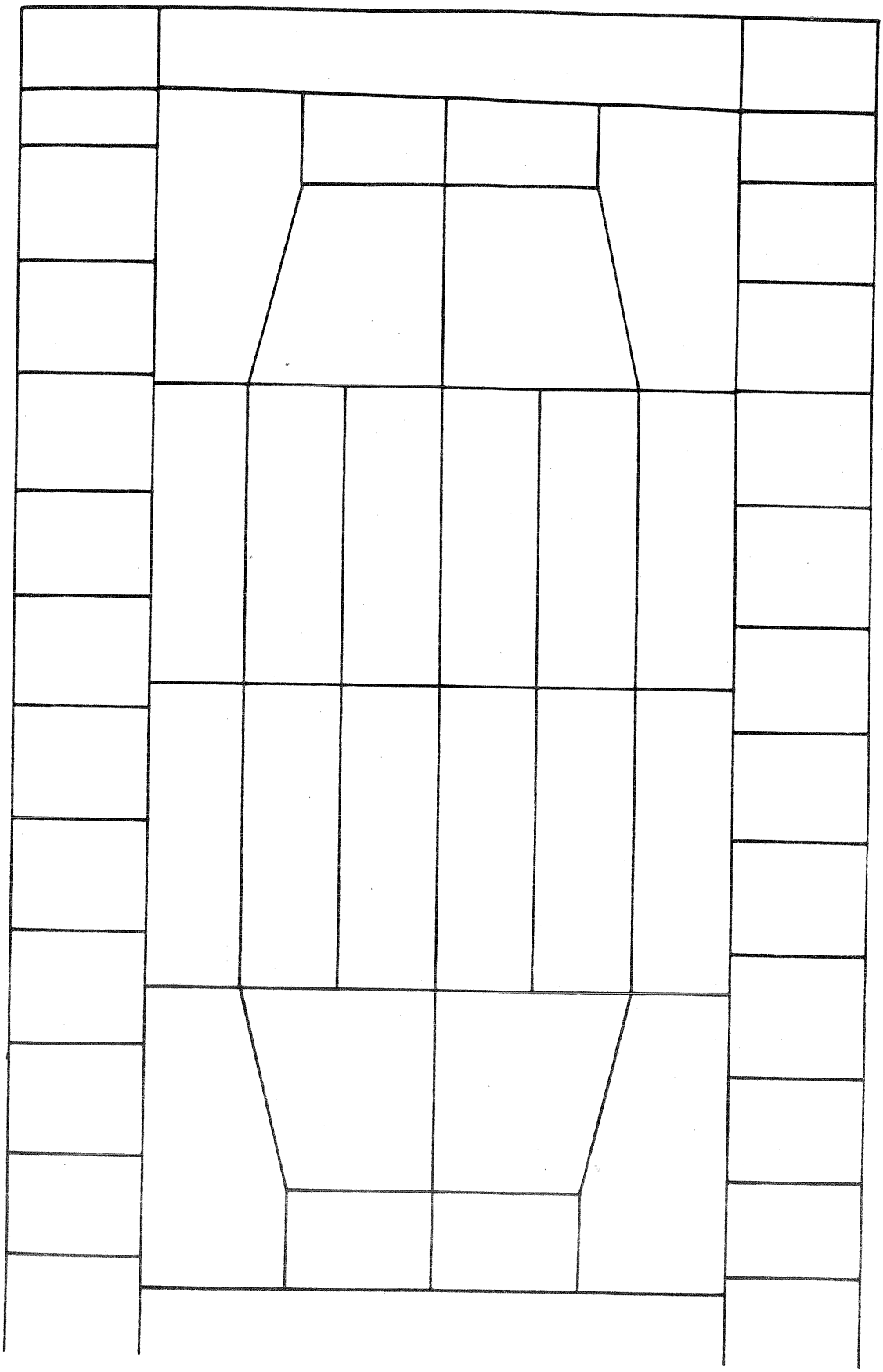

Figure 10.6 Arrangement of representative branches in gob for S.R.R. model.

necessary for the flowpaths leading into the gob from the longwall face. Similar to the other improved models, the airways surrounding the gob are assumed to carry turbulent air. Thus turbulent resistance values must be computed for these airways.

Output to expect from SRR model

With the use of a ventilation network program, modified to consider laminar airflow, a balanced network model can be obtained. Volume flow rates and frictional pressure drops will be computed for each representative branch. From these values the magnitude of the leakage and the leakage pattern can be visualized.

This model describes, in a simplified manner, the airflow magnitudes and patterns, relative to the stress distribution over the longwall gob. With fewer representative airways the leakage pattern can be well simulated. In addition, the simplicity of this design enables ventilation planners to analyze leakage characteristics of longwall gobs with minor modifications to existing network programs.

10.4. Application of the Models to the Thompson Creek No.1 Mine

The difference model and the simplified representative resistance (SRR) model were both applied to the gob area of the Thompson Creek No. 1 mine. Correlation studies were undertaken in order to compare the results from each of these models to the airflows measured in the mine. These models were incorporated into the ventilation network analysis program, VNET, which was also modified to accomodate airflow in the laminar flow regime. The modifications necessitated an amendment to the program in order to incorporate an additional input variable, the exponent of the general flow equation (equation 10.4).

For both models, the gob region was isolated from the rest of the mine and analyzed separately. Appropriate airflows into the gob were fixed as regulated quantities to simulate the airfow from the rest of the mine. This separation permitted the models to be designed to emphasize the airflow patterns in the gob. Both models were correlated with the actual measurements shown on the network on Figure (10.7). The correlations were deemed adequate when the face airflow pattern and the distribution of the airflows through the bleeder crosscuts were similar.

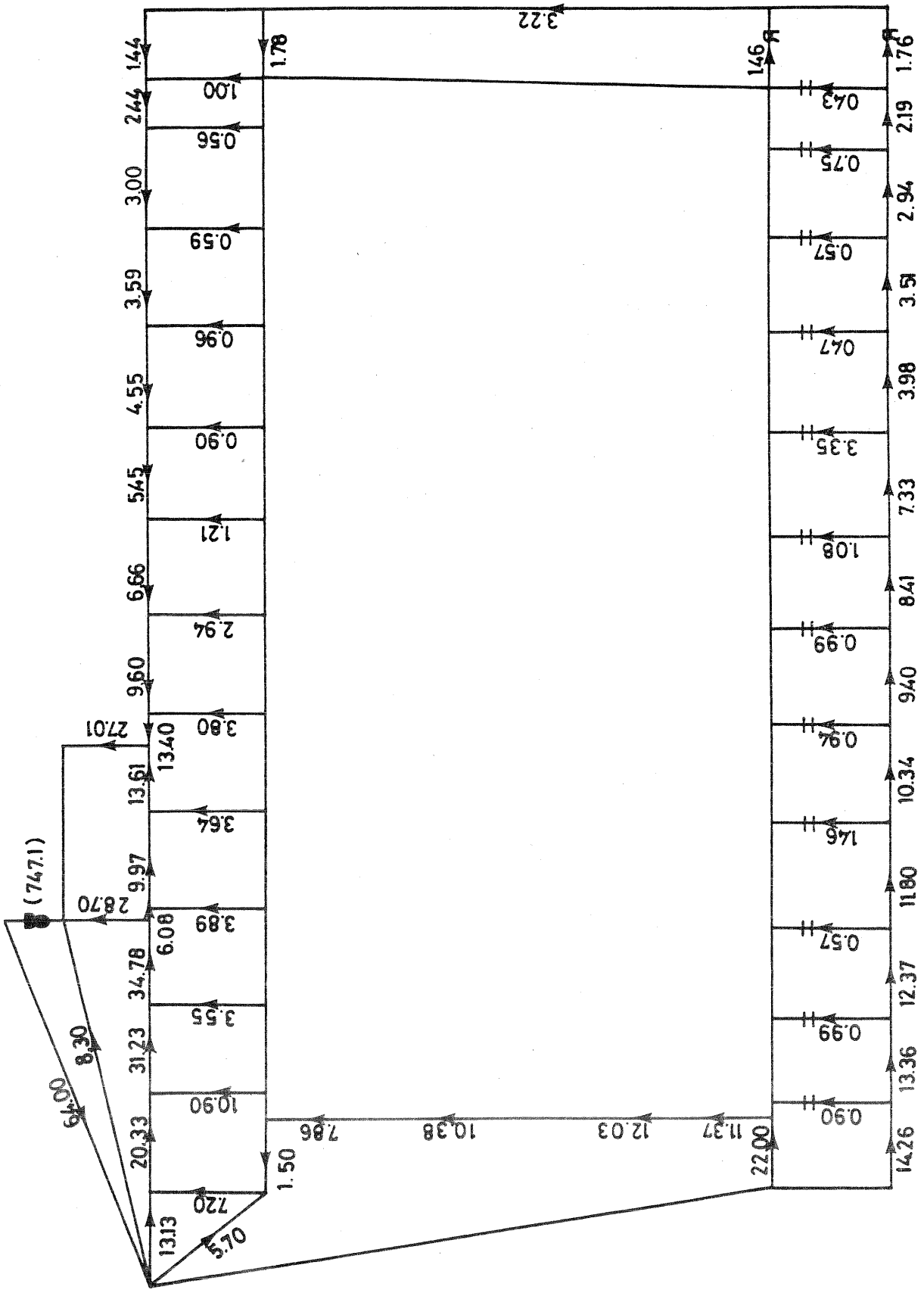

Figure 10.7 Measured airflows in m^3/s used for model correlations.

10.4.1. Snowmass Difference Model

This section discusses the construction procedure which was required to simulate the Thompson Creek No. 1 mine using the difference model. The resistances used and the results obtained will also be shown in detail.

10.4.1.1. Network design:

The isolated gob area was divided into a 12 by 6 grid leaving uniformly sized rectangles measuring 18 by 53.85 meters, Fig (10.8). The elements were constructed of equal size for simplicity, in that the resistances of the representative branches could be compared on a consistent length basis.

Permeability values in the range 10^{-6} m^2 to 10^{-8} m^2 were assigned to the elements, depending on their location. The lowest values of permeability were assigned to the 10 x 2 element region at the center of the gob, while the higher values were assigned to the perimeter elements. The permeability values of the remaining blocks were chosen such that symmetrical decreasing gradients of permeability existed, extending from the rib sides to the center.

From the values of permeability and the geometry of the blocks, laminar resistance values were computed and assigned to diagonal representative branches. This was performed with equation (10.6).

$$R_L = L\mu / kA$$

where the only variables per block were k, the permeability and A, the permeable cross-sectional area. The representative resistances required to simulate Snowmass are shown on Figure (10.8) and are also given in the form of element resistance contours on Figure (10.9). The large resistances assigned to the representative branches leading from the face are due to the shield sealing effects and were obtained by correlation with the measured data.

The resistances of the turbulent airways immediately around the gob, the caved headgate and tailgate airways were also obtained by correlation with survey data. The cross-sectional area of these airways decreases on moving away from the face. This results in the resistance gradients shown on Figure (10.10).

10.4.1.2. Results:

The correlating network, with the airflows ascribed to each representative branch, is shown on Figure (10.11). This correlation was obtained with the data given above and the modified VNET program.

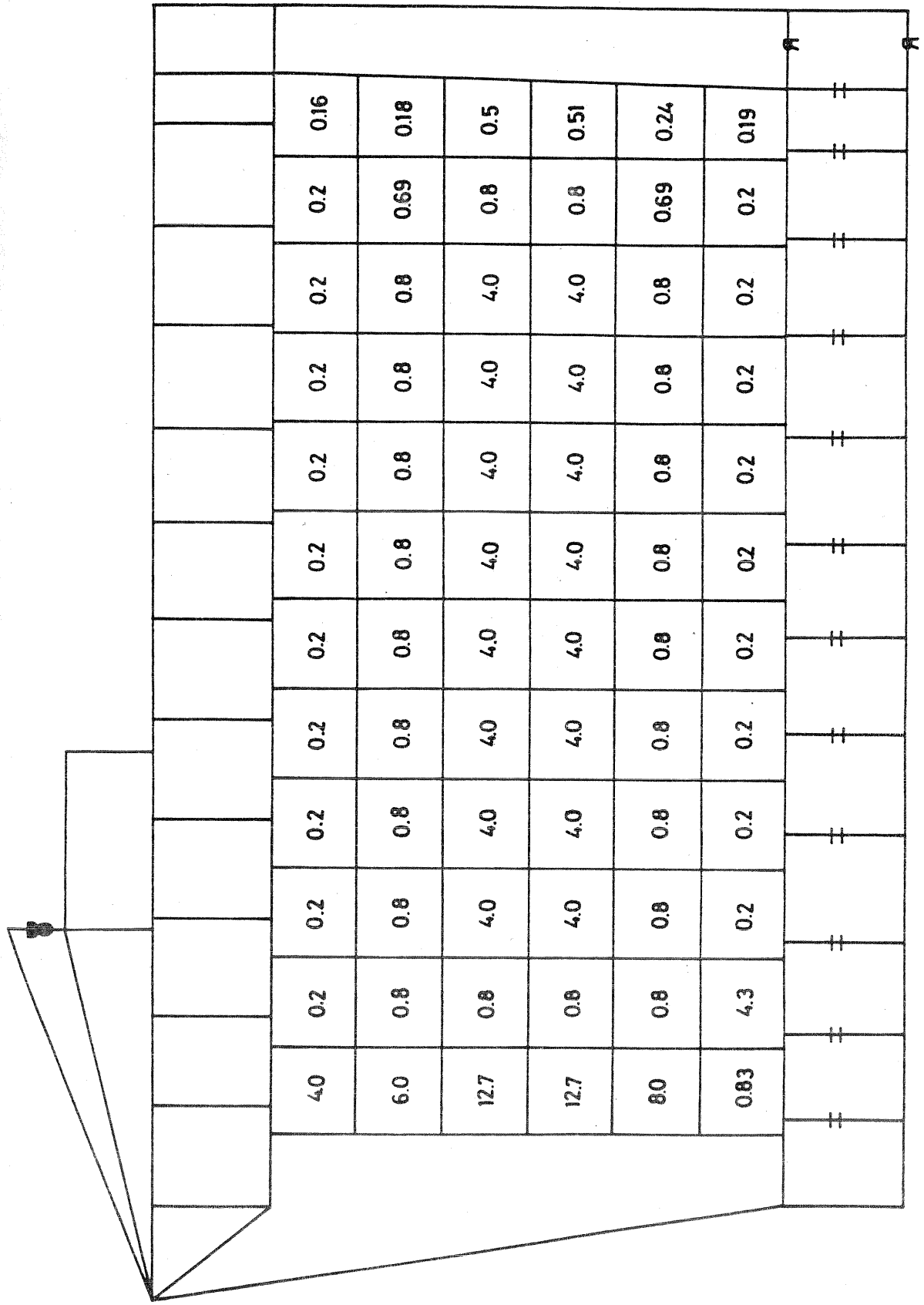

Figure 10.8 Element grid and representative resistances (Ns/m^5) used to simulate gob with Difference model.

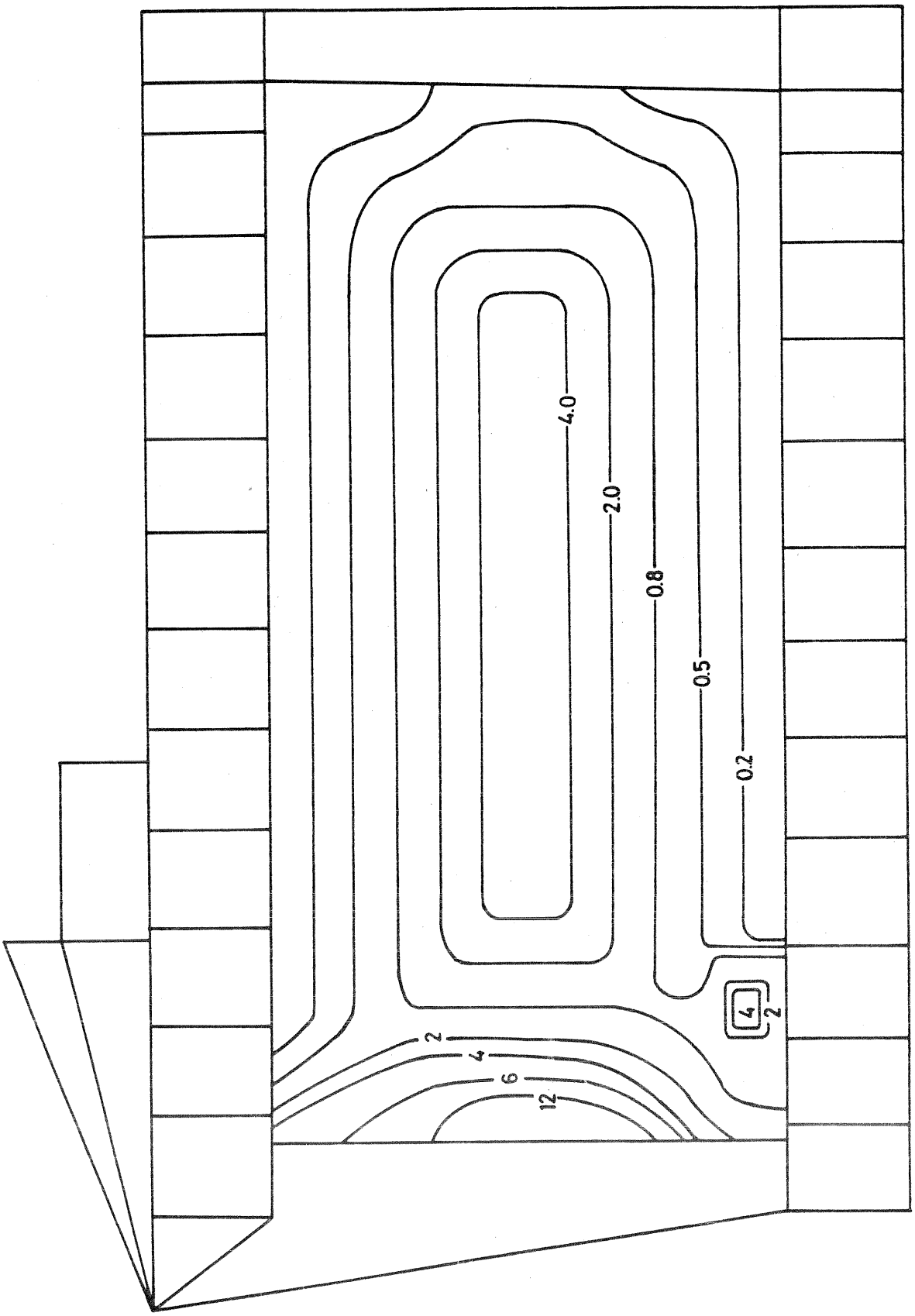

Figure 10.9 Contours of resistance elements used for Difference model.

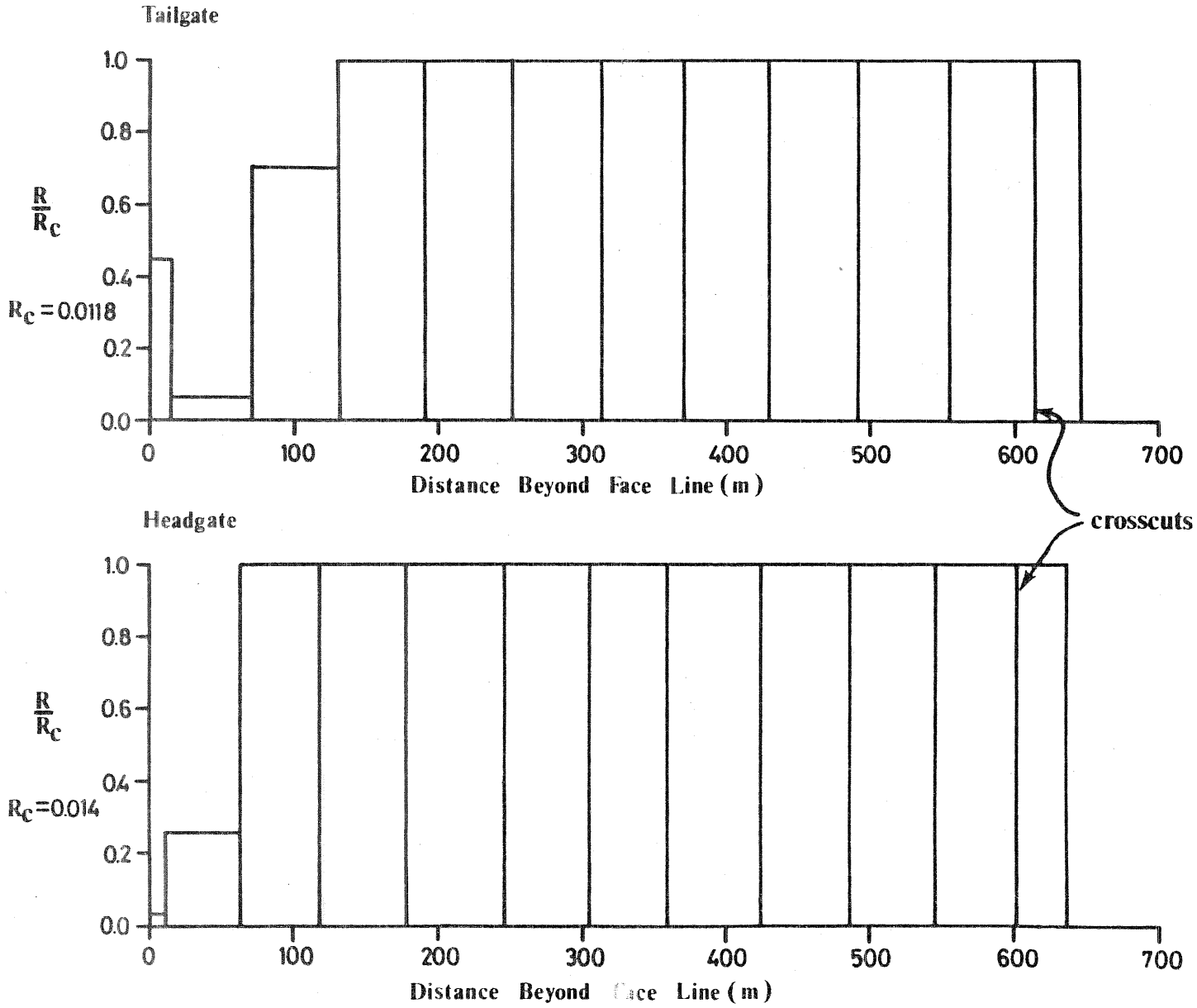

Figure 10.10 Normalized resistances (Ns^2/m^8 per meter) of the caved headgate and tailgate airways used for the Difference model correlation.

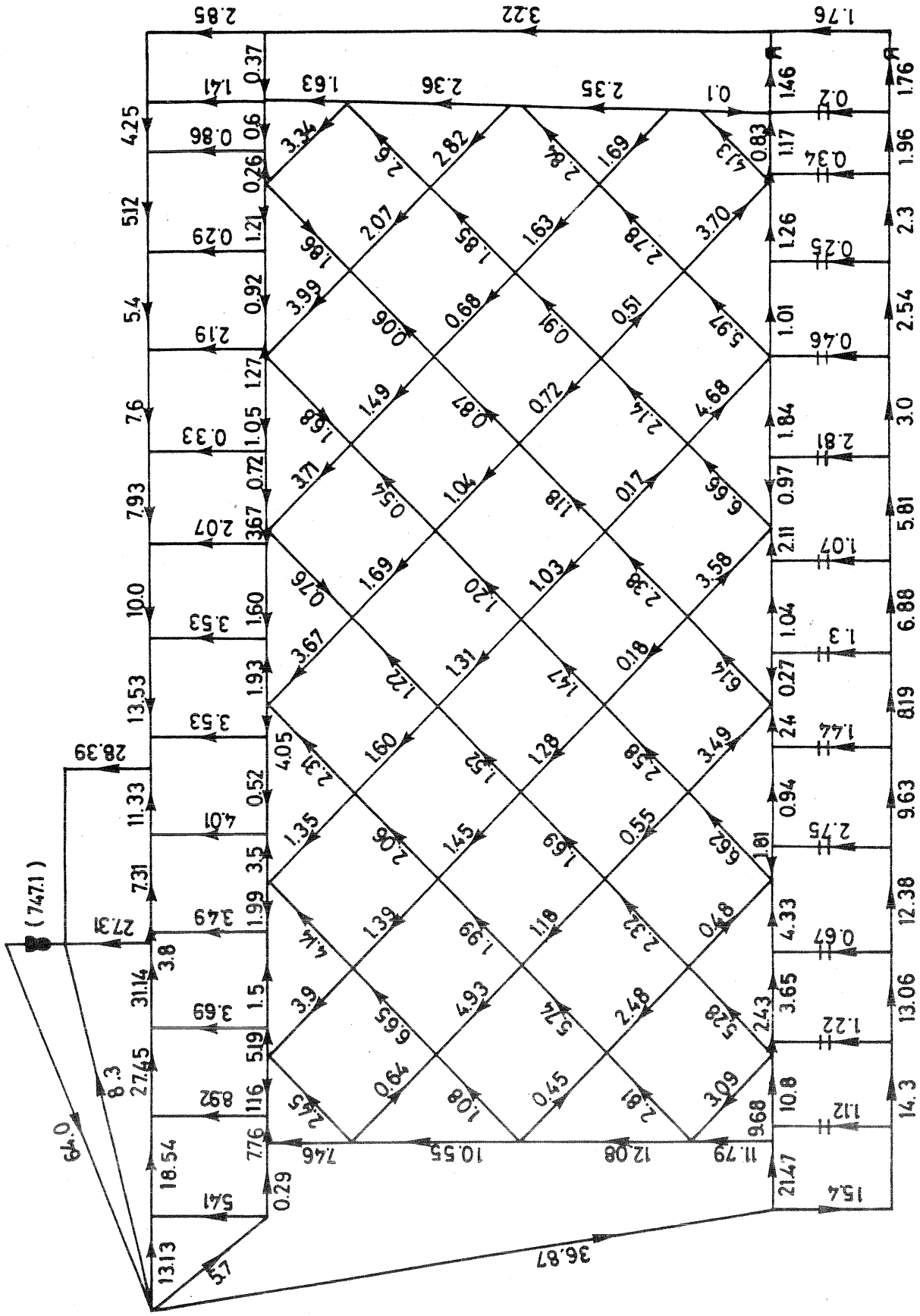

Figure 10.11 Simulation of the airflow distribution in the gob obtained with the Difference model.

Analysis of the airflow distribution indicates that the leakage air follows the same pattern as that described in the previous section. The leakage flows mainly behind the shields, near the caved headgate and around the highly consolidated center zone. Since this distribution pattern can be simulated by the SRR model, the research continued by investigating the correlation that could be obtained with this simpler model.

10.4.2. SRR Model applied to Thompson Creek No. 1 Mine Data

10.4.2.1. Design:

Using the grid layout obtained from the difference model, three feeder airways were constructed, evenly spaced, from each side of the gob. Connected to these were the leakage paths which encircle the highly consolidated center zone. These were, in turn, interconnected with branches leading through the gob center as shown on Figure (10.6).

Different values of laminar resistance were ascribed to the representative branches depending on their position and length. These resistances were lower than the resistances used in the difference model since each branch now represented a larger area. The relative resistance distribution of the airways in the gob remained similar to that of the difference model and is shown on Figure (10.12).

The resistances of the caved head and tailgate airways required some modification but remained of similar magnitude to the values ascribed in the difference model. The resistance distribution per unit length required for these airways is shown on Figure (10.13).

10.4.2.2. Results:

The results obtained from the network analysis program are shown on Figure (10.14). This correlation compares well with that obtained from the difference model, confirming that an adequate representation can also be attained with the SRR model.

From the known physical conditions apparent at the Thompson Creek No. 1 mine, a generalized model can now be suggested.

10.5. Recommended Modelling Procedure

The objective of this phase of the investigation was to develop a model for longwall waste areas which could, in turn, be recommended to ventilation planners. The model was to be accurate but simple enough to be used by ventilation planners in conjunction with conventional iterative network analysis programs.

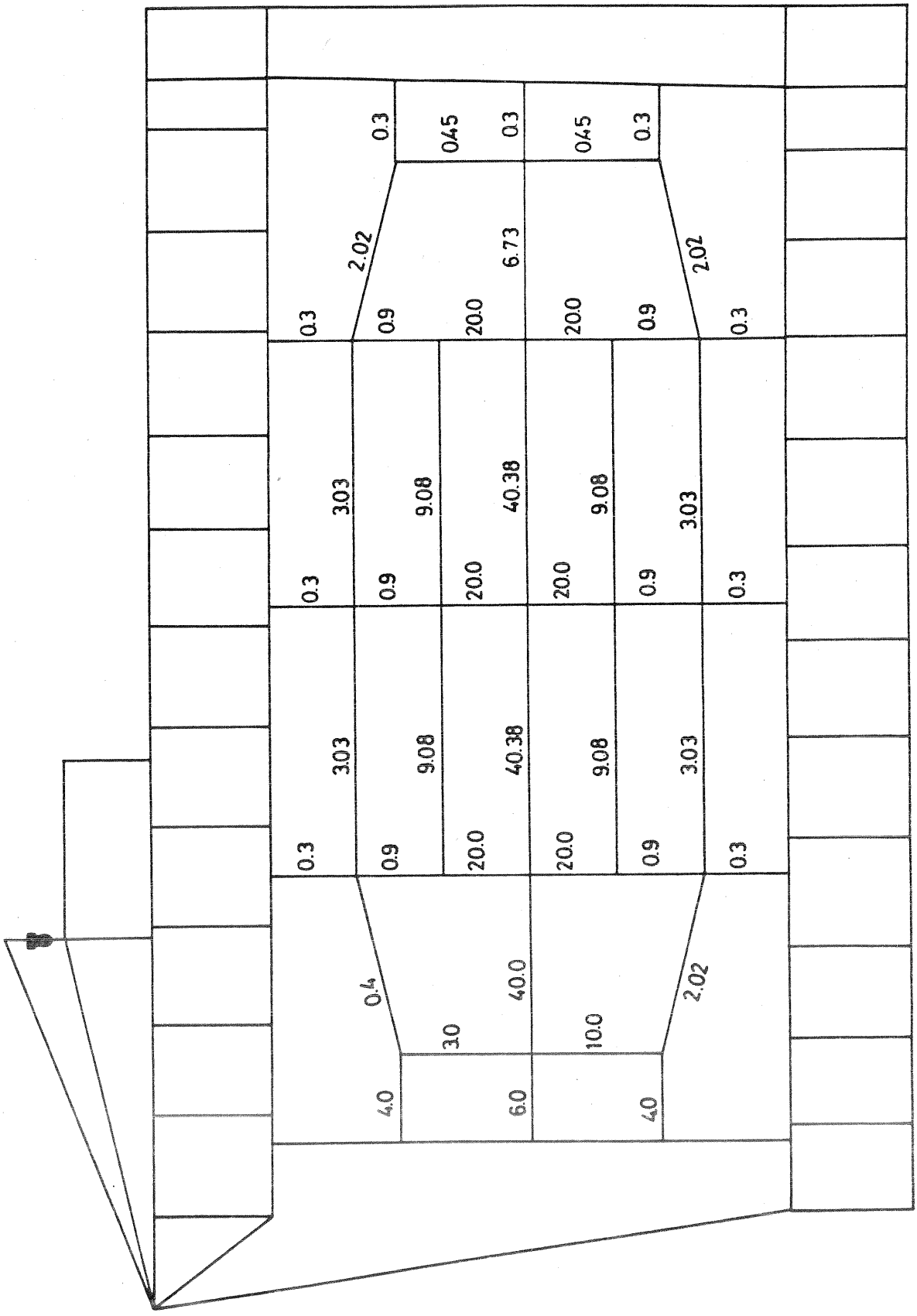

Figure 10.12 Resistances of the representative airways used for the S.R.R. model correlation.

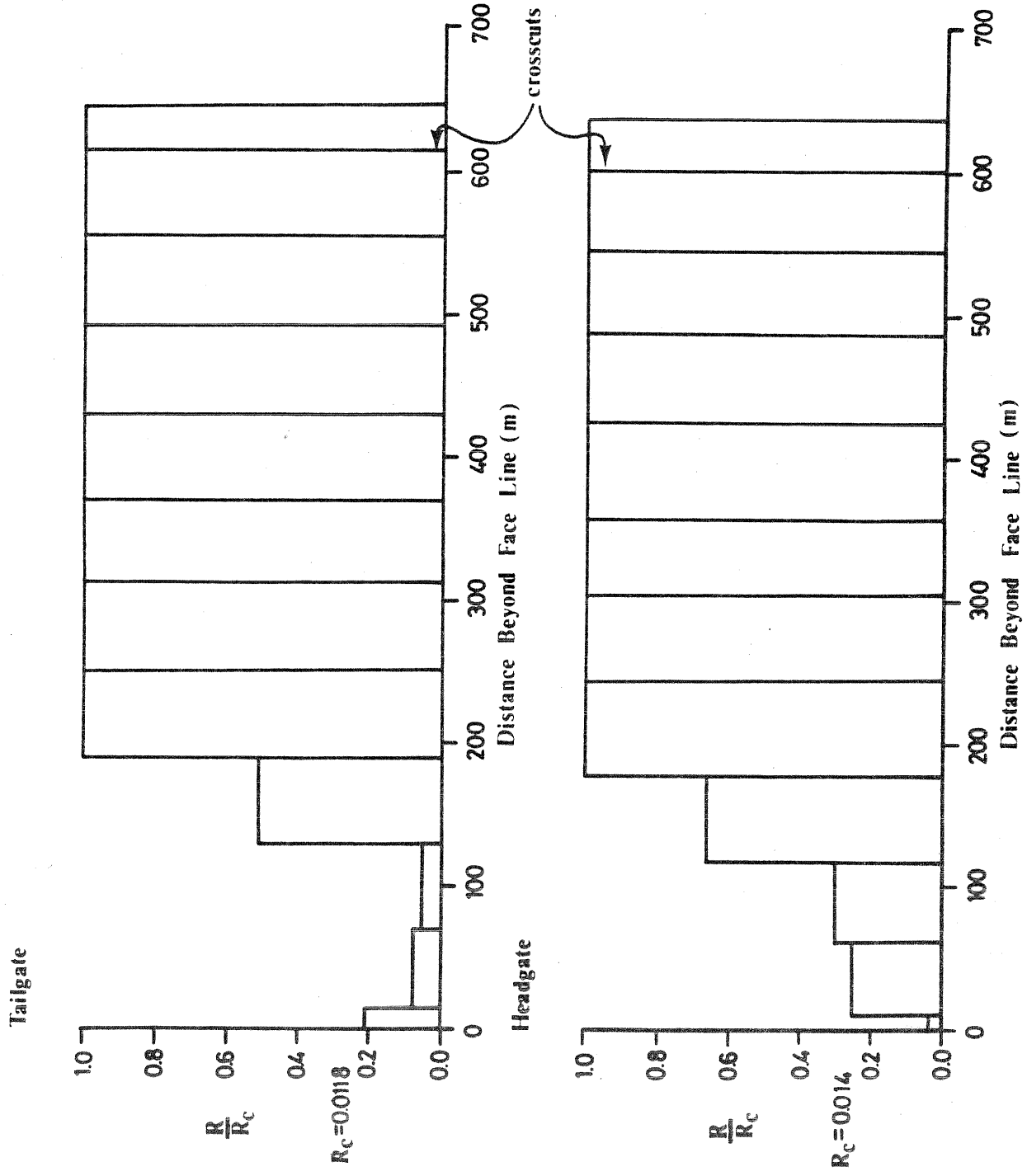

Figure 10.13 Normalized resistances (Ns^2/m^8 per meter) of the caved headgate and tailgate airways used for the S.R.R. model correlation.

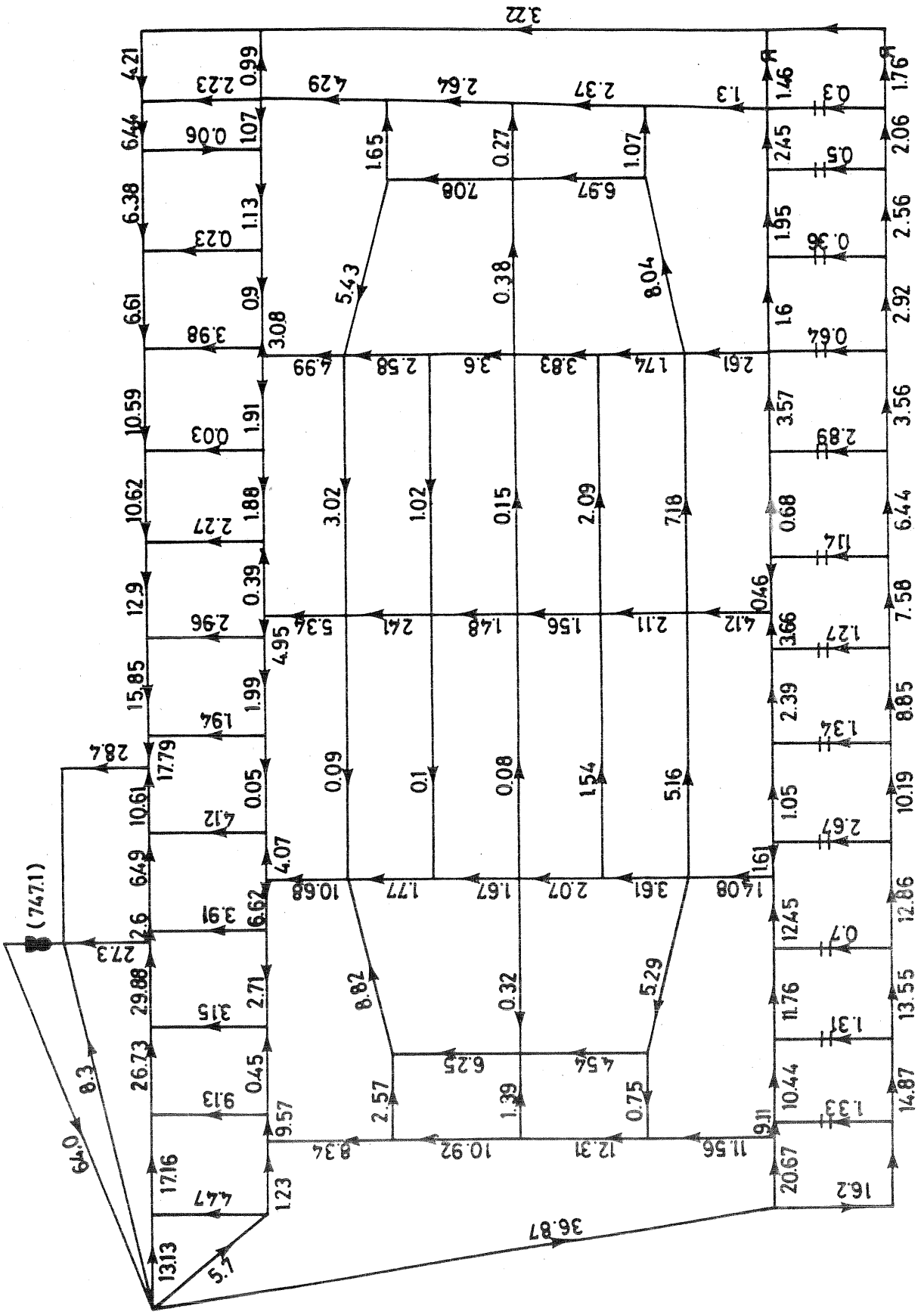

Figure 10.14 Simulation of the airflow distribution in the gob obtained with the S.R.R. model.

10.5.1. Generalizing the Field Observations

A generalized model for the simulation of air leakage through caved gob areas can be recommended from an analysis of the data obtained during the leakage survey, and by taking into account the particular conditions at the Thompson Creek No. 1 mine.

At the time of the survey, the longwall face was at a stand-still and had been idle for several weeks. In addition, the face encompassed a fault zone. These conditions caused the caved zone behind the face to be more consolidated than would be the case for a moving longwall. In particular, the gob exhibited a highly consolidated, low permeability zone directly behind the shields, especially around the fault zone, i.e. about half way along the face. The presence of this zone forced some of the leakage air to divert and flow from the gob back onto the face line.

The generalized gob model, on the other hand, assumes that a convergence zone of significant length exits behind the shields. This zone, apparent during normal face travel and fault free conditions, is assumed to be loosely consolidated and highly permeable. The loosely consolidated zone and the pressure difference between the bleeders, will cause the volume flow rate to drop steadily along the length of the face.

10.5.2. Description of Recommended Model.

The recommended model is based on the generalized case discussed above. In other words it assumes a fault free, steady, face advance. The model is designed on the basis of the simplified representative resistance model shown for the Thompson Creek No. 1 mine on Figure (10.14).

10.5.3. Design Procedure

This section suggests the procedure and the values to be used to develop the recommended gob model. The construction of the flow net geometry, the type of flow regime to assume, and the resistance values to use, are discussed.

10.5.3.1. Flownet geometry:

The recommended flownet pattern is shown on Figure (10.15). The pattern consists of a rectangular center grid, labeled A in the Figure, connected to two symmetrical end grids, B & C. The following construction procedure gives grid dimensions which must be followed if the recommended resistances are to be used.

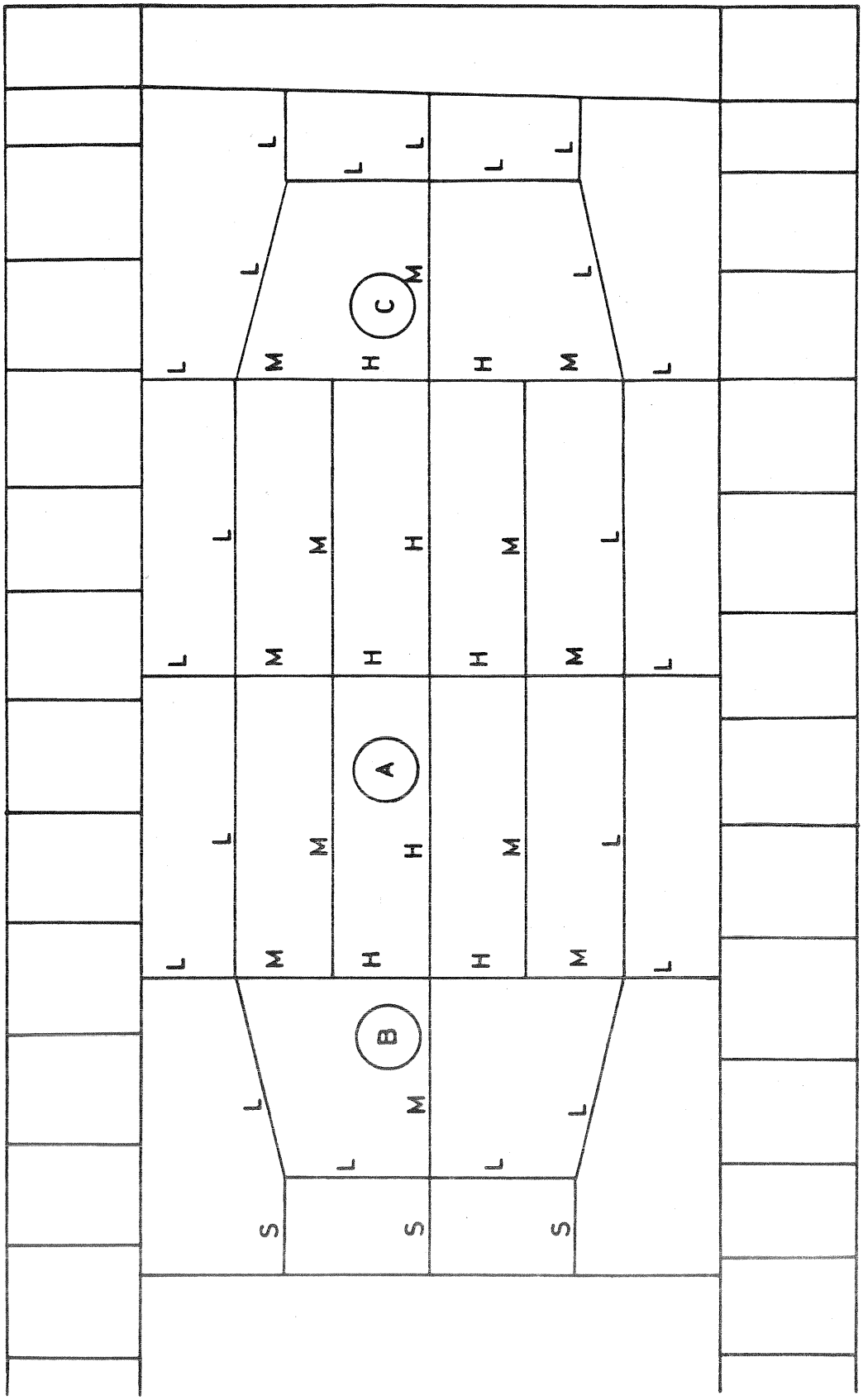

Figure 10.15 Recomended network to represent longwall gob.

Center grid:

To construct the center grid, labeled A on Figure (10.15) the following procedure should be adopted:

.1. Construct a scale representation of the gob.
.2. Divide the measured length of the gob into equal increments of approximately 150 meters.
.3. Divide the measured width of the gob into six equal increments.
.4. Construct the center grid as shown on Figure (10.15)

End grids:

To construct the two symmetrical end grids, B and C:

.1. Divide the measured face and stationary end into four equal increments.
.2. Construct rectangular elements on the two middle increments extending into the gob one third of the distance to the nearest center grid branch and complete grid as shown on Figure (10.15).

10.5.3.2. Flow regime:

The model utilizes the minimum amount of representative airways required for an adequate simulation. If the construction procedure is followed, the cross-sectional areas of the regions in the gob, represented by the airways, will be large. From the quantity relation,

$$Q = uA$$

where Q = volume flow rate (m^3/s)
u = velocity (m/s)
A = cross-sectional area (m^2)

It is evident that, with a constant volume flow rate, the velocity must decrease with an increased area. For low flow rates and large permeable cross sectional areas, the air velocity will be low enough to be able to assume laminar flow. On the other hand, if the flow rates are sufficiently large, the laminar assumption is no longer valid. If this is the case then equivalent turbulent resistances must be ascribed to the leakage branches.

The recommended model is based on the assumption that the airflow throughout the entire gob remains in the laminar flow regime. The airflow in the caved airways directly surrounding the gob is assumed to be turbulent.

10.5.3.3. Resistance values:

Resistances of the caved airways:

For practical utilizations, graphs were developed to determine the resistances of the caved airways relative to face height and location. These graphs are based on correlations performed with the resistance values obtained from the Thompson Creek analysis.

The caved airways are assumed to collapse to a height equivalent to (31%) of the face height. For the caved head and tailgate, this final height is attained at about 150 meters beyond the face line. These first 150 meters, incorporate a convergence zone in which it is assumed that the airways decrease linearly in height. The corresponding decrease in effective cross sectional area causes the resistance to rise at an accelerating rate until the convergence is complete. The resistance values for this region were calculated by integrating equation (10.5) along an airway of linearly decreasing height.

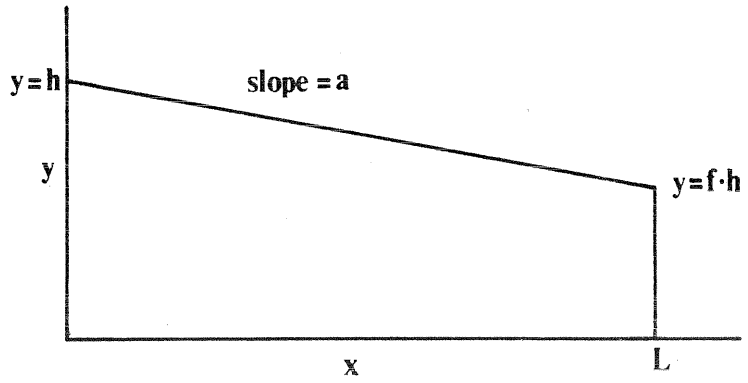

h = initial height of airway
f = fraction of initial height
a = slope of convergence
x = distance along caved airway

The linear decrease in height is described by

$$y = ax + h$$

The differential form of the resistance equation (10.5) is

$$dR = \frac{k\,O}{A3}\,dx$$

where dR is the resistance of the increment length dx.
Now at distance x,

area A = Xy and perimeter O = 2 (X + y)

giving

$$dR = k\,\frac{2\,(X + y)}{(Xy)3}\,dx$$

But $y = ax + h$

and

$$dy = a\,dx$$

Substituting for $dx = dy/a$ gives

$$dR = \frac{2k}{aX3}\,\frac{(X + y)}{y3}\,dy$$

Integrating

$$R = \frac{2k}{aX3}\int_1^2 \left\{\frac{X}{y3} + \frac{1}{y2}\right\} dy$$

$$= \frac{2k}{aX3}\left\{-\frac{X}{2y2} - \frac{1}{y}\right\}_1^2$$

or

$$-\frac{2k}{aX3}\left\{\frac{X}{2\,(ax + h)2} + \frac{1}{(ax + h)}\right\}_x^{x+1}$$

between the incremental distance (x) through (x + 1)

$$= \frac{-2k}{aX3}\left\{\frac{1}{ax + h}\cdot\frac{X}{2\,(ax + h)} + 1\right\}_x^{x+1}$$

giving

$$\left(R \right)_{X}^{X+1} = \frac{-2k}{aX3} \left\{ \frac{1}{a\ (x+1)\ +h} \left(\frac{X}{2(a(x+1)+h} + 1 \right) - \frac{1}{ax+h} \left(\frac{X}{2(ax\ +h)} + 1 \right) \right\}$$

Using the following values determined from data correlation:

k = 0.03 kg/m3
L = 150 m
f = 0.31
X = 4.0m

incremental resistances were calculated from 0 to L for varying face height, h. this produced the resulting graphs, Figures (10.16 - 10.18)

Recommended resistance values for the caved surrounding airways are determined by using the following procedure:

Caved headgate and tailgate:

(1) . Use the face height to select the appropriate curve from Figures (10.16 - 10.18).

(2) . For each length of caved airway increment, use the distance beyond the face line and obtain an average resistance value per unit length from the appropriate curve.

(3) . Multiply the length of the increment by this value.

(4) . Repeat 2-3 for all remaining increments.

Caved airway along stationary end of gob (face start line):

(1) . For each airway increment, use the face height and the <u>flat part</u> of the curves on Figs (10.16 - 10.18), to obtain a resistance value per unit length.

(2) . Multiply the length of the increment by this value.

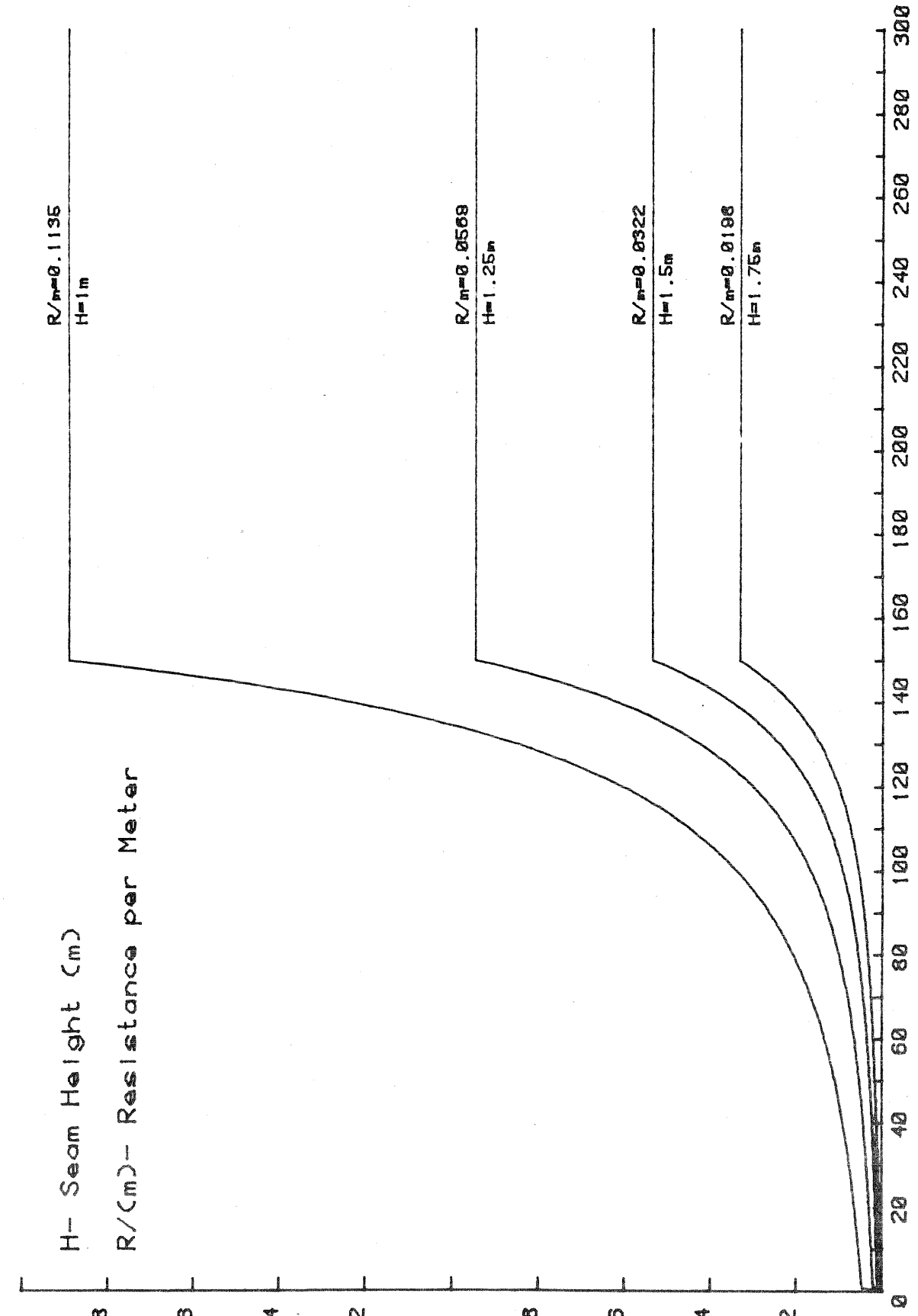

Figure 10.16 Nomogram to determine resistances of caved airways for face heights ranging from 1.0 to 1.75 meters.

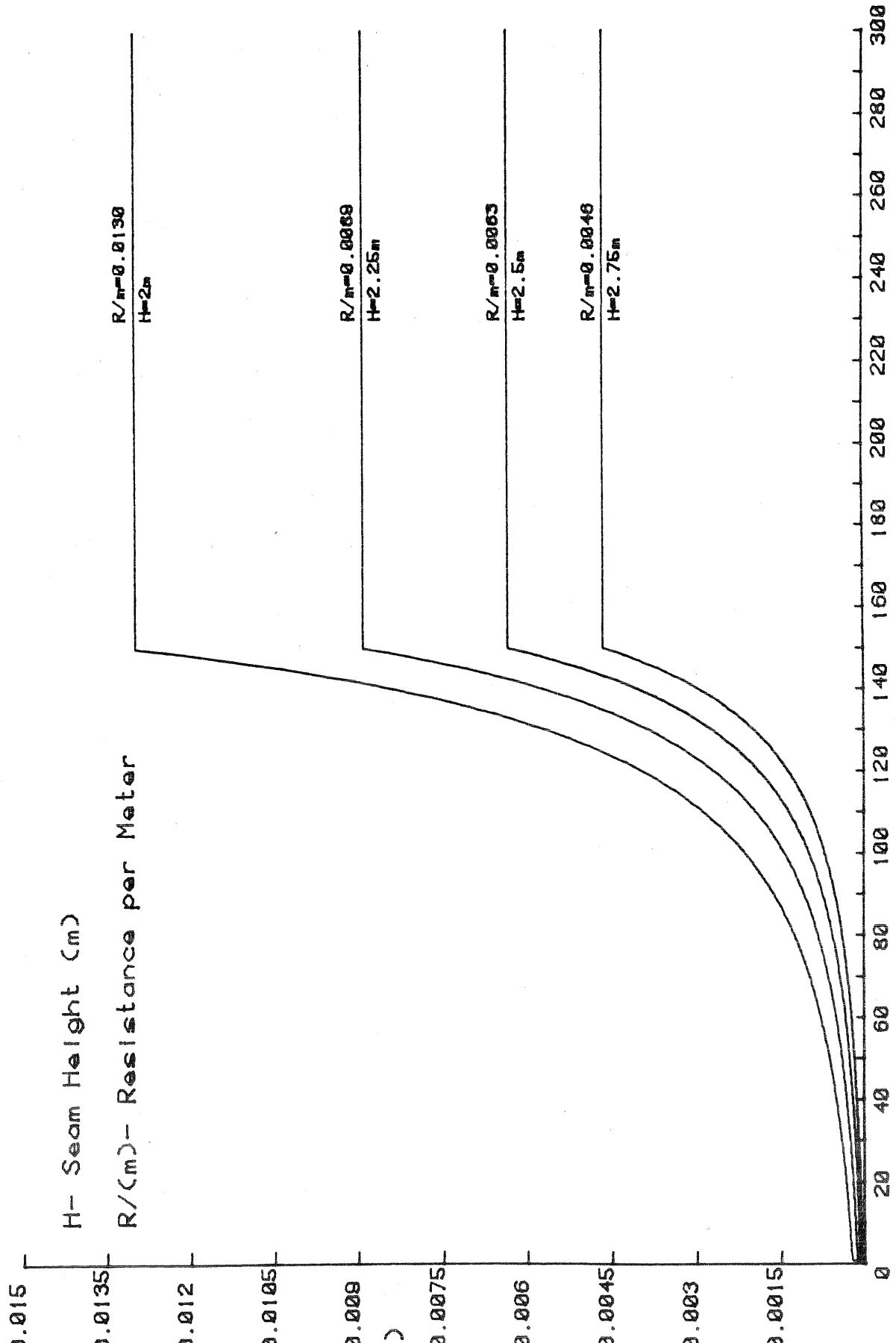

Figure 10.17 Nomogram to determine resistance of caved airways for face heights ranging from 2.0 to 2.75 meters.

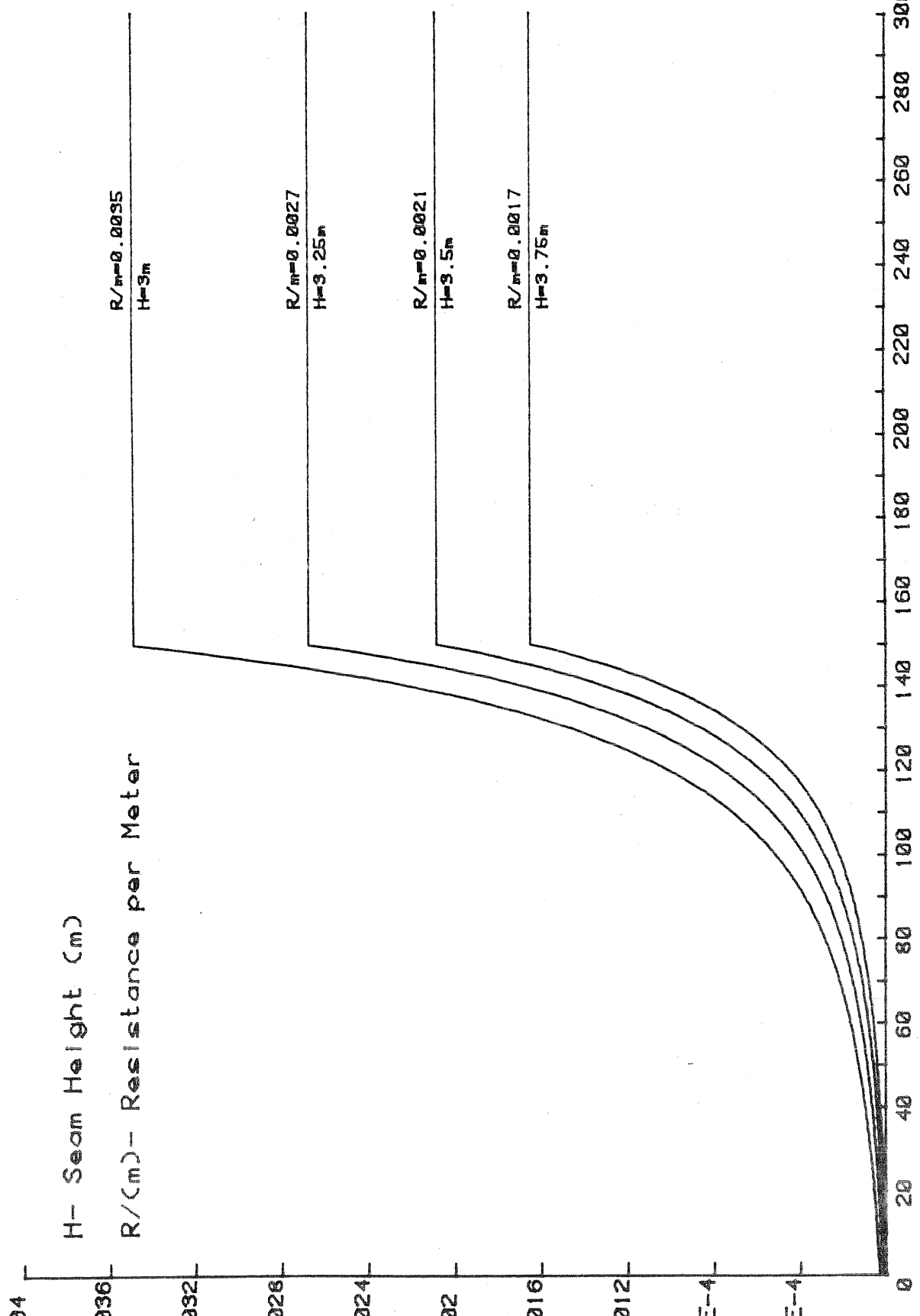

Figure 10.18 Nomogram to determine resistance of caved airways for face heights ranging from 3.0 to 3.75 meters.

Resistances of flowpaths in the caved area:

Owing to the dependence on cross-sectional area, recommended laminar resistance values are based on the branch spacing suggested in Section 10.5.3.1. Furthermore, laminar resistance values are given in terms of 10 meter lengths and as functions of location and seam height.

Four different resistance values exist, each assigned to represent a different degree of consolidation in the gob.

(1) Shield Resistance - S
(2) High Resistance - H
(3) Medium Resistance - M
(4) Low Resistance - L

The shield resistances are assigned to the branches leading into the gob from the face. The high resistance values are assigned to the branches in the center of the gob, while the medium values are distributed directly around the center zone. In addition, the low resistance values are assigned to the branches along the perimeter of the gob. The exact locations of these resistances are shown on Figure (10.15). The actual resistance values to use are shown as functions of face height on figure (10.19). These values are based on the modelling performed with the Thompson Creek No. 1 mine where the face height was approximately 2 meters. Altering the face height reduces the permeable cross-sectional area A, in equation (10.6)

$$R_L = \mu L/kA \qquad 10.6$$

Since laminar resistance is inversely proportional to the cross-sectional area, extrapolation was employed to determine the resistance values for varying face heights.

10.6. Worked Example

This section describes a worked example which illustrates longwall face resistance calculations using the algorithim devised in Section 8, and the recommended gob modelling method. In addition, the example illustrates one possible application of a detailed longwall simulation.

10.6.1. Description

Network:

The network which is used for the example is a single longwall district ventilated by a through flow system, as shown on Figure

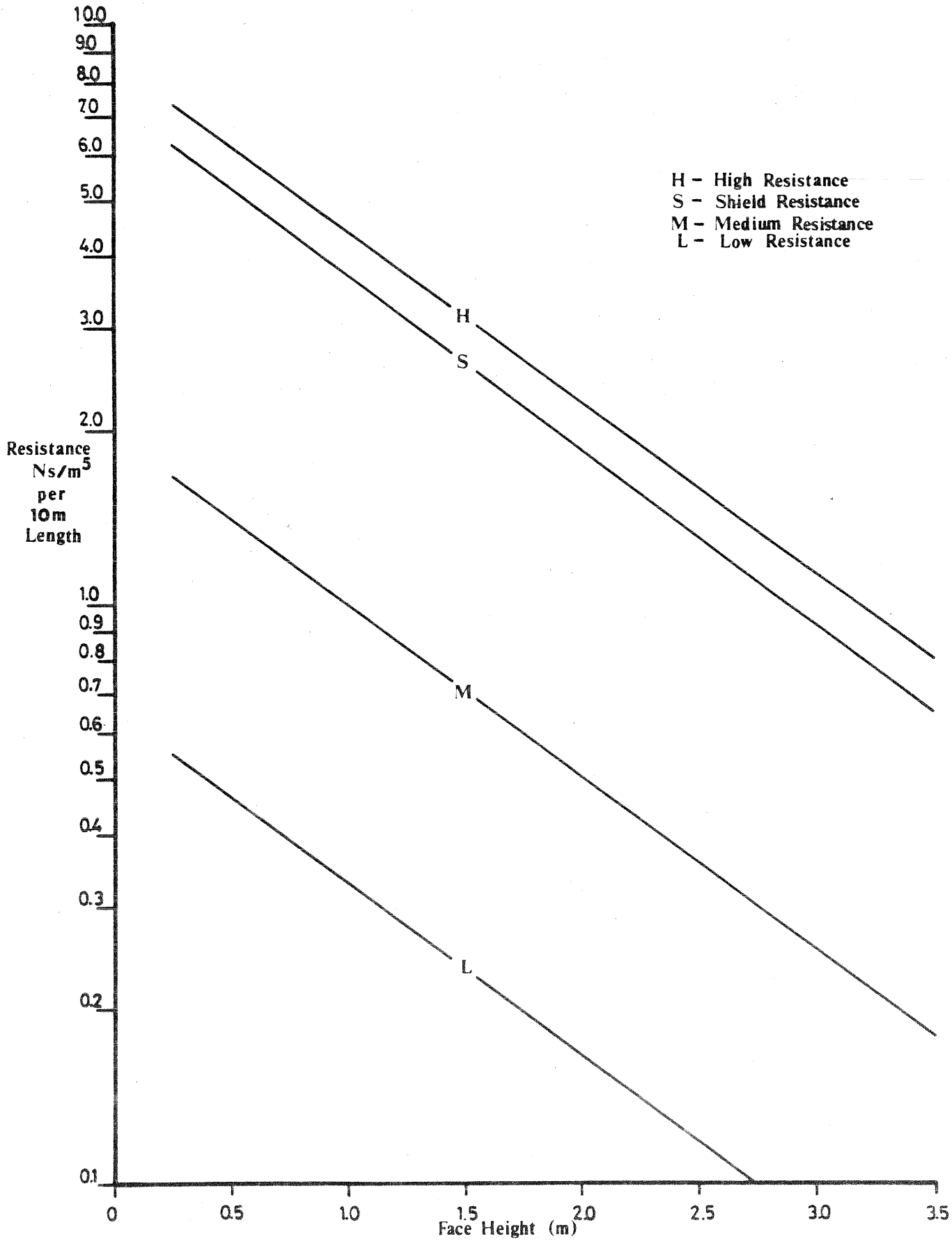

Figure 10.19 Nomogram to determine laminar resistance values as functions of face height and location in the gob.

(10.20). Air is supplied to the longwall district by a fan which exhibits the fan characteristics shown on Figure (10.21). The gob itself, is ventilated with a bleeder system similar to that of the Thompson Creek No. 1 mine where the crosscuts along the main intake side are sealed while those on the return side are left unobstructed.

The longwall is mined in retreat and, for this example the face has travelled a distance of 650 meters. The 120 meter face has an average width of 3 meters, while the face height is 1.5 meters.

Procedure:

The values obtained from the face line resistance algorithm and the gob model, were input, along with the remaining airway resistances, as data for the ventilation network analysis program VNET. For this example, the VNET program was used to simulate the effect of shearer location on face airflow patterns. This was accomplished by assigning a shearer resistance value, as determined from the face resistance algorithim, to different increments of the face line.

10.6.2. Calculations of Face Resistances

The techniques used to calculate face resistance values were those derived in Section 8.

Face height:	1.5m	
Face width:	3.0m	
Face friction factor:	0.05	$\frac{kg}{m^3}$

Using equation (10.5):

$$R_{fl} = \frac{k\ L\ O}{A^3}$$

where $O = 2 \times (1.5 + 3.0) = 9m$

$A = (1.5 \times 3.0) = 4.5m^3$

$L = 1$ meter

$$= \frac{0.05 \times 1x9}{(4.5)^3} \quad \frac{(kg).(m).(m)}{m^3 \quad m^6} = \frac{Ns^2}{m^8}$$

$= 0.004938 \quad Ns^2/m^8$ per meter length

Dividing the face length into <u>four</u> equal increments:

$L = 120/4 = 30m$

$R_{fl} = .004938 \times 30 = 0.1481 \quad \frac{Ns^2}{m^8}$

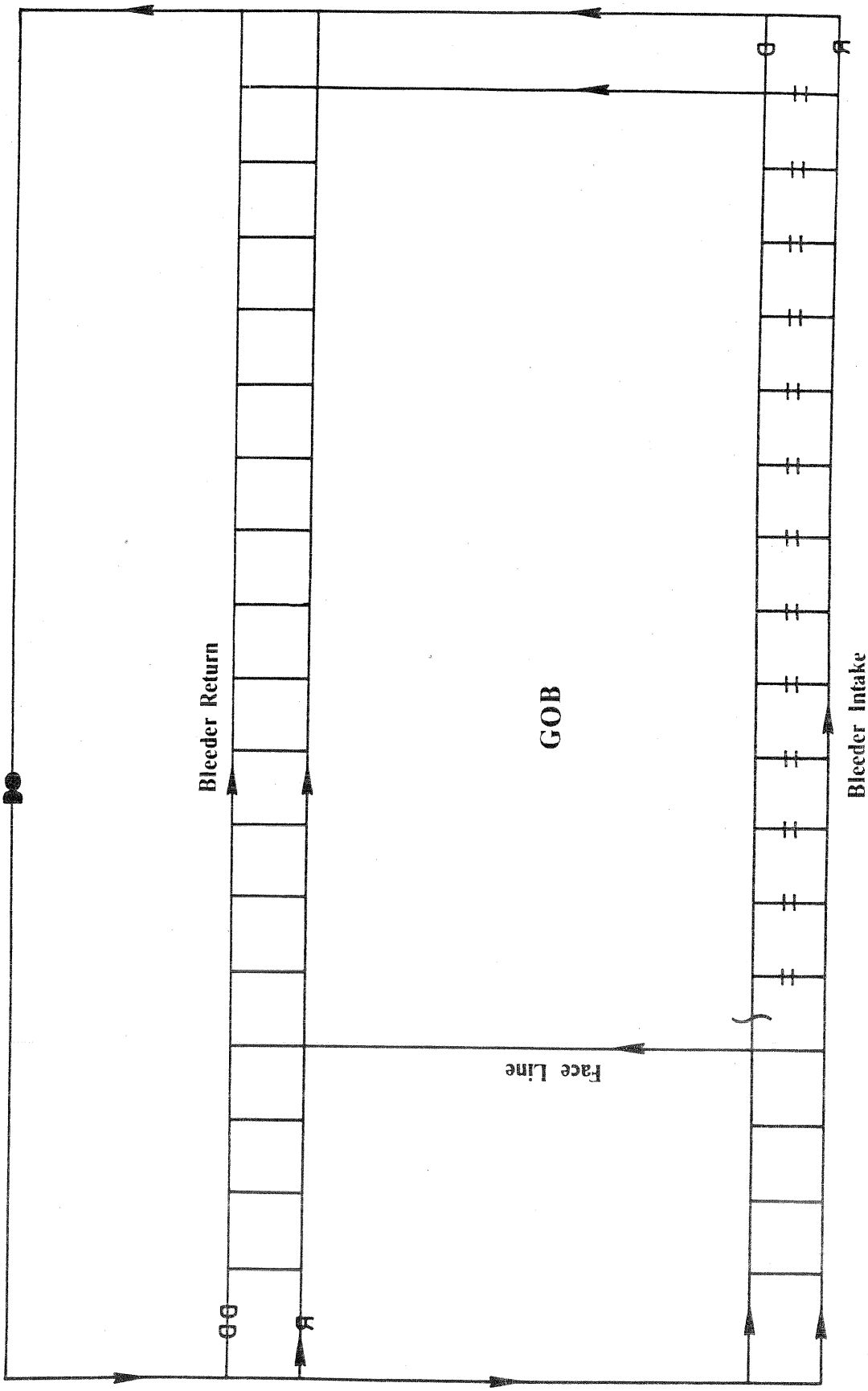

Figure 10.20 Ventilation schematic of longwall district used for worked example.

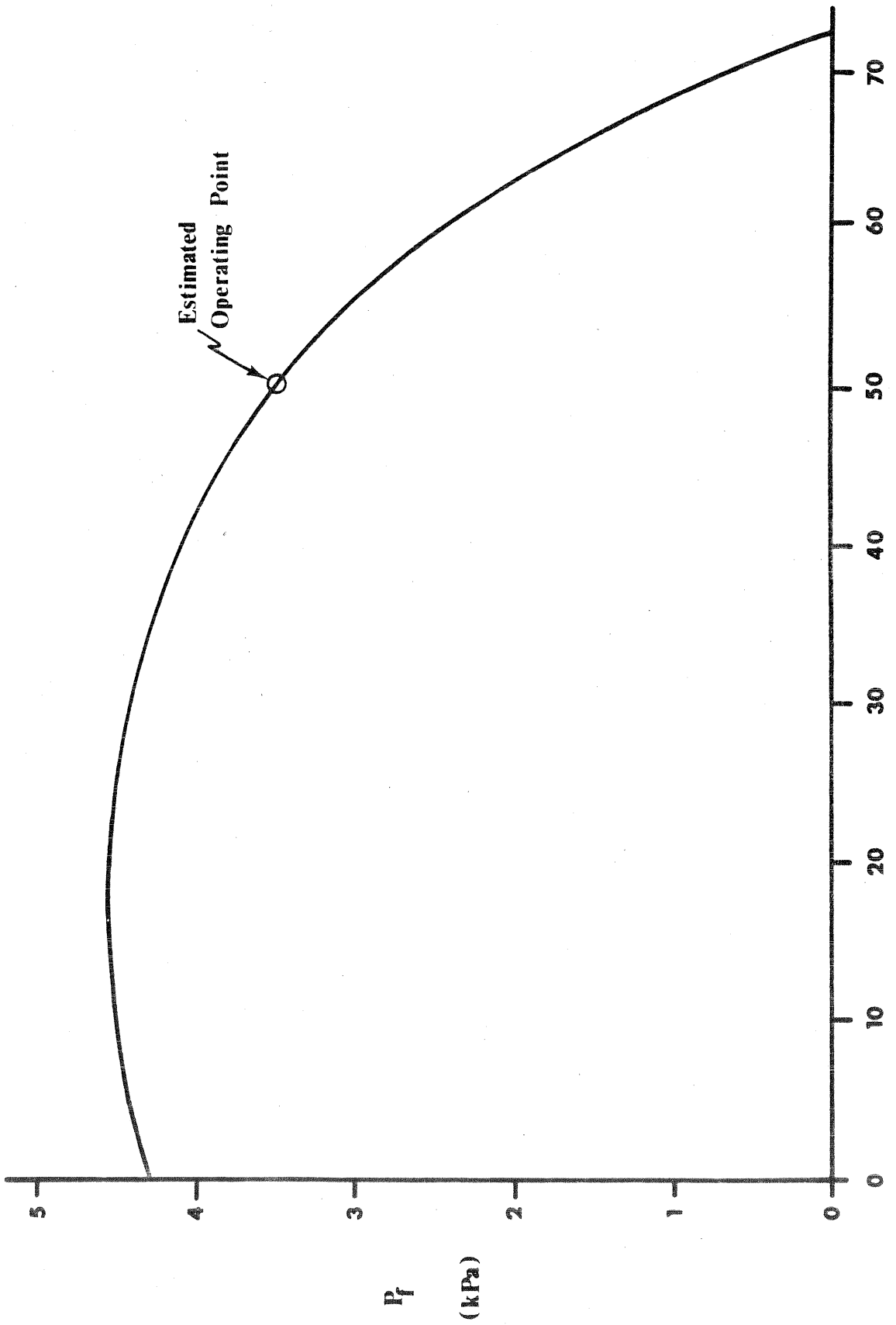

Figure 10.21 Fan characteristic curve of fan used for worked example.

Face Intake:
Conditions:

(1) sharp right angle bend
(2) panzer gear head - $2.5m^2$

shock loss factors:

X_{bend} = 1.4 velocity heads
$X_{contraction}$ = 0.184 velocity heads

X obstruction:

$A = 4.5m^2$, $a = 2.5m^2$

$$X \text{ obstruction} = \left\{ \frac{A}{0.7\ (A-a)} - 1 \right\}^2$$

$$= \left\{ \frac{4.5}{0.7(2)} - 1 \right\} 2$$

= 4.903 velocity heads

Total shock loss, $\Sigma X = 1.4 + .184 + 4.903 = 6.487$

Resistance due to shock losses:

$$R_{sh} = \frac{\Sigma X \rho}{2A^2} = \frac{(6.487) \times 1.2}{2 \times 4.5^2} = 0.1922 \quad Ns^2/m^8$$

Face Return:

conditions: (1) sharp right angle bend
shock loss factor: X bend = 1.4 velocity heads

Resistance due to shock loss:

$$R_{sh} = \frac{(1.4) \times (1.2)}{2 \times (4.5)^2} = 0.04148\ Ns^2/m^8$$

Shearer:

shockloss factor: X shearer = 4 velocity heads

Resistance due to shock loss:

$$R_{sh} = \frac{(4) \times (1.2)}{2 \times (4.5)^2} = 0.1185\ Ns^2/m^8$$

TOTAL Face line Resistance:

1st quarter:

$$R = R_{fl} + R_{shock}$$
$$= 0.1481 + 0.1922$$
$$= 0.3404 \ Ns^2/m^8$$

2nd quarter:

$$R = R_{fl}$$
$$R = 0.1481 \ Ns^2/m^8$$

3rd quarter:

$$R = R_{fl}$$
$$R = 0.1481 \ Ns^2/m^8$$

4th quarter:

$$R = R_{fl} + R_{shock}$$
$$R = 0.1481 + 0.04148 = 0.1896 \ Ns^2/m^8$$

shearer resistance to be added to quarters 1,2,3 and 4 alternatively.

$$R_{shearer} = 0.1185 \ Ns^2/m^8$$

Total face line resistance =

$$R_T = .3404 + .1481 + .1896 + .1185$$
$$= 0.9447 \ Ns^2/m^8$$

10.6.3. Gob Model (Figure 10.22)

Branch dimensions:
center grid

Gob length - L = 650m

Divide into equal increments of around 150m
= 650m/150m
= 4.33
= 4 increments of 162.5m

Divide width into 6 increments
W = 120m
= 120/6
= 6 increments of 20m

End grids

Face line was divided into 4 increments of 30m.

Dimensions of rectangular end grid elements:

162.5m/3 = 54.17m

54.17m x 30m

Length of diagonal passages connecting end grid to center grid:

$$\left\{(162.5 \times 2/3)^2 + (30 - 20)^2\right\}^{1/2}$$

$$= 108.8\text{m}$$

The model was constructed in the gob region and the branches are numbered as shown in Figure (10.22).

Laminar Resistance computations:

Laminar resistances are determined with Figure (10.19) using the face height of 1.5 meters.

Resistance	Location	Length(m)	R/10m	R Ns/m^5
Low	center grid	20	0.235	0.47
Low	centergrid	162.5	0.235	3.818
Low	connecting	108.8	0.235	2.56
Low	end grid	54.17	0.235	1.273
Low	end grid	30	0.235	0.705
Medium	center grid	20	0.71	1.42
Medium	centergrid	162.5	0.71	11.537
Medium	connecting	108.3	0.71	7.69
High	centergrid	20	3.12	6.24
High	centergrid	162.5	3.12	50.7
Shield	shield	54.16	2.6	14.08

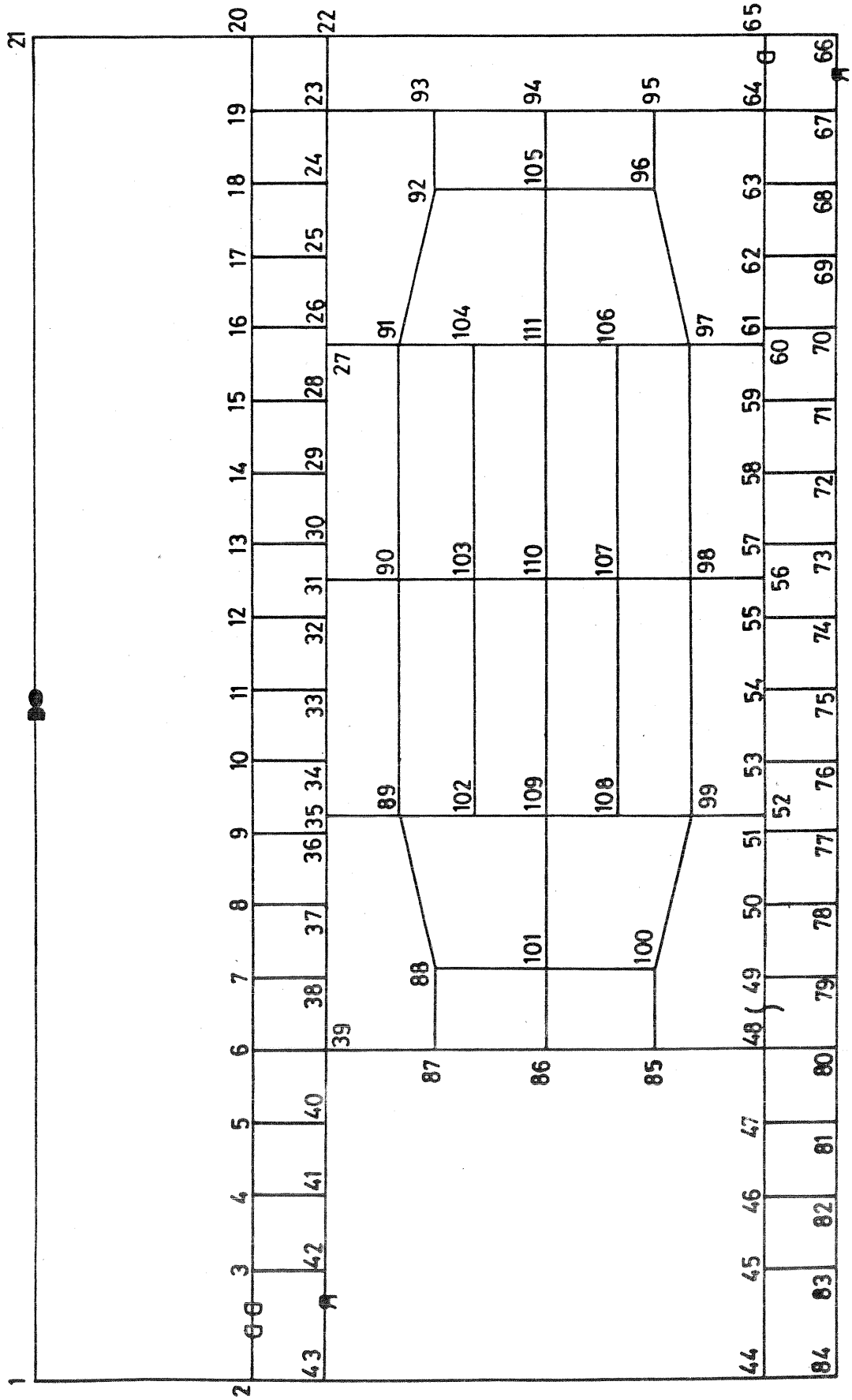

Figure 10.22 Network with gob model and branch junction numbers.

Caved Airway Resistance Computations:

Turbulent resistance values of the caved airways were determined using Figure (10.16), with a face height of 1.5m.

Caved headgate and tailgate:

Distance between crosscuts = 50m

location of increments between crosscuts relative to face line (m)	average res. per m	L (m)	R $\frac{Ns2}{m8}$
0 50	0.0034	50	0.017
50 100	0.007	50	0.35
100 150	0.012	50	0.6
150 162.5	0.012	12.5	0.15

For all remaining increments beyond 162.5m from the face line:

R/m = 0.0322 $Ns2/m8$ per m
L = 50m
R = 1.61 $Ns2/m8$

caved airway at stationary end

R/m = 0.0322 $Ns2/m8$ per m
L = 30m
R = 0.966/30m increment

10.6.4. Network Simulation

The resistances of the remaining airways were calculated using equation (10.5). The values used are shown on Figure (10.23).

After input data, the VNET program produced the results shown on Figures (10.24 - 10.27). From these figures, the effect of shearer position on the total ventilation system is evident. For each figure, the shearer is located in the labelled increment of the face line. On analyzing these figures, it is apparent that the shearer location has only a localized effect on the ventilation of the face and caved zone. The leakage into the caved area is increased on the upstream (high

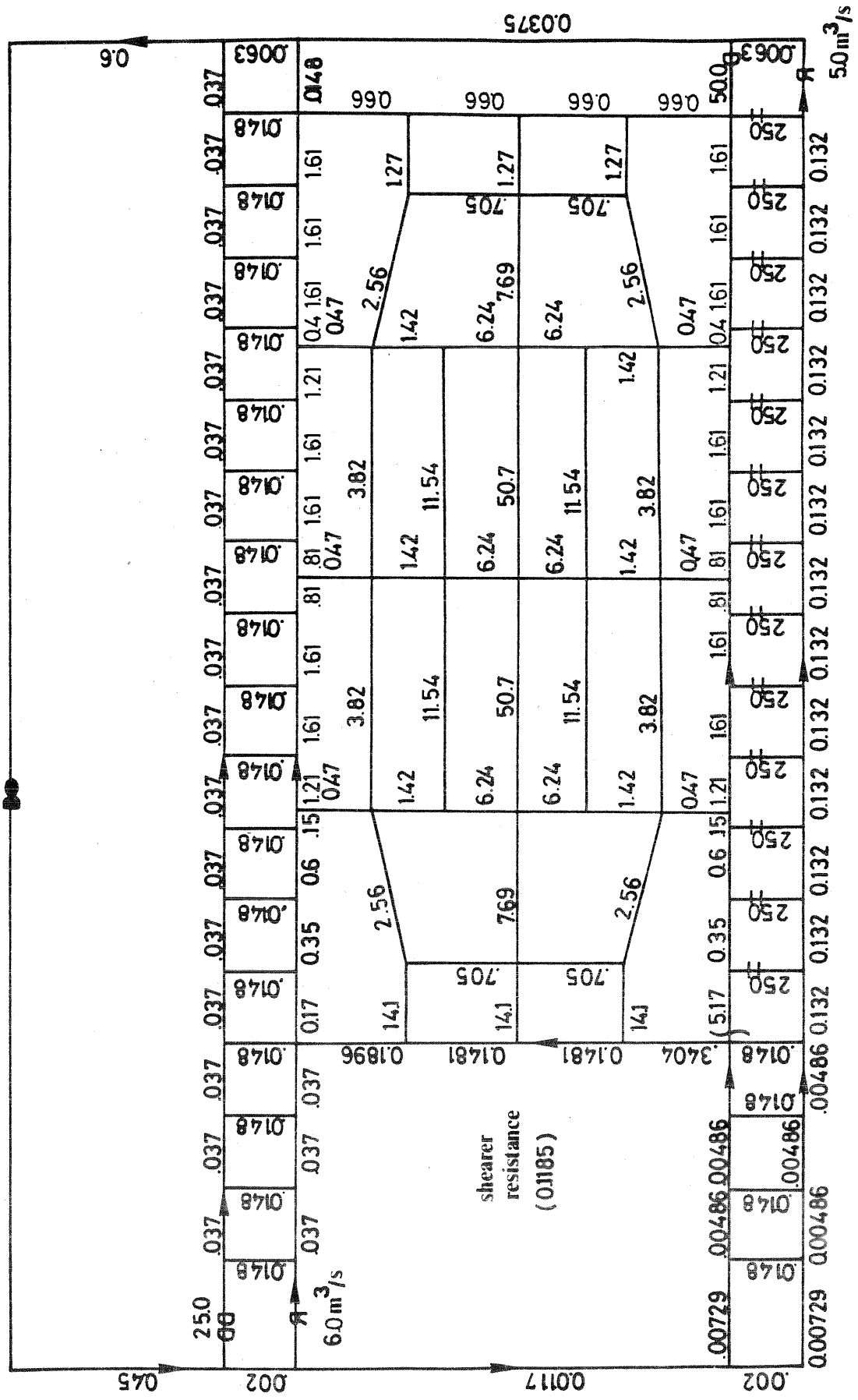

Figure 10.23 Resistance values used for worked example.

pressure) side of the shearer, and decreased on the downstream (low pressure) side of the shearer. In this example, the bleeder airway system was sufficient to maintain the leakage direction from the face into the gob. Without bleeder airways, the shearer may cause leakage into the gob upstream of the machine and out of the gob (possibly containing methane) downstream from the machine.

The amount of air flowing onto the face line is reduced only when the shearer is moved to the intake of the face. In general, however, all the other flow magnitudes remain sensibly constant.

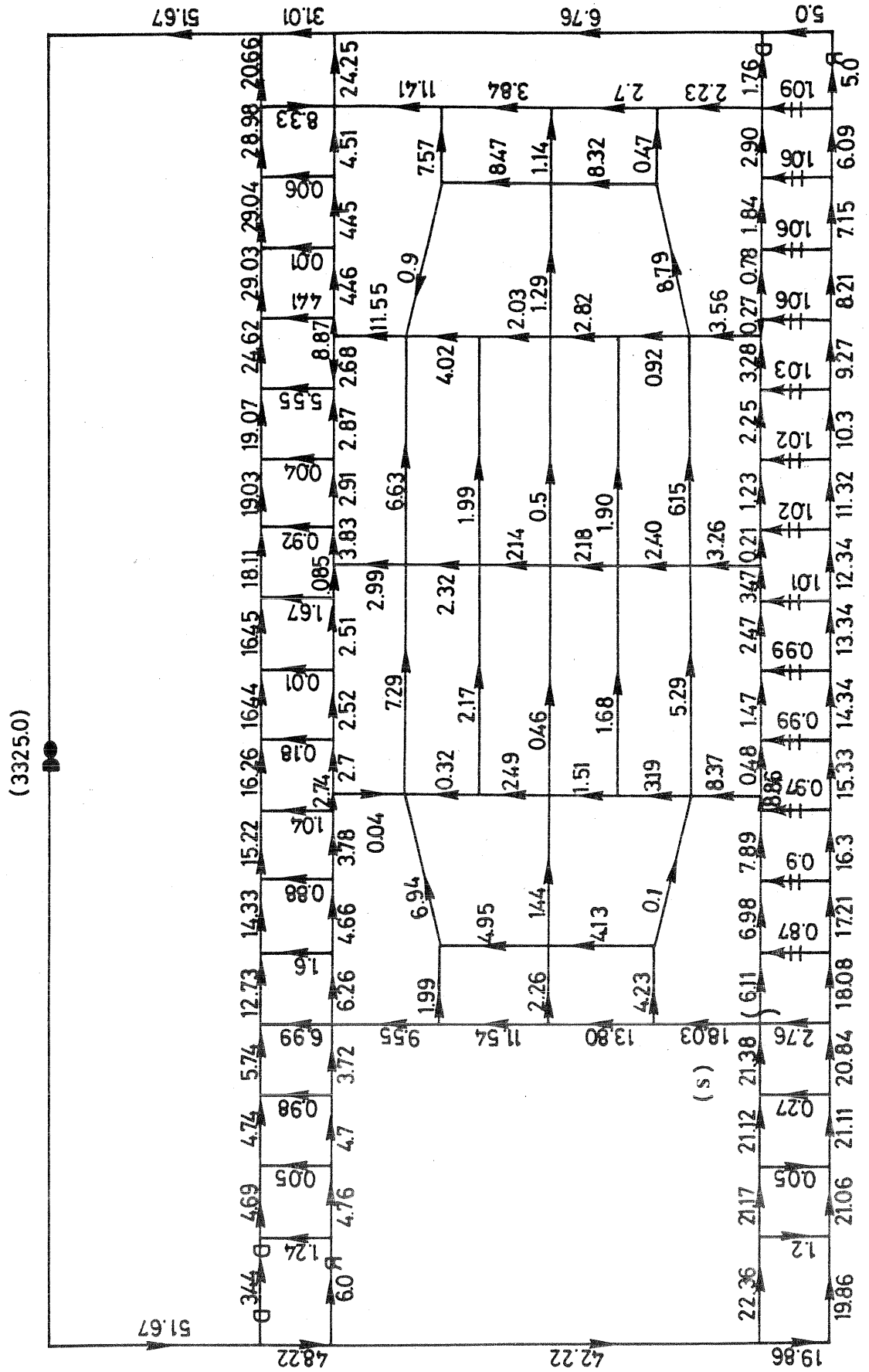

Figure 10.24 Simulation showing resulting airflows (m^3/s) with shearer in branch 48-85.

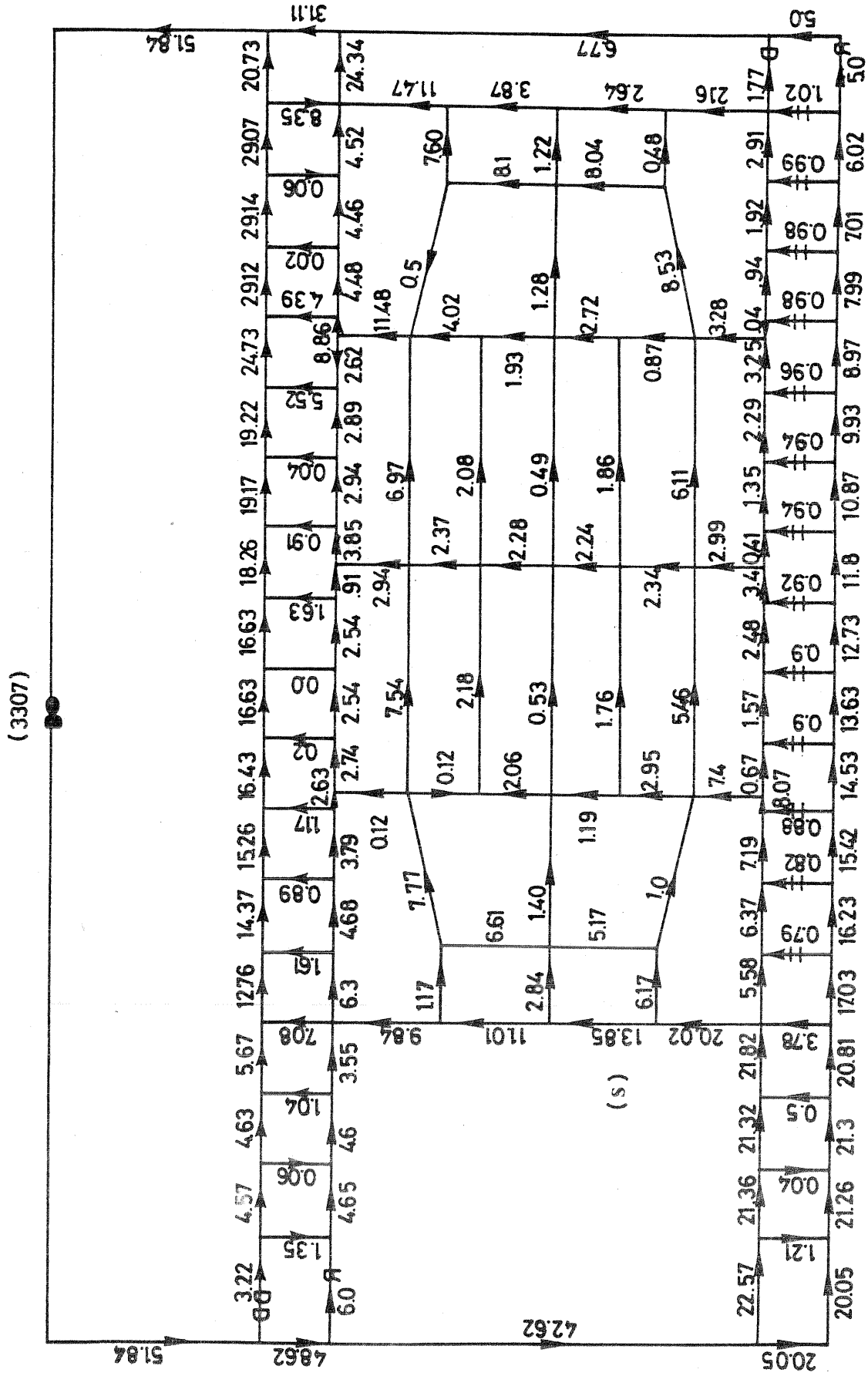

Figure 10.25 Simulation showing resulting airflows (m^3/s) with shearer in branch 85-86.

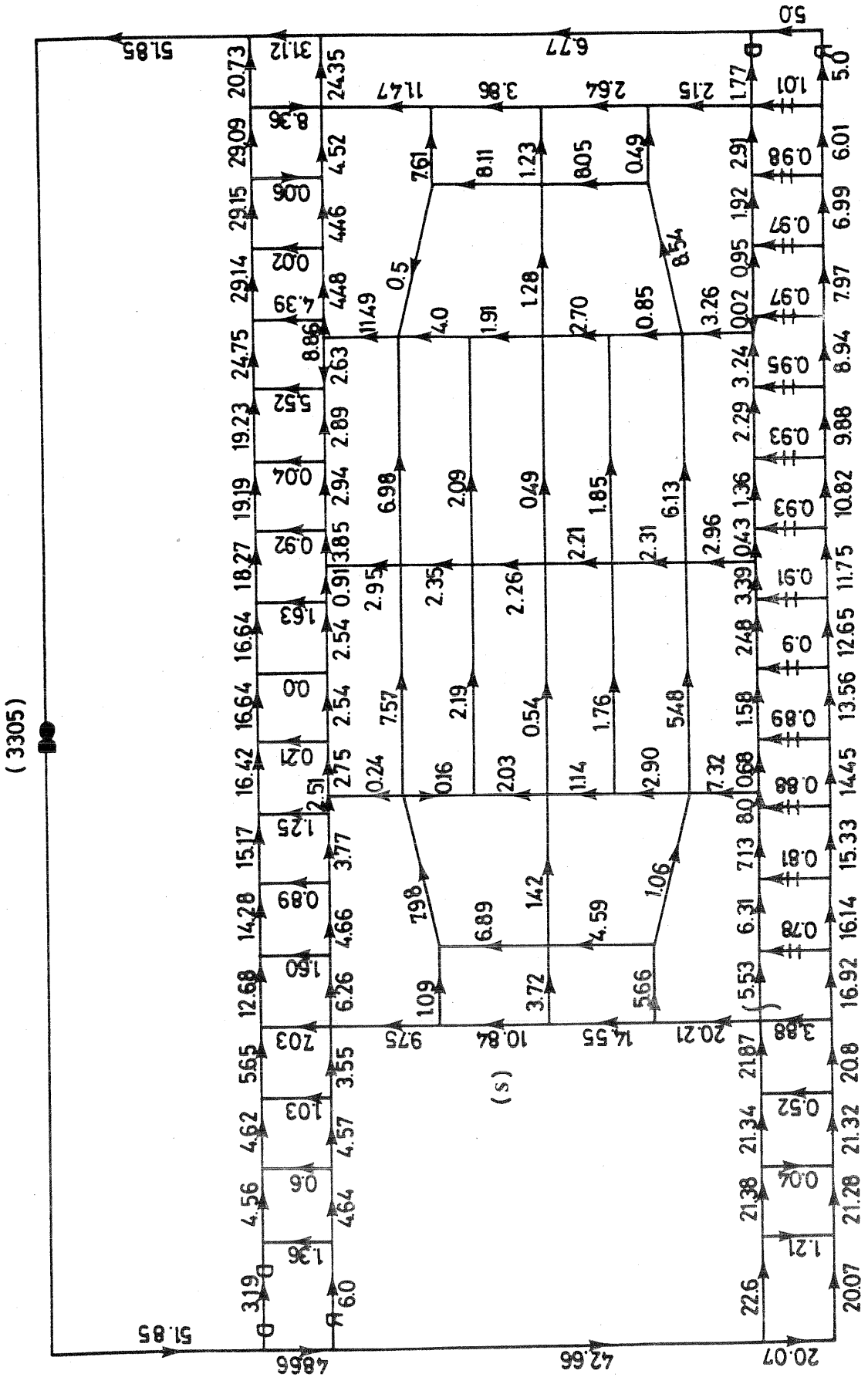

Figure 10.26 Simulation showing resulting airflows (m^3/s) with shearer in branch 86-87.

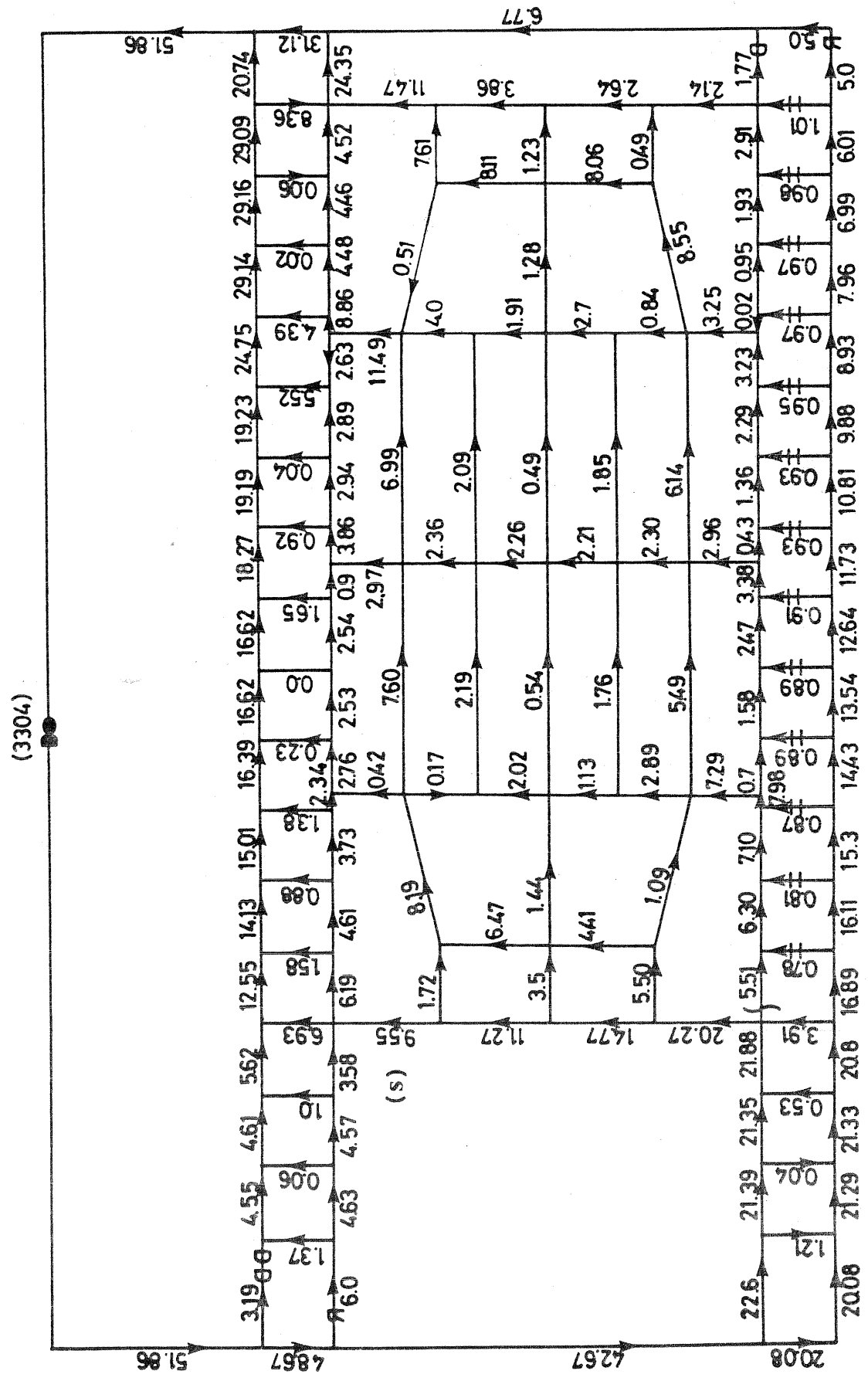

Figure 10.27 Simulation showing resulting airflows (m^3/s) with shearer in branch 87-39.

11. CONCLUSIONS

This project has encompassed a thorough investigation into the mechanisms of airflow distribution on a longwall face, the caved area behind the face and the intake, return and bleeder airways comprising the complete longwall district.

Following a pressure-quantity survey to establish and quantify the main ventilation routes of the mine, four major tests were carried out. First, detailed measurements at each of a number of stations on the longwall face allowed the variations in airflow along, and across, the face to be determined. These measurements also indicated the extent to which the bleeder airways were successful in preventing methane accumulations in the caved waste from migrating on to the face.

Second, a survey of frictional pressure drops and corresponding airflows was conducted at the face ends and at increments of length along the entire longwall. This allowed friction factors to be established for a mechanized face fitted with shield powered supports. The results also provided the information necessary to establish the values of resistance to be allocated to the complex interaction of shock losses at face ends, across the shearer and for the airflow along the faceline.

Third, a carefully controlled experiment was carried out to establish the relationship between frictional pressure drops and airflows on a longwall face.

Fourth, a survey of air leakage at all points connecting into the caved waste was conducted. This provided correlation data for the development of a computer model designed to simulate the leakage airflow patterns in the caved zone behind a longwall.

Within each of those Sections of the report that involve the four tests, the significance of the work and the theoretical background (where relevant) has been described. The procedures employed in carrying out the practical work, and the data obtained, have been delineated. Furthermore, the results have been used as a basis for the development of design data and improved procedures for the study and planning of ventilation in other longwall mines.

The specific accomplishments of this project include the following:

1. It was verified that a system of bleeder airways, combined with an adequate pressure differential between intakes and returns, can be successful in maintaining leakage from the faceline into the waste and, hence, preventing waste gas migration on to the face. In particular, the positions of stoppings, brattice cloths and regulators must be such that the air pressure in the waste remains below that on the face, throughout the faceline. A further provision is that the caved material immediately behind the chocks must be sufficiently permeable to allow the leakage air to migrate towards the bleeder return. If the caved material

becomes consolidated at the rear of the chocks due to geological disturbance or a delay in turning over the face, then it is likely that leakage will occur from the waste on to the faceline immediately upstream of the consolidated zone.

2. Some 50 per cent of the face airflow travels in the conveyor track with the remainder divided between the face front and the travelling track. Very little passes through the constricted passage between the chock legs. The proportions of airflow at the face front and the travelling track depend mainly upon the relative cross sectional areas but also upon the rate of leakage into the waste area.

3. A range of friction factors from 200 x 10^{-10} to 350 x 10^{-10} lbf min^2/ft^4 (0.037 to 0.065 kg/m^3) was established for a mechanized longwall face with powered supports. These very high values, compared with other airways, are a direct result of the aerodynamic drag of the chocks and, to a lesser extent, the armored face conveyor. Nomograms were produced to assist in establishing faceline resistances for planned longwall faces.

4. Procedures were developed, and data established, to enable the resistances to airflow to be estimated at face ends and across power-loading machinery. The summation of the individual components of resistance gives much more precise values of longwall face resistance than have been available to the present time.

5. It was established that the airflow on a longwall face adheres very closely to the theoretical Square Law, i.e. the frictional pressure drop varies with the square of the air volume flowrate. As far as the authors are aware, this is the first time that the Square Law has been verified on a full-scale longwall face. This finding allays a doubt that has been expressed by some authorities.

6. A survey of airflows passing through the caved waste indicated that in the system investigated, some 54 per cent of the airflow available to the district was utilized in waste ventilation.

7. A mathematical model was developed to simulate airflow patterns in longwall caved areas. This model represents the differential consolidation which arises from the stress pattern on a mined-out area. The caved material is simulated as a geometric pattern of leakage paths with laminar flow through the waste, and turbulent flow through the caved airways that provide the boundaries to the caved zone. The model was correlated with observed data, and is sufficiently efficient to be incorporated into existing programs for ventilation network analysis. This allows a new level of detail and precision in the ventilation planning of longwall mines.

8. A complete procedure was developed, and illustrated by a worked example, of modelling the ventilation of an entire longwall district including the patterns of air migration through the caved area.

The worth of any research project is measured by the extent to which the results are used by others. The authors hope that the publication of this report will result in a better understanding of the mechanisms of airflow in and around longwall faces. The report has endeavored to combine theory and practice in order to produce data and procedures that will lead to the improved design, planning and control of ventilation in longwall mines.

ACKNOWLEDGEMENTS

The authors are grateful to the United States Department of Energy for providing the funding that enabled this project to be undertaken.

The project would not have been possible had it not been for the Snowmass Coal Company making available their Thompson Creek No. 1 Mine for the field study. Acknowledgements are paid particularly to the Mine Manager, Mr. Jay Reynolds and Chief Engineer, Mr. Stephen Self for their ready co-operation and assistance.

REFERENCES

[1] McPherson, M.J. and Hood, M., "Ventilation Planning for Underground Coal Mines," DOE. Report, Contract No. W-7405 ENG-48, October 1981.

[2] Atkinson, J.J., "On the Theory of Airflow in Mines" Transactions North of England Institute of Mining Engineers, 3, 1854 pp. 73-222.

[3] McPherson, M.J., "The Metrication and Rationalization of Mine Ventilation Calculations", The Mining Engineer No. 131, August, 1971.

[4] Wallace Jr., K. and McPherson, M.J. "Mine Ventilation Economics", DOE Report, contract No. DC AC03-768 F000 98, September 1982.

[5] "A Review of Spontaneous Combustion Problems and Controls with Application to U.S. Coal Mines." D.O.E. Report TID - 28879, September, 1978.

[6] Bear, J., "Dynamics of Fluids in Porous Media, American Elsevier, N.Y., N.Y., 1972.

[7] Whittaker, B.N., "An appraisal of strata control practice", Trans. Inst. Mining Engineers, October 1974.

APPENDIX I

Calculation of airflow distribution across face at each measuring station

1. face track - 12 ft^2 adjacent to coal front
2. conveyor track - across armored face conveyor
3. travelling track - from spill plate to shield leg
4. chock track - between chock legs

A2-A3, cross-section 1

travelling track: 10.1 ft^2

A ft^2	u ft/min
0.9	800
2.8	650
2.4	575
1.5	525
2.5	400
10.1	u_{mean} = 565.1
	Q = 5.708 kcfm

chock track: 2.35 ft^2

A-ft^2	u ft/min
.35	400
2.0	200
2.35	u_{Mean} = 229.8
	Q = 0.54 kcfm

conveyor track: 19.83 ft^2

A-ft^2	u ft/min
1.53	800
8.3	650
4.59	575
2.73	525
2.68	400
19.83	u_{mean} = 593.5
	Q = 11.77 kcfm

face track: 12 ft^2

A-ft^2	u ft/min
2.9	650
3.1	575
2.6	525
3.4	400
12.0	u_{mean} = 532.7
	Q = 6.39 kcfm

A3-A4, cross-section 2

travelling track: 10.8 ft^2

A-ft^2	u ft/min
.90	550
2.0	450
4.2	350
2.4	250
1.3	150
10.8	u_{mean} = 335.0
	Q = 3.62 kcfm

chock track: 2.31 ft^2

A ft^2	u ft/min
1.71	80
0.6	150
2.31	u_{mean} = 98.2
	Q = 0.226 kcfm

Conveyor track: 21.13 ft^2

A ft^2	u ft/min
0.54	800
6.06	750
4.77	675
4.29	625
3.86	550
0.52	450
0.82	350
0.27	250
21.13	u_{mean} = 642.7
	Q = 13.58 kcfm

Face track: 12 ft^2

A ft^2	u ft/min
1.4	750
1.7	675
2.7	625
3.2	550
1.75	450
0.9	350
0.2	250
.15	150
12	u_{mean} = 568.3
	Q = 6.82 kcfm

A4-A5, cross-section 3

travelling track: 14.2 ft^2

A ft^2	u ft/min
.16	625
.62	550
1.39	450
2.2	350
3.4	250
3.07	150
2.86	80
0.5	10
14.2	

u_{mean} = 239.85
Q = 3.405 kcfm

chock track: 2.0 ft^2

A ft^2	u ft/min
0.5	80
1.5	10
2.0	

u_{mean} = 65
Q = .130 kcfm

Conveyor track: 29.31 ft^2

A ft2	u ft/min
0.52	780
4.7	740
5.46	675
5.39	625
7.34	550
2.82	450
1.76	350
1.32	250
29.31	

u_{mean} = 586
Q = 17.18 kcfm

face track: 12 ft^2

A ft2	u ft/min
0.6	740
1.9	675
1.8	625
2.2	550
2.4	450
1.9	350
1.2	250
12	

u_{mean} = 508.9
Q = 6.11 kcfm

A5-A6, cross-section 4

travelling track: A = 18.7 ft^2

A ft^2	u ft/min
1.25	550
3.6	450
4.1	350
5.2	250
4.55	150
18.7	u_{mean} = 306.15
	Q = 5.73 kcfm

chock track: A = 2.2 ft^2

A	u ft/min
0.2	150
2.0	48
2.2	u_{mean} = 57.3
	Q = .126 kcfm

Conveyor track: A = 28.77 ft^2

A ft^2	u ft/min
1.03	625
3.14	612.5
10.04	550
8.15	450
3.4	350
1.52	250
1.49	150
28.77	u_{mean} = 470.9
	Q = 13.55 kcfm

face track: A = 12 ft^2

A ft^2	u ft/min
0.9	550
2.7	450
4.6	350
2.4	250
1.4	150
12	u_{mean} = 344.2
	Q = 4.13kcfm

A6-A7, cross-section 5

travelling track: A = 19.2

A ft^2	u ft/min
5.5	250
0.3	325
4.5	175
5.0	125
3.9	75
19.2	

u_{mean} = 165.49
Q = 3.178 kcfm

chock track: 2.2

A ft^2	u ft/min
2.0	40
0.2	75
2.2	

u_{mean} = 43.2
Q = .095 kcfm

Conveyor track: A = 39.24 ft^2

A ft^2	u ft/min
0.97	450
9.09	425
11.47	375
8.16	325
5.56	250
3.32	175
0.67	125
39.24	

u_{mean} = 338.9
Q = 13.3 kcfm

face track: 12 ft^2

A ft^2	u ft/min
1.3	375
2.1	325
2.8	250
3.2	175
2.0	125
0.6	75
12	

u_{mean} = 227.08
Q = 2.73 kcfm

A9 over shearer, cross-section 6

travelling track: A = 9.9 ft^2

A ft^2	u ft/min
2.2	300
2.8	260
2.9	225
2.0	150
9.9	u_{mean} = 236.4
	Q = 2.34 cfm

chock track: A = 2.2 ft^2

A ft^2	u ft/min
2.0	80
0.2	150
2.2	u_{mean} = 86.3
	Q = .190 kcfm

Conveyor Track : A = 53.33 ft^2

A ft^2	u ft/min
0.93	300
12.91	260
8.91	245
15.89	225
14.69	150
55.33	u_{mean} = 217.5
	Q = 11.6 kcfm

Face track : A = 12 ft^2

A ft^2	u ft/min
0.8	260
1.8	245
3.6	225
5.8	150
12	u_{mean} = 194.1
	Q = 2.33 kcfm